SYNTHESIS, CHARACTERIZATION, AND TRANSFORMATIONS OF α-BORYLCARBONYL COMPOUNDS CONTAINING 1,2-AZABORINE

Jennifer Sara LaPoff

A Thesis

submitted to the Faculty of

the Department of Chemistry

in partial fulfillment

of the requirements for the degree of

Master of Science

Boston College

Morrissey College of Arts and Sciences

Graduate School

May 2024

Synthesis, Characterization, and Transformations of α-Borylcarbonyl Compounds Containing 1,2-Azaborine

Jennifer Sara LaPoff

Advisor: Shih-Yuan Liu, Ph.D.

ABSTRACT:

Organoboron compounds are widely used in organic synthesis and medicinal chemistry. It has been shown that organoboron compounds can undergo a vast quantity of transformations, especially stereospecific reactions. Boron enolates and their reactivity are less explored in the field of organic chemistry. In enolates, boron can be bound to oxygen or carbon. The boron-carbon enolates are of interest for having the potential to engage in stereospecific organoboron chemistry via the stereospecific carbon connected to the boron atom. Two methods of synthesizing boron-carbon enolates are through quaternized and unquaternized boron centers. While quaternized boron-carbon enolates are more studied, unquaternized boron-enolates represent a gap in the field. To date only four unquaternized boron-carbon enolates have been isolated and characterized with only one of the compounds engaging in organoboron chemistry. Herein I report the synthesis, isolation, and characterization of a boron-carbon enolate containing 1,2-azaborine as the organoboron analog.

For my mom, my dad, my brother, my friends, my dogs, my therapist

TABLE OF CONTENTS

LIST OF FIGURES

Figure 1.18: Comparison of Experimental and Theoretical Bond Lengths for Compound **1**.

LIST OF SCHEMES

LIST OF TABLES

LIST OF ABBREVIATIONS

1,2-Azaborine: monocyclic 1,2-dihydro-1,2-azaborine

Å: Angstrom

Ac: acetyl

Ar: aryl

Bcat: catecholborane

BIAN: bis(aryl)acenaphthenequinonediimine

BINAP: (2,2’-bis(diphenylphosphino)-1,1’-binaphthyl

Bn: benzyl

Bpin: pinacolborane

Bu: butyl

Cat.: catalyst

Cp: cyclopentadienyl

Cy: cyclohexyl

DART: direct analysis in real time

dba: dibenzylideneacetone

DDQ: 2,3-dichloro-5,6-dicyano-1,4-benzoquinone

DIPA: diisopropylamine

DMAP: 4-dimethylaminopyridine

DMFU: dimethyl fumarate

d.r.: diastereomeric ratio

DTBP: di-tert-butyl peroxide

EAS: electrophilic aromatic substitution

Et: ethyl

eq: equation

equiv: equivalent(s)

Gen.: generation

h: hour(s)

HMPA: hexamethylphosphoramide

HPLC: high performance liquid chromatography

HRMS: high resolution mass spectroscopy

KHMDS: potassium bis(trimethylsilyl)amide

IR: infrared spectroscopy

L: ligand

LDA: lithium diisopropylamine

$LiAlH_4$: lithium aluminum hydride

M: molar

Me: methyl

MIDA: N-methyliminodiacetic acid

Min: minute(s)

mol: mole

MS: mass spectroscopy

M.S.: molecular sieves

NAS: nucleophilic aromatic substitution

nbd: norbornadiene

n.d: not detected

nm: nanometers

NMR: nuclear magnetic resonance spectroscopy

OAc: acetoxyl

ODCB: ortho-dichlorobenzene

OMe: methoxyl

OTf: trifluoromethanesulfonate

Parent azaborine: N-H, B-H 1,2-dihydro-1,2-azaborine

pent: pentane

Ph: phenyl

PIDA: pinene-derived iminodiacetic acid

PPh_3: triphenylphosphine

(R)-DTBM-SEGPHOS: (R)-(–)-5,5'-Bis[di(3,5-di-*tert*-butyl-4-methoxyphenyl)phosphino]-4,4'-bi-1,3-benzodioxole

RBF: round-bottomed flask

RCM: ring-closing metathesis

RT: room temperature

SKA: silylketene acetal

SOP: Standard Operating Procedure

t: *tert*

TBAF: tetrabutylammonium fluoride

TBDPS: *tert*-butyldiphenylsilyl

TBS: *tert*-butyldimethylsilyl

tBu: *tert*-butyl

temp: temperature

Tf: triflyl

THF: tetrahydrofuran

TIPS: triisopropylsilyl

TMS: trimethylsilyl

Tol: toluene

Triflate: trifluoromethanesulfonate

TTMSS: Tris(trimethylsilyl)silyl

wt: weight

CHAPTER 1: SYNTHESIS, CHARACTERIZATION, AND TRANSFORMATIONS OF ALPHA-BORYLCARBONYL COMPOUNDS CONTAINING 1,2-AZABORINE

1.1 Introduction

1.1.1 BN/CC Isosterism and Properties of 1,2-Azaborine

An attractive method for expanding chemical space is isosterism. In 1919, Langmuir defined isosterism first as the similarity between molecules or ions that have the same number of atoms and valence electrons.[1] This idea of isosterism continued to expand through the work of Grimm,[2] then Penny and Sutherland.[3] For an organic compound B to be an isostere of compound A, compound B needs to be isoelectronic and isostructural. Being isoelectronic is when two or more molecules or compounds have the same total number of atoms and electrons, while being isostructural is when there is a similar geometric structure.[3]

Among the different forms of isosterism, a growing research field is the replacement of a carbon-carbon double bond with a boron-nitrogen single bond, which is

[1] Langmuir, I. *J. Am. Chem. Soc.* **1919**, *41*, 1543-1559.
[2] (a) Grimm, H.G.Z. *Elektrochem.* **1925**, *31*, 474-480. (b) Grimm, H.G.Z. *Naturwissenshaften* **1929**, *17*, 557-564.
[3] (a) Penney, W.G.; Sutherland, G.B.B.M. *Force Constants of Triatomic Systems* **1936**, 654-678. (b) Rayner-Canham, G. *Found Chem.* **2009**, *11*, 123-129.

referred to as BN/CC isosterism (Figure 1.1).[4] BN-heterocycles have been studied in various fields including materials science,[4] ligand chemistry,[5] organic synthesis,[4] hydrogen storage,[6] and biomedical research.[7] BN isosteres are of interest because they can expand the chemical space of hydrocarbon compounds due to the electronic difference generated with the incorporation of boron and nitrogen.

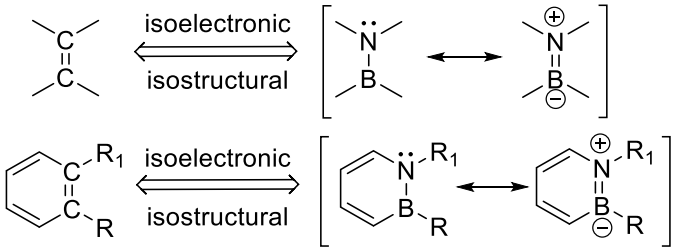

Figure 1.1: BN/CC Isosterism and its Incorporation in Benzene.

Isosterism can also be applied to benzene where the replacement of one CC unit with nitrogen and boron creates the 1,2-dihydro-1,2-azaborine (parent 1,2-azaborine) and a variety of different substitutions throughout the ring that is stable with aromatic character. A key distinguishing feature of 1,2-azaborine compared to benzene is its ability

[4] For perspective pieces: (a) Lamm, A.N.; Garner, E.B.; Dixon, D.A.; and Liu, S.-Y. *Angew. Chem. Int. Ed.* **2011**, *50*, 8157-8160. (b) Campbell, P.G.; Marwitz, A.J.V.; and Liu, S.-Y. *Angew. Chem. Int. Ed.* **2012**, *51*, 6074-6092. (c) Giustra, Z.X. and Liu, S.-Y. *J. Am. Chem. Soc.* **2018**, *140*, 1184-1194.

[5] (a) Marwitz, A.J.V.; Jenkins, J.T.; Zakharov, L.N.; and Liu, S.-Y. *Organometallics* **2011**, *30*, 52-54. (b) McConnell, C.R.; Campbell, P.G.; Fristoe, C.R. Memmel, P.; Zakharov, L.N.; Li, B.; Darrigan, C.; Chrostowska, A.; and Liu, S.-Y. *Eur. J. Inorg. Chem.* **2017**, 2207-2210.

[6] (a) Campbell, P.G.; Zakharov, L.N.; Grant, D.J.; Dixon, D.A.; and Liu, S.-Y. *J. Am. Chem. Soc.* **2010**, *132*, 3289-3291. (b) Giustra, Z.X.; Chou, L.-Y.; Tsung, C.-K.; and Liu, S.-Y. *Organometallics* **2016**, *35*, 2425-2428.

[7] (a) Liu, L.; Marwitz, A.J.V.; Matthews, B.W.; and Liu, S.-Y. *Angew. Chem. Int. Ed.* **2009**, *48*, 6817-6819. (b) Knack, D.H.; Marshall, J.L.; Harlow, G.P.; Dudzik, A.; Szaleniec M.; Heider, J.; and Liu, S.-Y. *Angew. Chem. Int. Ed.* **2013**, *52*, 2599-2601. (c) Lee, H.; Fischer, M.; Shoichet, B.K.; and Liu, S.-Y. *J. Am. Chem. Soc.* **2016**, *138*, 12021-12024. (d) Zhao, P.; Nettleton, D.O.; Karki, R.G.; Zécri, F.J.; and Liu, S.-Y. *ChemMedChem* **2017**, *12*, 358-361. (e) Boknevitz, K.; Italia, J.S.; Li, B.; Chatterjee, A.; and Liu, S.-Y. *Chem. Sci.* **2019**, *10*, 4994-4998. (f) Liu, Y. and Liu, S.-Y. *Org. Biomol. Chem.* **2019**, *17*, 7002-7006.

to act as a nucleophile or electrophile at the two heteroatoms. Boron is the most electrophilic position since it has a partially occupied p-orbital due to resonance through the ring;[4] therefore, boron can be attacked nucleophilically.

Liu and co-workers unveiled physical properties of parent 1,2-azaborine, e.g. melting point, boiling point, etc. 1,2-Azaborine has a melting point of –45 ºC and a boiling point of 117 ºC.[7,8] It is generally understood that 1,2-azaborine is water stable and can withstand oxidative degradation depending on the boron substitution,[9] e.g. a bulkier substituent (i.e, mesityl group) impacts greater stability. This could allow certain 1,2-azaborine substrates to be utilized without the necessity of inert atmosphere techniques. All atoms in 1,2-azaborine are coplanar as determined by crystallographic and microwave spectroscopic analysis.[10] Besides those characteristics, the parent 1,2-azaborine has a λ_{max} of 269 nm, which is slightly red shifted relative to the alpha band of benzene at 255 nm.[8]

The aromatic character of 1,2-azaborine represents an important topic in BC/CC isosterism of polycyclic aromatic hydrocarbon. 1,2-Azaborine is considered an aromatic compound, but it is less aromatic than benzene. How aromatic it is in comparison to benzene? Experimentally, 1,2-azaborines have been shown to engage in electrophilic aromatic substitution (EAS)[11] and nucleophilic aromatic substitution (NAS) reactions.[12] Experimental hydrogenation enthalpies determined via reaction calorimetry revealed a potentially resonance stabilization energy (RSE) for a 1,2-azaborine to be 16.6

---

[8] (a) Marwitz, A.J.V.; Matus, M.H.; Zakharov, L.N.; Dixon, D.A.; and Liu, S.-Y. *Angew. Chem. Int. Ed.* **2009**, *48*, 973-977. (b) Abbey, E.R.; Lamm, A.N.; Baggett, A.W.; Zakharov, L.N.; and Liu, S.-Y. *J. Am. Chem. Soc.* **2013**, *135*, 12908-12913.
[9] Lamm, A.N. and Liu, S.-Y. *Mol. BioSyst.* **2009**, *5*, 1303-1305.
[10] (a) Abbey, E.R.; Zakharov, L.N.; and Liu, S.-Y. *J. Am. Chem. Soc.* **2008**, *130*, 7250-7252. (b) Daly, A.M.; Tanjaroon, C.; Marwitz, A.J.V.; Liu, S.-Y.; and Kukolich, S.G. *J. Am. Chem. Soc.* **2010**, *132*, 5501-5506.
[11] Pan, J.; Kampf, J.W.; and Ashe, A.J. *Org. Lett.* **2007**, *9*, 679-681.
[12] McConnell, C.R. and Liu, S.-Y. *Chem. Soc. Rev.* **2019**, *48*, 3436-3453.

kcal/mol.[13] Kistiakowsky and co-workers determined the RSE of benzene as 36 kcal/mol.[14] Recognizing the aromatic character of 1,2-azaborine, we hypothesized it could be used to access a kinetically stabilized C-Boron enolate, which is the topic of this thesis.

1.1.2 Syntheses of 1,2-Azaborines

Historically, there have been many attempts at synthesizing and characterizing 1,2-azaborines.[13] Dewar and White pioneered BN heterocycle research in the 1960's where they researched monocyclic and ring-fused polycyclic 1,2-azaborine derivatives (Scheme 1.1).[15] In 1962, Dewar and co-workers synthesized compound **1.4** from a substituted thiophene compound **1.1** which underwent a reduction of the nitro group to obtain compound **1.2**. From compound **1.2**, a borylative cyclization followed by a Ni-mediated desulfurization to yield compound **1.4**. In 1963, White and co-workers synthesized compound **1.8** via a borylative cyclization to furnish compound **1.7**. Subsequent dehydrogenation over Pd/C at high temperatures produced **1.7**.

[13] Campbell, P.G.; Abbey, E.R.; Neiner, D.; Grant, D.J.; Dixon, D.A.; and Liu, S.-Y. *J. Am. Chem. Soc.* **2010**, *132*, 18048-18050.
[14] Kistiakowksy, G.B.; Ruhoff, J.R.; Smith, H.A.; and Vaughan, W.E. *J. Am. Chem. Soc.* **1936**, *58*, 146-153.
[15] (a) Fritsch, A.J. *Chem. Heterocycl. Compd.* **1977**, *30*, 381-440. (b) Dewar, M.J.S. and Marr, P.A. *J. Am. Chem. Soc.* **1962**, *84*, 3782. (c) White, D.G. *J. Am. Chem. Soc.* **1963**, *85*, 3634-3636.

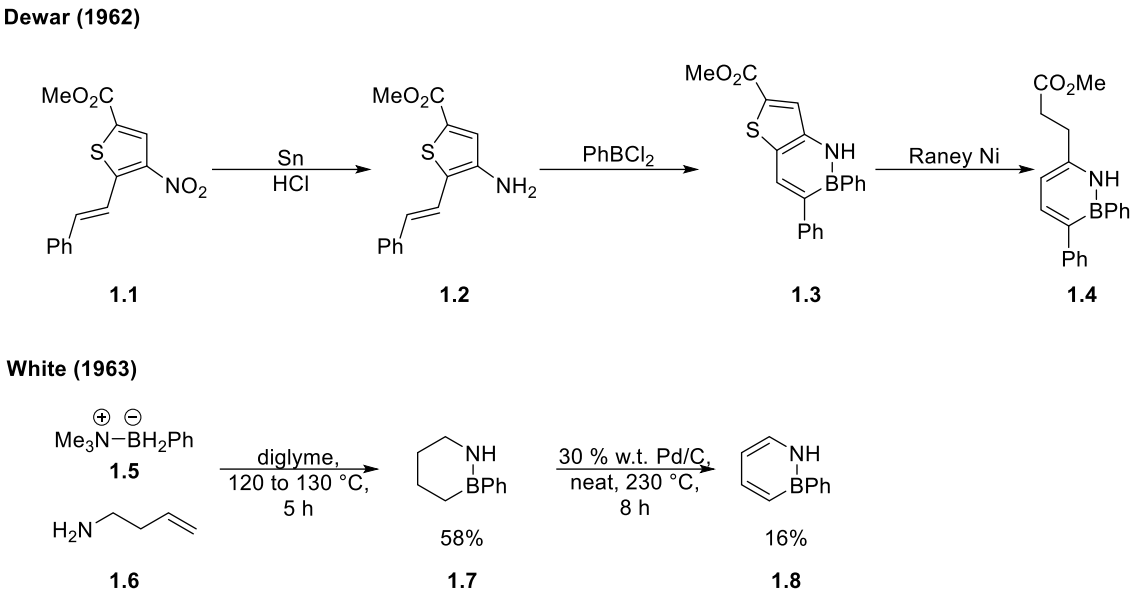

Scheme 1.1: Dewar's and White's Syntheses of Substituted 1,2-Azaborine.

There was a paucity in BN-heterocyclic research until 2000, when Ashe and co-workers reignited the field for research. Ashe and co-workers developed two complementary syntheses for N-Et, B-Ph 1,2-azaborine. The first synthesis included a ring-closing metathesis[16] and the second utilized a Katz-type ring expansion[14,17] (Scheme 1.2). In the first synthesis, allyltributyltin (**1.19**) reacted with boron trichloride to generate allylboron dichloride *in situ* that then reacted with ethylallylamine in the presence of triethylamine to yield product (**1.10**) in 68% yield. The BN-adduct (**1.10**) then reacted with phenyllithium in diethyl ether to exchange the chloride with a phenyl in the adduct to generate (**1.11**) in 81% yield. A ring-closing metathesis of **1.11** using Grubbs first-generation catalyst[18] afforded product (**1.12**) in 86% yield. The aromatic product (**1.13**) was obtained by oxidation using DDQ in pentane (Scheme 1.2 equation 1). In the second

[16] Ashe, A.J. and Fang, X. *Org. Lett.* **2000**, *2*, 2089-2091.
[17] Ashe, A.J.; Fang, X.; Fang, X.; and Kampf, J.W. *Organometallics* **2001**, *20*, 5413-5418.
[18] Schwab, P.; France, M.B.; Ziller, J.W.; and Grubbs, R.H. *Angew. Chem. Int. Ed.* **1995**, *34*, 2039-2041.

synthesis, RCM of the diene adduct (**1.14**) afforded a five-membered ring (**1.15**) in 85% yield. Deprotonation with lithium diisopropylamine (LDA) afforded the lithium azaborolide (**1.16**) in 77% yield, which following by a Katz-type ring expansion gives the desired product (**1.13**) in 64% yield (Scheme 1.2 equation 2).

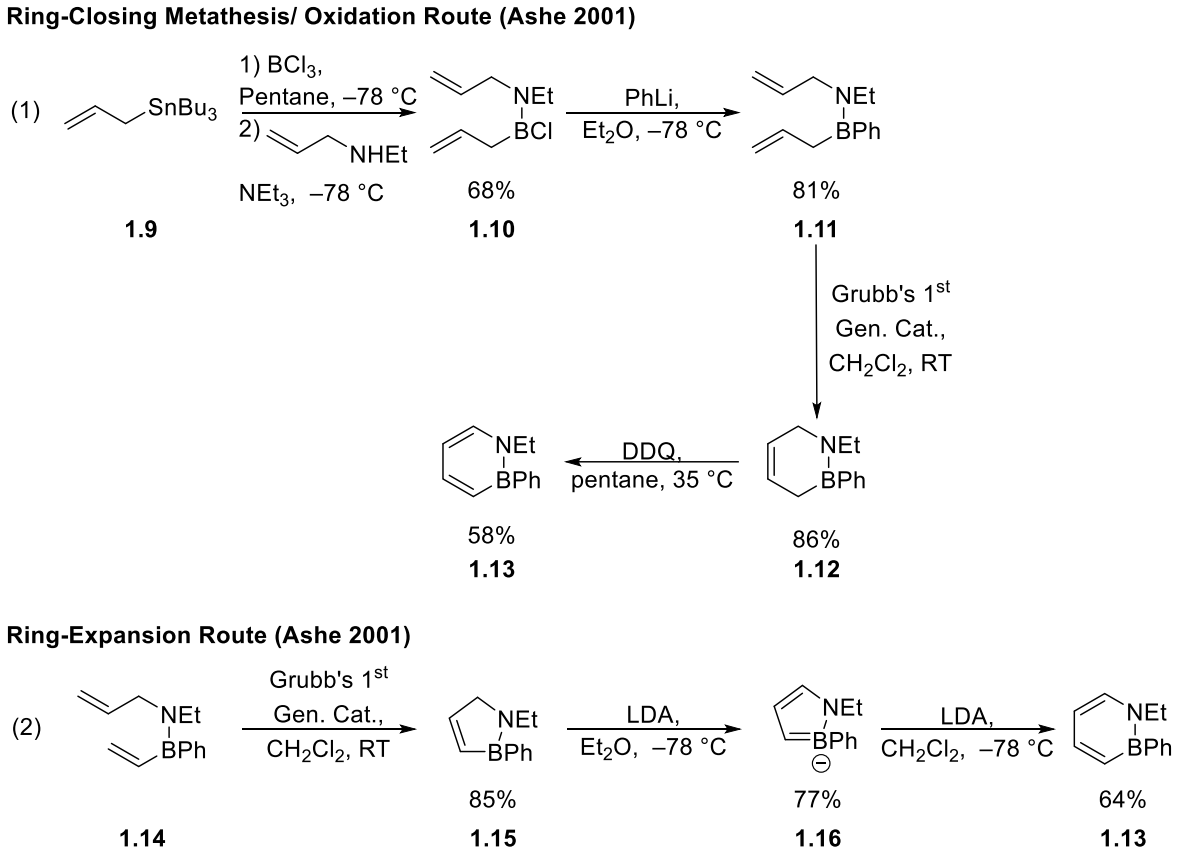

Scheme 1.2: Ashe's Syntheses of N-Et, B-Ph 1,2-Azaborine.

After Ashe's syntheses reignited the field of BN-heterocyclic research, Liu and co-workers developed a synthesis of a versatile 1,2-azaborine building block N-TBS, B-Cl 1,2-azaborine (**1.20**) through a modified version of Ashe's synthesis (Scheme 1.3).[19]

[19] Marwitz, A.J.V.; Matus, M.H.; Zakharov, L.N.; Dixon, D.A.; and Liu, S.-Y. *Angew. Chem. Int. Ed.* **2009**, *48*, 973-977.

In Liu's synthesis, the use of TBS-allylamine afforded the BN-adduct product (**1.18**) in 58% yield, and sequential RCM to finished the product (**1.19**) in 82% yield. The desired building block (**1.20**) was then achieved in 35% yield using Pd/C dehydrogenation (Scheme 1.3). Similarly, triallyborane (**1.21**) reacts with boron trichloride *in situ* to generate allylboron dichloride that reacts with TBS-allylamine to obtain adduct (**1.18**) in 81% yield (Scheme 1.3).

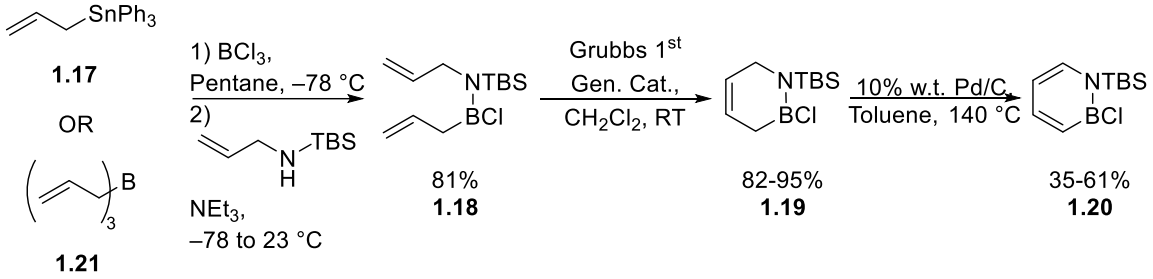

Scheme 1.3: Liu's Syntheses of N-TBS, B-Cl 1,2-Azaborine.

Along with the synthesis of N-TBS, B-Cl 1,2-azaborine, Liu and co-workers accomplished the synthesis of the long-sought parent (N-H, B-H) 1,2-azaborine (**1.25**) (Scheme 1.4).[8,17] Two synthesis exist for parent 1,2-azaborine. In the first one, reduction of **1.20** yielded BH product **1.22** in 99% yield followed by coordination to $(MeCN)_3Cr(CO)_3$ to achieve complex (**1.23**) in 71% yield. Subsequently, desilylation with HF·pyridine to obtain product (**1.24**) in 76% yield, which was followed by decomplexation to obtain parent 1,2-azaborine (**1.25**) in 10% isolated yield (Scheme 1.4 equation 1). The second synthesis provides a more straightforward route starting with addition of acetamide to **1.20**, to obtain product **1.26** in 62% yield with concurrent desilylation. An amide exchange occurred with an alcohol to afford product (**1.27**) in

90% yield followed by reduction achieve the parent 1,2-azaborine (**1.25**) in 57% yield (Scheme 1.4 equation 2).

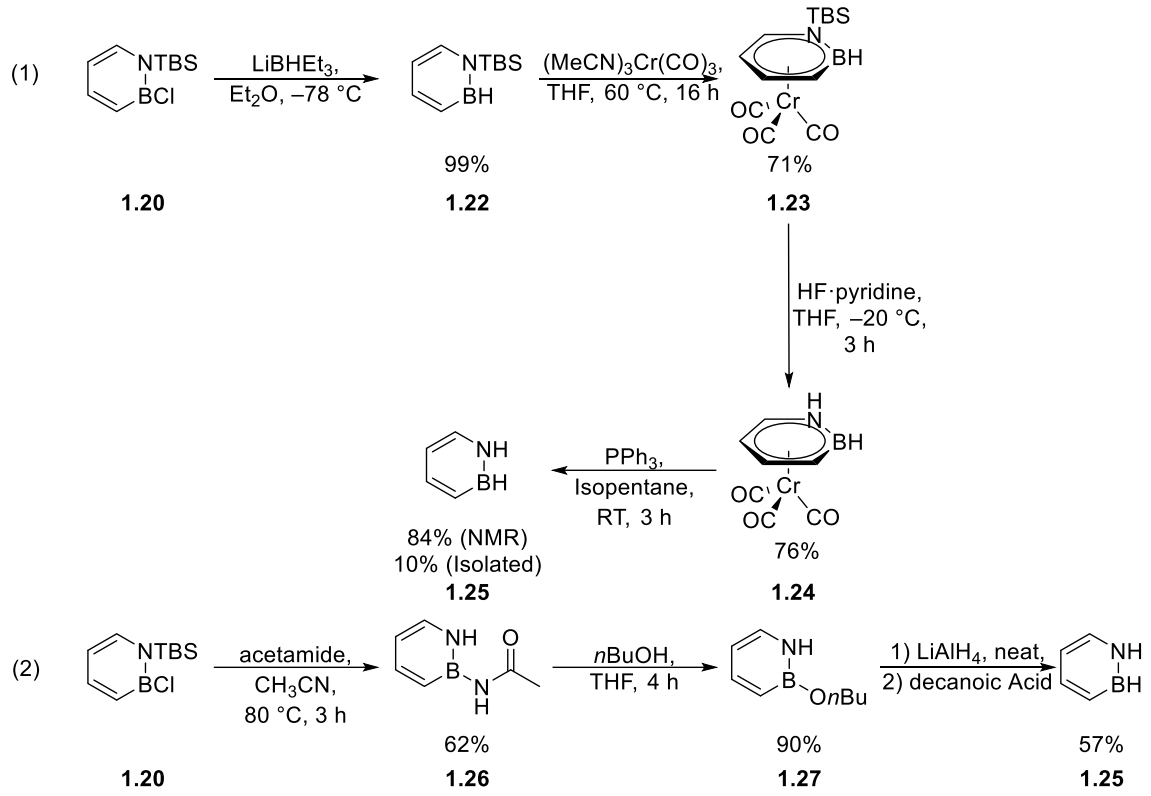

Scheme 1.4: Liu's Syntheses Toward Parent 1,2-Azaborine.

1.1.3 Functionalization at the Boron Position in 1,2-Azaborine

The 1,2-azaborine scaffold allows for selective substitutions due to its distinct electronic structure. On the 1,2-azaborine ring, boron can be functionalized using various transformations such as transmetalation,[4] dehydrogenative borylation,[20] nucleophilic aromatic substitution (NAS),[8,21] and arylation reactions.[22] The ability to functionalize the

[20] Brown, A.N.; Zakharov, L.N.; Mikulas, T.; Dixon, D.A.; and Liu, S.-Y. *Org. Lett.* **2014**, *16*, 3340-3343.
[21] (a) Marwitz, A.J.V.; Abbey, E.R.; Jenkins, J.T.; Zakharov, L.N.; and Liu, S.-Y. *Org. Lett.* **2007**, *9*, 4905-4908. (b) Lamm, A.N.; Garner, E.B.; Dixon, D.A.; and Liu, S.-Y. *Angew. Chem. Int. Ed.*

boron position is essential when it comes to using 1,2-azaborine as a handle for further transformations. Examples of 1,2-azaborine building blocks include α-boryl diazo compound,[23] cyano-substituted boron,[24] and a cationic 1,2-azaborine species[25] have shown to be used in further transformations (Figure 1.2). Specifically, the α-boryl diazo compound containing 1,2-azaborine has been shown to undergo carbonyl olefination, O-alkylation of carboxylic acids, [3+2] reactions, and C-H activation of terminal alkynes. Not only can boron substitution be used to construct building blocks, but it can also be used to generate analogs of 1,2-azaborine all-carbon counterparts in the fields of ligand design,[5] materials science,[4,19,26] and medicinal chemistry[7] (Figure 1.2).

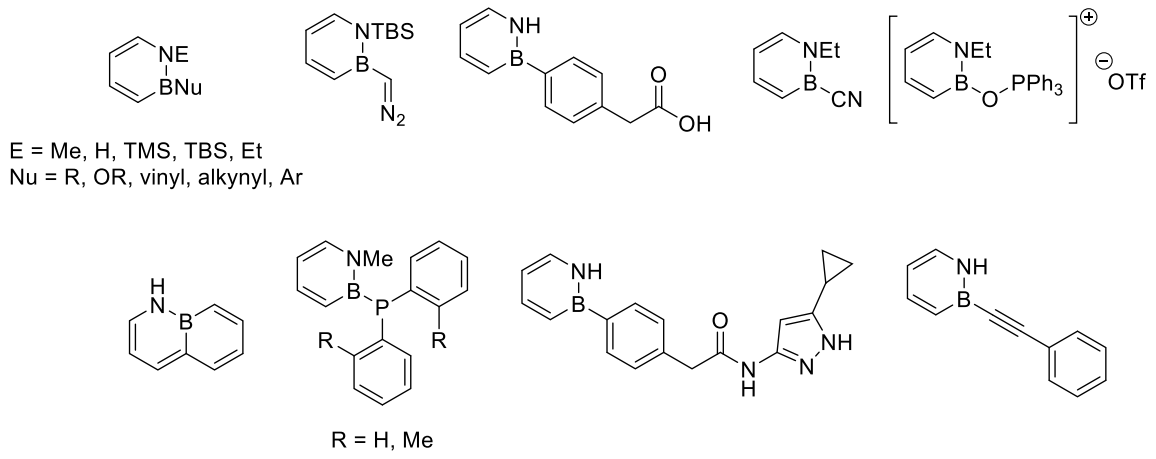

Figure 1.2: Select 1,2-Azaborine Compounds Substituted at the Boron

---

2011, *50*, 8157-8160. (c) Brown, A.N.; Li, B.; and Liu, S.-Y. *J. Am. Chem. Soc.* **2015**, *137*, 8932-8935.

[22] Rudebusch, G.E.; Zakharov, L.V.; and Liu, S.-Y. *Angew. Chem. Int. Ed.* **2013**, *52*, 9316-9319.

[23] Liu, Y.; Puig de la Bellascasa, R.; Li, B.; Cuenca, A.B.; and Liu, S.-Y. *J. Am. Chem. Soc.* **2021**, *143*, 14059-14064.

[24] Marwitz, A.J.V.; McClintock, S.P.; Zakharov, L.N.; and Liu, S.-Y. *Chem. Commun.* **2010**, *46*, 779-781.

[25] Marwitz, A.J.V.; Kenkins, J.T.; Zakharov, L.N.; and Liu, S.-Y. *Organometallics* **2011**, *30*, 52-54.

[26] Marwitz, A.J.V.; Lamm, A.N.; Zakharov, L.N.; Vasiliu, M.; Dixon, D.A.; and Liu, S.-Y. *Chem. Sci.* **2012**, *3*, 825-829.

1.2 Stereospecific Organoboron Functionalizations and Transformations

1.2.1 Background

Organoboron compounds have profound usage in organic chemistry, asymmetric synthesis, and medicinal chemistry.[27] The boron handle in these types of compounds allows for a wide array of transformations and late-stage functionalizations that would otherwise be difficult to accomplish. In 1961, Brown and co-workers reported the first asymmetric hydroboration, demonstrating that organoboron molecules can be prepared with high enantioselectivity.[28] An appealing transformation of an organoboron compound is the stereospecific oxidation of chiral alkylborane, which allows for alkylboranes to be converted to a wide range of functional groups.[29] One disadvantage of using alkylboranes is that they are susceptible to decomposition in air and moisture.[26,27] Boronic esters have been utilized instead for their increased stability especially when it comes to purification.[27] The usage of boronic acids has opened a new stream of products that can be synthesized.[30] Preparing these boronic ester compounds has been well-established through a vast array of reactions such as diboration,[31] hydroboration,[32] and homologations.[33]

---

[27] For Review see: (a) Defrancesco, H.; Dudley, J.; and Coca, A. *ACS Symposium Series* **2016**, *1236*, 1-25. (b) Sandford,C. and Aggarwal, V.K. *Chem. Commun.* **2017**, *53*, 5481. (c) Yangm, X.; Kalita, S.J.; Maheshuni, S.; and Huang, Y.-Y. *Coord. Chem.* **2019**, *392*, 35-48. (d) Fernandes, G.F.S.; Denny, W.A.; and Dos Santos, J.L. *Eur. J. of Med. Chem.* **2019**, *179*, 791-804. (e) Shoji, Y.; Kashida, J.; and Fukushima, T. *Chem. Commun.* **2022**, *58*, 4420-4434.
[28] Brown, H.C. and Bigley, D.B. *J. Am. Chem. Soc.* **1961**, *83*, 486-487.
[29] Brown, H.C. and Singaram, B. *Acc. Chem. Res.* **1988**, *21*, 287-293.
[30] Lennox, A.J.J. and Lloyd-Jones, G.C. *Chem. Soc. Rev.* **2014**, *43*, 412-443.
[31] Coombs, J.R. and Morken, J.P. *Angew. Chem. Int. Ed.* **2016**, *55*, 2636-2649.
[32] Crudden, C.M. and Edwards, D. *Eur. J. Org. Chem.* **2003**, 4695-4712.
[33] Matteson, D.S. *Chem. Rev.* **1989**, *89*, 1535-1551.

1.2.2 Overview of Stereospecific Transformations

Enantioenriched secondary or tertiary boronic esters can be used in stereospecific transformations with either stereoretentive or stereoinvertive manner to yield a variety of enantioenriched products. These boronic esters have been shown to engage in a variety of transformations such as oxidation,[34] amination,[35] protodeboronation,[36] olefination,[37] and many more (Figure 1.5).[38] These transformations have been shown to tolerate a variety of sensitive functional groups and as a result organoboron compounds have become one of the most versatile building blocks in organic synthesis.

[34] (a) Brown, H.C. and Zweifel, G. *J. Am. Chem. Soc.* **1961**, *83*, 2544-2551. (b) Fontani, P.; Carboni, B.; Vaultier, M.; and Maas, G. *Synthesis* **1991**, 605-609. (c) Stymiest, J.L.; Bagutski, V.; Grench, R.M.; and Aggarwal, V.K. *Nature* **2008**, *456*, 778-782.
[35] (a) Brown, H.C.; Kim, K.-W.; Cole, T.E.; and Singaram, B. *J. Am. Chem. Soc.* **1986**, *108*, 6761-6764. (b) Bagutski, V.; Elford, T.G.; and Aggarwal, V.K. *Angew. Chem. Int. Ed.* **2011**, *50*, 1080-1083. (c) Mlynarski, S.N.; Karns, A.S.; and Morken, J.P. *J. Am. Chem. Soc.* **2012**, *134*, 16449-16451.
[36] (a) Brown, H.C. and Murray, K.J. *Tetrahedron* **1986**, *42*, 5497-5504. (b) Nave, S.; Sonawane, R.P.; Elford, T.G.; and Aggarwal, V.K. *J. Am. Chem. Soc.* **2010**, *132*, 17096-17098. (c) Rasappan, R. and Aggarwal, V.K. *Nat. Chem.* **2014**, *6*, 810-814.
[37] (a) Zweifel, G.; Arzoumanian, H.; and Whitney, C.C. *J. Am. Chem. Soc.* **1967**, *89*, 3652-3653. (b) Evans, D.A.; Crawford, T.C.; Thomas, R.C.; and Walker, J.A. *J. Org. Chem.* **1976**, *41*, 3947-3953. (c) Sonawane, R.P.; Jheengut, V.; Rabalakos, C.; Larouche-Gauthier, R.; Scott, H.K.; and Aggarwal, V.K. *Angew. Chem. Int. Ed.* **2011**, *50*, 3760-3763. (d) Fletcher, C.J.; Blair, D.J.; Wheelhouse, K.M.P.; and Aggarwal, V.K. *Tetrahedron* **2012**, *68*, 7598-7604. (e) Armstrong, R.J.; Garcia-Ruiz, C.; Myers, E.L.; and Aggarwal, V.K. *Angew. Chem. Int. Ed.* **2017**, *56*, 786-790.
[38] For review see: Sandford, C. and Aggarwal, V.K. *Chem. Commun.* **2017**, *53*, 5481-5494.

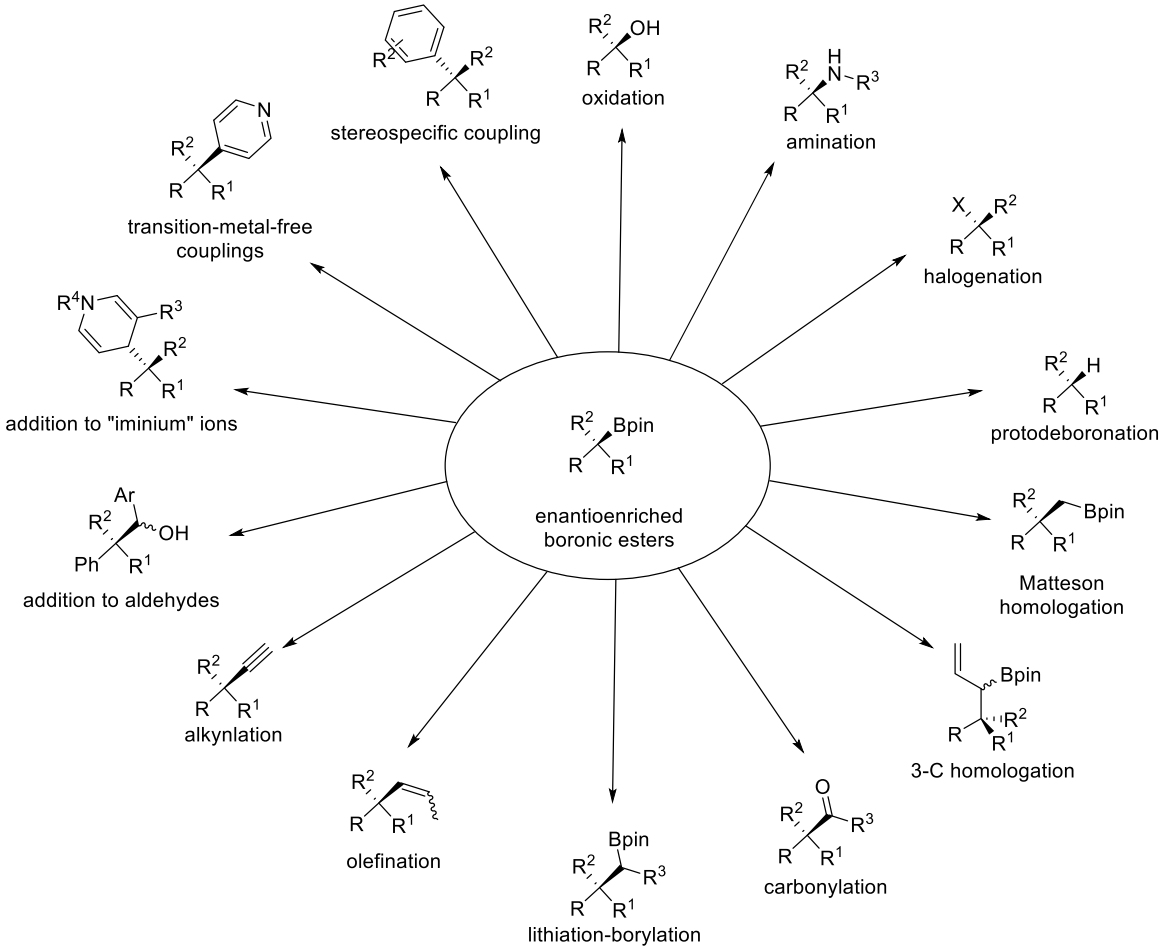

Scheme 1.5: Stereospecific Transformations of Enantioenriched Boronic Esters.

One prominent transformation for boronic is the stereospecific Suzuki-Miyuara cross-coupling reaction.[39] This reaction involves a boronic ester or acid that will couple with an aryl or alkyl halide electrophile in the presence of a transition metal catalyst and a base. Suzuki and co-workers first reported this transformation in 1979.[40] In this cross-coupling reaction, there are a variety of factors that influence the stereochemical outcome for the product which arises from the transmetalation. Biscoe and Sigman studied the

[39] For review see: Ma, X.; Murray, B.; and Biscoe, M.R. *Nat. Rev.* **2020**, *4*, 584-599.
[40] Miyaura, N.; Yamada, K.; and Suzuki, A. *Tetrahedron. Lett.* **1979**, *36*, 3437-3440.

stereochemical outcome of the transmetalation as a function of the ligand properties.[41] A bulky electron deficient ligand promotes the stereoretentive pathway and decreases the β-H elimination side pathway.[39] If the ligand is a bulky and electron rich, the reaction the goes through a stereoinvertive pathway.[38] Ligand sterics can also be used to tune the reactivity. When a bulky phosphine ligand is used, the reaction is stereoretentive due to axial shielding from the ligand blocking access to the stereoinvertive transmetalation pathway.[42] Finally, the substrate may override the influence of the ligand electronics.[43] The ability to control the reactivity of boronic esters in stereospecific transformations has merited considerable attention in organometallics and asymmetric synthesis.

1.3 Boron Enolates

1.3.1 Background

In enolates, boron can be used in place of the classic lithium.[44,59] Boron has the potential to be bound to the carbonyl oxygen (BO) or the α-carbon (BC) enolate (Figure 1.3).[45] It is generally energetically more favorable (by ~20 kcal/mol) for boron to be bound to oxygen.[46] The BO enolate is more thermodynamically stable but is achiral because of the presence of a mirror plane. Between BO (O-boron) and BC (C-boron)

---

[41] (a) Neimeyer, Z.L.; Milo, A.; Hickey, D.P.; and Sigman, M.S. *Nat. Chem.* **2016**, *8*, 610-617. (b) Chen, L.; Ren, P.; and Carrow, B.P. *J. Am. Chem. Soc*. **2016**, *138*, 6392-6395. (c) Zhao, S.; Gensch, T.; Murray, B.; Niemeyer, Z.L.; Sigman, M.S.; and Biscoe, M.R. *Science* **2018**, *362*, 670-674.
[42] Lehmann, J.W.; Crouch, I.T.; Blair, D.J.; Trobe, M.; Wang, P.; Li, J.; and Burke, M.D. *Nat. Commun.* **2019**, *10*, 1263-1272.
[43] Dreher, S.D.; Dormer, P.G.; Sandrock, D.L.; and Molander, G.A. *J. Am. Chem. Soc.* **2008**, *130*, 9257-9259.
[44] Braun, M. *Helvetica Chiminica Acta* **2015**, *98*, 1-31.
[45] Wang Hei Ng, E.; Low, K.-H.; and Chiu, P. *J. Am. Chem. Soc.* **2018**, *140*, 3537-3541.
[46] He, Z.; Zajdlik, A.; and Yudin, A.K. *Acc. Chem. Res.* **2014**, *47*, 1029-1040.

enolates, BO enolates have been widely used to be intermediates in cross-coupling reactions and are more readily isolated.[45,44] The compound itself can engage in enolate chemistry such as aldol and/or alkylation reactions.[45]

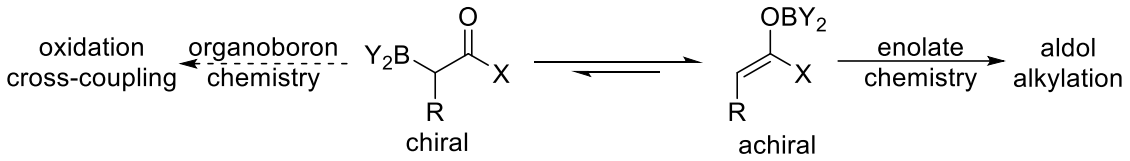

Figure 1.3: Boron Enolate Isomerization from Carbon to Oxygen.

The more underdeveloped organoboron BC enolate compound is significantly less stable, harder to isolate, and tends to isomerize to the BO enolate. BC enolates have only been proposed as intermediates in reactions until 2001.[45,47] It is widely understood that carbon-bound metal and metalloid enolates are thermodynamically unstable and hard to isolate.[48] The BC enolate is chiral and has the potential to engage in stereospecific organoboron chemistry such as cross-coupling and/ or oxidation reactions. One idea to increase the stability of BC enolate would be to have an electron rich boron center to decrease the ability for it to coordinate to the carbonyl oxygen.[45] Two families of BC enolates have been characterized; quaternized and unquaternized BC enolates.

1.3.2 Boron-Carbon Enolates

1.3.2.1 Quaternized Boron-Carbon Enolates

Quaternized BC enolates are more stable because boron is tetracoordinated and the lewis acidity of boron is thus quenched. However, since boron is tetracoordinated, it

[47] For perspective pieces: (a) Mukaiyama, T.; Murakami, M.; Oriyama, T.; and Yamaguchi, M. *Chemistry Letters* **1981**, 1193-1196. (b) Wei, W.; Li, C.; Wang, T.; Liu, D.; and Zhang, Z. *Organometallics* **2008**, *27*, 443-4454.
[48] He, Z. and Yudin, A.K. *J. Am. Chem. Soc.* **2011**, *133*, 13770-13773.

is less reactive towards typical organoboron functionalization chemistry. The first example of an isolated quaternized BC enolate (**1.28**) was reported in 1977 by Pickardt and co-workers (Figure 1.4).[49] Ten examples of quaternized BC enolates have been reported and fully characterized (Figure 1.5).

Pickardt (1977)

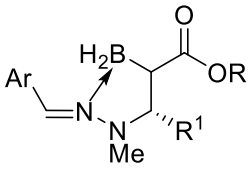

1.28

Figure 1.4: First Example of Isolated and Characterized Quaternized BC Enolate.

Paetzold (1979)

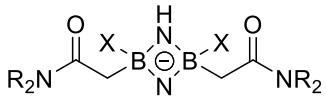

1.29

Burger (1993)

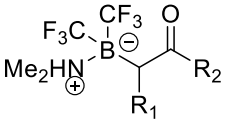

1.30

Burger (1996)

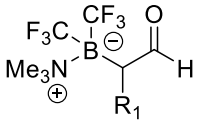

1.31

Burger (1999)

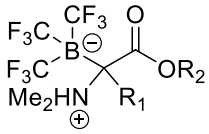

1.32

Yudin (2011)

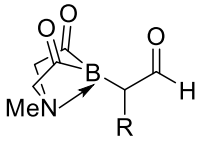

1.33

Burke (2011)

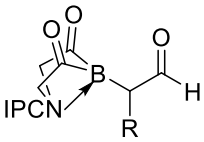

1.34

Curran (2013)

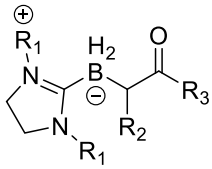

1.35

Zhou (2013)

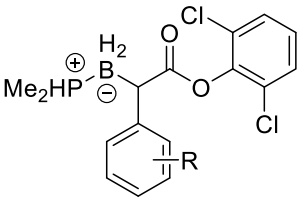

1.36

Yudin (2018)

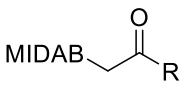

1.37

Zhang (2023)

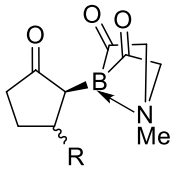

1.38

Figure 1.5: Quaternized BC Enolates.

[49] Sucrow, W.; Zühlke, L.; Slopianka, M.; and Pickardt, J. *Chem. Ber.* **1977**, *110*, 2818-2833.

In 1979, Paetzold isolated a bridged enolate (**1.29**) that isomerized from oxygen to carbon.[50] Burger and co-workers synthesized three quaternized BC enolates using esters (**1.32**), aldehydes (**1.31**), or ketones (**1.30**).[51] In 2011, Burke[52] and Yudin[44] simultaneously published their findings which used a 1,2-boryl migration to open an epoxide to access a BC enolate. Burke and co-workers were able to perform a deuterium-labeling study that showed the rearrangement of boron through a 1,2-boryl migration to form product **1.34**. They were also able to use the quaternized BC enolate to perform carbonyl chemistry where the PIDA or MIDA boron entity remained intact. Yudin and co-workers concluded the BO to BC isomerization occurs through a 1,3-boryl shift with a barrier of ~11 kcal/mol.[53] In 2013, Curran[54] and Zhou[55] both reported the preparation of BC enolates via metal carbene intermediates. Curran and co-workers used NHC-boranes with rhodium carbenes to access **1.35**. Zhou and co-workers use phosphine-boranes for B-H bond insertion into carbenes via copper (Cu)-catalysis to generate product **1.36**. In 2018, Yudin and co-workers expanded the substrate scope for their quaternized BC enolates beyond aldehydes to make ketone **1.37**.[56] Finally in 2023, Zhang and co-workers generated cyclic substrates that included quaternized BC enolates (**1.38**).[57]

---

[50] Paetzold, P. and Kosma, S. *Chem. Ber.* **1979**, *112*, 654-662.
[51] (a) Ansorge, A.; Vrauer, D.J.; Bürger, H.; Hagen, T.; and Pawelke, G. *J. Organomet. Chem*. **1993**, *444*, 5-14. (b) Brauer, D.J.; Bürger, H.; Dittmar, T.; and Pawelke, G. *Chem. Ber.* **1996**, *129*, 1541-1545. (c) Brauer, D.J.; Bürger, H.; Buchheim-Spiegel, S.; and Pawelke, G. *Eur. J. Inorg. Chem* **1999**, *1999*, 255-261.
[52] Li, J. and Burke, M.D. *J. Am. Chem. Soc***. 2011**, *133*, 13774-13777.
[53] St. Denis; J.D.; He, Z.; and Yudin, A.K. *ACS Catal.* **2015**, *5*, 5373-5379.
[54] Li, X. and Curran, D.P. *J. Am. Chem. Soc.* **2013**, *135*, 12076-12081.
[55] Cheng, Q.-Q.; Zhu, S.-F.; Zhang, Y.-Z.; Xie, X.-L.; and Zhou, Q.-L. *J. Am. Chem. Soc.* **2013**, *135*, 14094-14097.
[56] Corless, V.B.; Holownia, A.; Foy, H.; Mendoza-Sanchez, R.; Adachi, S.; Dudding, T.; and Yudin, A.K. *Org. Lett.* **2018**, *20*, 5300-5303.
[57] Zheng, Y.; Jiang, J.; Li, Y.; Wei, Y.; Zhang, J.; Hu, J.; Ke, Z.; Xu, X.; and Zhang, L. *Angew. Chem. Int. Ed.* **2023**, *62*, e202218175.

1.3.2.2 Unquaternized Boron-Carbon Enolates

Unquaternized BC enolates can also be prepared but are studied less compared to quaternized BC enolates due to their increased ability to isomerize. In unquaternized BC enolates, the boron has the potential to engage in organoboron chemistry. Prior to 2023, there were only four isolated and characterized BC enolates (Figure 1.6). These BC enolates have only been hypothesized as intermediates in reactions until 2001, when Abiko and co-workers showed the first isolation and characterization of a BC enolate (**1.39**), albeit as a 7:1 mixture of BC:BO enolate.[58]

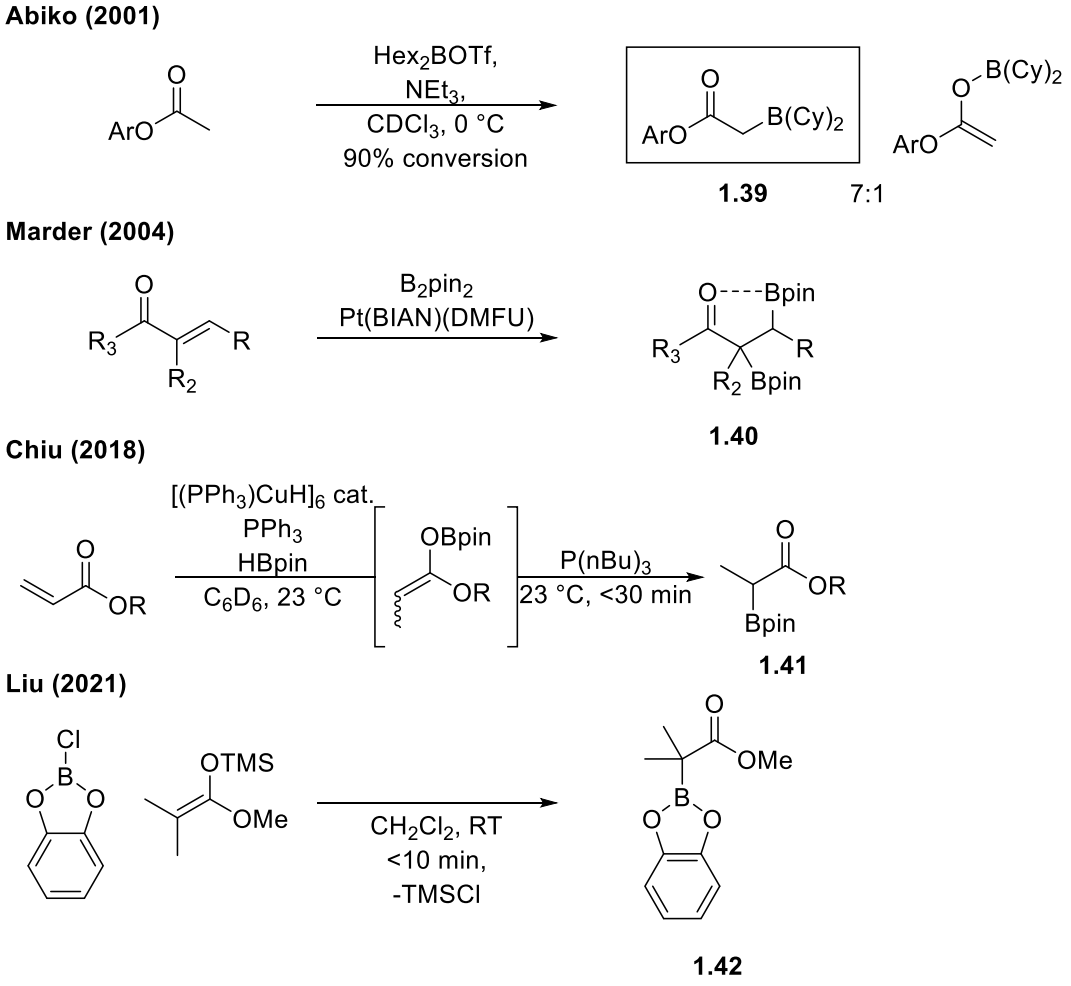

[58] Abiko, A.; Inoue, T.; and Masamune, S. *J. Am. Chem. Soc.* **2002**, *124*, 10759-10764.

Figure 1.6: Syntheses of Unquaternized BC Enolates.

Marder and co-workers isolated and characterized **1.40** in 2004.[59] This BC enolate was synthesized through a diboration of an enone where the β-Bpin group coordinates to the carbonyl oxygen to help stabilize the product for isolation. They determined that the isolated BC enolate is stable in air but observed slow hydrolysis with water.

Chiu and co-workers reported **1.41** in 2018.[45] Chiu and co-workers obtained the desired BC enolate through Cu-catalyzed hydroboration where they initially observed and characterized the BO enolate. Upon the addition of tributylphosphine ($PnBu_3$), a 1,3-isomerization from BO to BC occurred. The rate of isomerization is positively correlated with ligand nucleophilicity and negatively correlated with an increase in ligand sterics. A control experiment without copper was conducted, and no reaction occurred, so it was assumed that copper is needed to form the desired BC enolate.

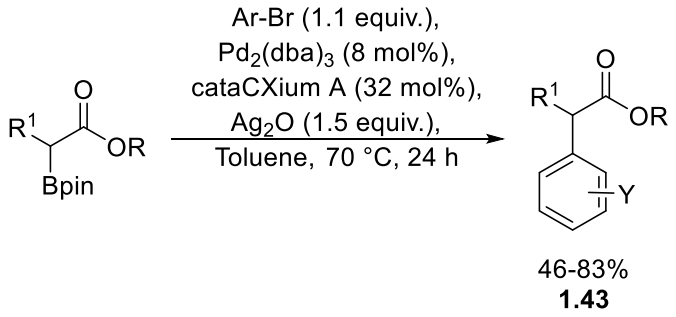

Scheme 1.6: Suzuki Cross-Coupling Reaction using an Unquaternized BC Enolate.

Chiu and co-workers were also able to show the first examples of BC enolates engaging in organoboron functionalization chemistry. The BC enolate was prepared and immediately subjected to an anhydrous cross-coupling reaction without isolation

[59] Bell, N.J.; Cox, A.J.; Cameron, N.R.; Evans, J.O.; Marder, T.B.; Duin, M.A.; Elsevier, C.J.; Baucherel, X.; Tulloch, A.A.D.; and Tooze, R.P. *Chem. Commun.* **2004**, 1854-1855.

(Scheme 1.6). The scope of aryl bromides electrophiles included electron-withdrawing groups at the *para*-position and electron-donating groups at the *ortho*, *meta*, and *para*-positions. To assess the competency of the BC enolate in the reaction, they isolated the enolate and subjected it to the cross-coupling reaction. This was done to rule out the BO enolate engaging in the reaction via a Curtin-Hammett scenario, in which the BC and BO enolate would be in rapid equilibrium. The corresponding BO enolate did not produce the cross-coupling product under otherwise identical reaction conditions. Stereospecific oxidation utilizing their BC enolate was achieved to finish **1.44** (Scheme 1.7). For the oxidation, an anhydrous oxidant was used to afford the desired product in an 8.3:1 d.r. with the syn being the major diastereomer.

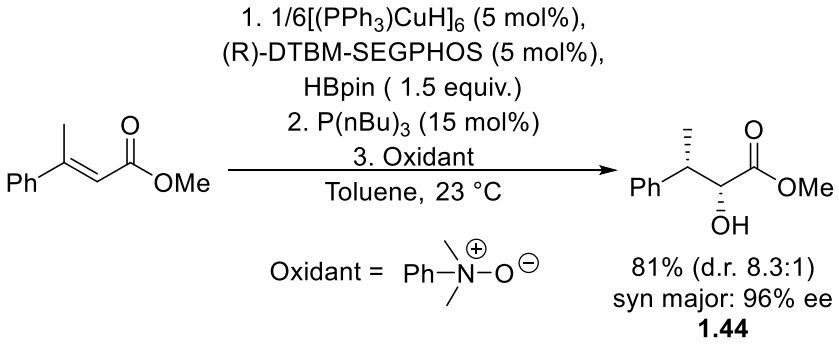

Scheme 1.7: Stereospecific Oxidation of Unquaternized a BC Enolate.

In 2021, Liu and co-workers characterized BC enolate (**1.42**) with catechol borane. A crystal structure of the BC enolate was obtained and calculations were performed to determine the mechanism of its formation.[60] A stepwise mechanism for the formation of **1.42** was proposed. The use of 1,2-azaborine as the organoboron analog in unquaternized BC enolates was proposed as an extension of this chemistry. This would

[60] Wang, Z.; Lamine, W.; Miqueu, K.; and Liu, S.-Y. *Chem. Sci.* **2023**, *14*, 2082-2090.

expand the scope of functionalization of boron in 1,2-azaborine as well as expanding research for unquaternized BC enolates.

1.4 Alpha-Borylcarbonyl Compounds Containing 1,2-Azaborine

1.4.1 Initial Investigations

Jason Wu began the initial investigations into synthesizing BC enolates containing 1,2-azaborine. Initially, metal enolates were surveyed to form BC enolates by utilizing 1,2-azaborine electrophiles. Two different types of metals were screened: alkali metals and transition metals. The alkali metals that were investigated were lithium,[61] sodium, and potassium enolates.[62] However, these metal enolates were not compatible with 1,2-azaborine due to decomposition of 1,2-azaborine or a BO species forming. Palladium,[63] tin,[64] copper,[65] iron,[63] and zinc[66] enolates of methyl 2-bromoacetate were also investigated and did not afford the desired product. Different solvents, temperatures, reaction times, and ester substrates were investigated but the desired BC enolate product was not obtained. It was concluded that metal enolates were not feasible precursors for the synthesis of a BC enolate containing 1,2-azaborine. Instead, the desired BC enolate was successfully prepared using silylketene acetals (SKAs) and an N-TBS, B-OTf 1,2-azaborine electrophile.

---

[61] Juaristi, E.; Beck, A.K.; Hansen, J.; Matt, T.; Mukhopadhyay, T.; Simson, M.; and Seebach, D. *Synthesis* **1993**, *12*, 1271-1290.
[62] Hudrlik, P.F. and Takacs, J.M. *Org. Chem.* **1978**, *43*, 3861-3865.
[63] Sullivan, B.P. and Meyer, T.J. *Organometallics* **1986**, *5*, 15000-1502.
[64] Mukaiyama, T. and Kobayashi, S. (**2004**). Tin(II) Enolates in the Aldol, Michael, and Related Reactions. In Organic Reactions, (Ed.). https://doi.org/10.1002/0471264180.or046.01
[65] Chattopahdyay, A. and Dubey, A.Kr. *J. Org. Chem.* **2007**, *72*, 9357-9359.
[66] Sailer, M.; Dubicki, K.I.; and Sorensen, J.L. *Synthesis* **2015**, *47*, 79-82.

1.4.2 Synthesis and Characterization of BC Enolate

The discovery of the first BC enolate containing 1,2-azaborine was enabled by the synthesis of the super electrophilic 1,2-azaborine containing B-OTf (**1.45**).[21] A silylketene acetal (**SKA1**) was able to react to achieve the finish product (**1**) (Scheme 1.8). However, the isolation of this compound was challenging. The BC enolate (**1**) decomposed when subjected to silica gel column chromatography (both open to air and under inert atmosphere). Compound **1** was successfully isolated by distillation under reduced pressure when heated with a 145 ºC oil bath.

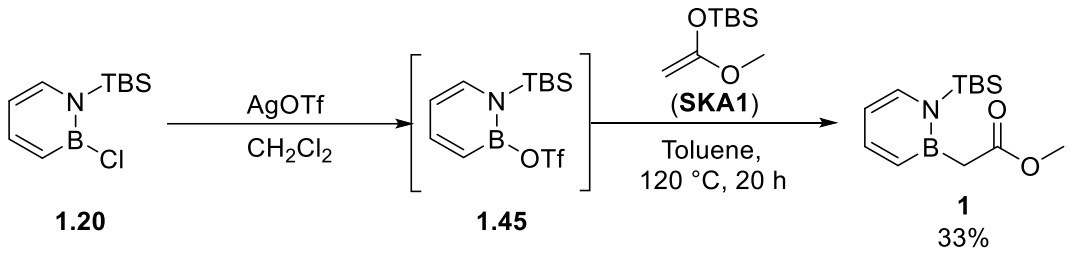

Scheme 1.8: Synthesis of Achiral BC Enolate (**1**) containing 1,2-Azaborine.

Compound **1** was characterized by ^{1}H NMR, ^{13}C NMR, IR, and high-resolution mass spectrometry (HRMS). The enolate (**1**) was compared to the all-carbon analog methyl phenylacetate (**1.46**) (Figure 1.7) using a variety of spectroscopic techniques. The stretching frequency for the CO bond was analyzed using IR spectroscopy. The CO stretching frequency for **1** was observed as weaker than **1.46**[67] which may be due to the BC σ-bond donating to the CO π^{*}-orbital.

[67] (a) Brown, T.L. and Darensbourg, D.J. *Inorg. Chem.* **1967**, *6*, 971-977. (b) do Amaral, A.T. and do Amaral, L. *J. Org. Chem.* **1976**, *41*, 1623-1627.

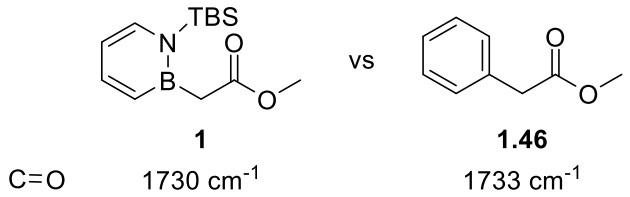

Figure 1.7: Comparison of CO Stretching Frequencies from IR Spectroscopy.

Single crystals suitable for x-ray diffraction were grown from pentane at –20 ºC for 24 hours and analyzed by Bo Li, Ph.D. (Figure 1.8, See Experimental Section). The bond length of B-C_1 is 1.604(2) Å which is longer than the expected B-C_1 bond length of the two previous BC enolate crystal structures (1.578 Å),[45,58] while the C_1-C_2 is 1.491(2) Å is shorter than the expected C_1-C_2 bond length of the two previous BC enolate crystal structures (1.519 Å, Figure 1.8)[45,58]. This is consistent with the C_1-C_2 bond having double bond character. As a result of B-C_1 σ-bond donation to the π^*-orbital of the C_2-O bond (1.200(2) Å, Figure 1.8). Yuping Dai, a collaborator at the University of Pau, was able to compare the experimental data collected for the bond lengths to the calculated bond lengths with reasonable agreement observed (See Experimental Section, Figure 1.19).

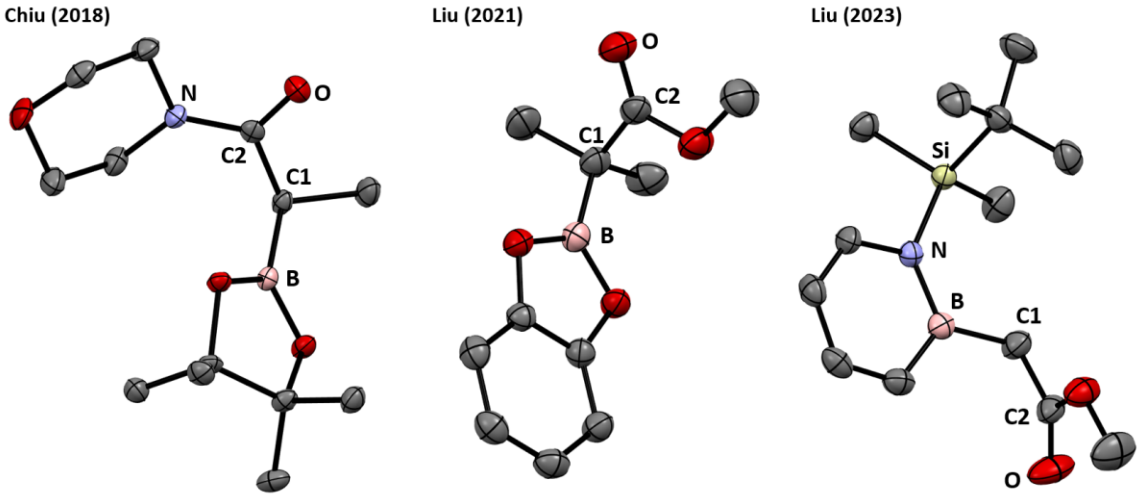

Figure 1.8: X-ray Structures of Unquaternized BC Enolates**.**

Compound **1** was also compared to the BO enolate which was synthesized using a Reformatsky-type reaction (Scheme 1.9).[56] 1,2-Azaborine derivative **1.20** reacts with zinc and methyl 2-bromoacetate to produce product **1.47** in 6.7% isolated yield. The BO enolate was characterized and was compared to BC enolate using IR spectroscopy (Figure 1.9). One key observation while looking at the IR spectra is the absence of a C=O stretch in compound **1.47** while **1** has a peak at 1730 cm^{-1}. This is consistent with an O-bound enolate.

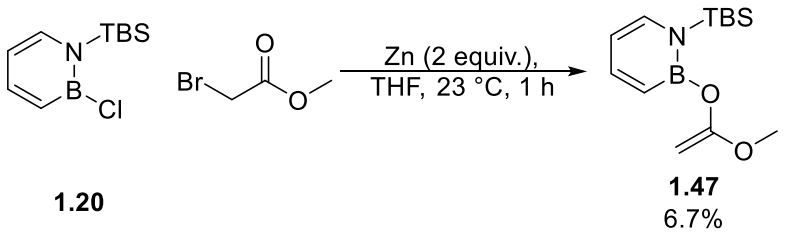

Scheme 1.9: Synthesis of BO Enolate containing 1,2-Azaborine

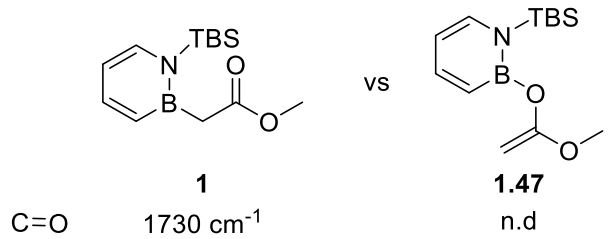

Figure 1.9: Comparison of CO Stretching Frequencies for BC and BO Enolate.

1.4.3 Optimization

The conditions for the preparation of unquaternized BC enolates containing 1,2-azaborine were investigated next. The preparation of BC enolates was evaluated by Aimee Henderson, my undergraduate mentee, and myself. The reactions were run in J-young NMR tubes, and the reactions were monitored by ^{1}H NMR in the presence of an

internal standard hexamethylbenzene (Table 1.1). Switching the solvent from toluene to THF or 1,1,2,2-tetrachloroethane or benzene provided little to no desired product (Table 1.1 entries 1-4). It was determined that toluene is the optimal solvent for this reaction. Next, the temperature was screened. Reaction temperatures of 110 ºC and 130 ºC were found to be inferior to the standard temperature of 120 ºC with a significant decrease in yield (entries 5 and 6 vs. entry 1). So, we concluded that the standard conditions in entry 1 are the optimal conditions for BC enolate formation.

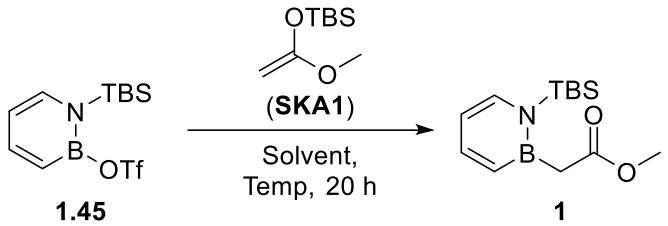

1.45 **1**

Entry	Solvent	Temp (°C)	Yield[a] (%)
1	Toluene-d8	120	80
2	THF-d8	120	0
3	1,1,2,2-tetrachloroethane-d2	120	0
4	Benzene-d6	120	<5
5	Toluene-d8	110	44
6	Toluene-d8	130	45

[a]NMR yield determine by internal standard hexamethylbenzene

Table 1.1: Optimization of Conditions for the Synthesis of Achiral BC Enolate.

1.4.4 Reaction Scope

A series of SKAs were prepared with different substituents on the α-carbon of the enolate as well as different silyl groups. First, **1.49** was tested with the standard conditions, but the major product was the BO enolate. SKA **1.50**, which contains a

bulkier silyl group, was then subjected to the standard conditions and a mixture of BC and BO enolates were observed by ^{1}H NMR with a 1:1 ratio of BC:BO enolate (Figure 1.10). We; therefore, hypothesized that the larger the silyl group is, the higher the preference for the BC enolate to form. With this in mind, SKAs **1.51**, **1.52**, and **1.53** were prepared and subjected to the standard conditions. We did not observe a clear pattern relating to the sterics of the silyl group's influence on the ratio of BC vs. BO enolate formation. These reactions all provided a mixture of the BC and BO enolate, which we were unable to separate via vacuum distillation.

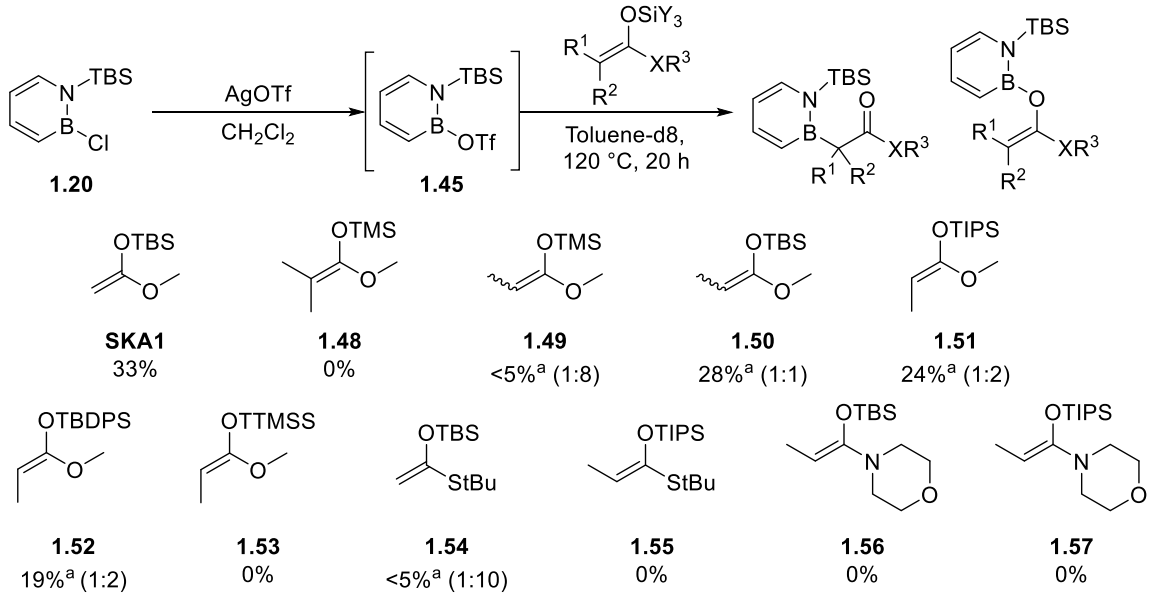

[a]Yield from internal standard, dibromomethane. [b]Ratio of BC:BO enolates within parentheses

Figure 1.10: Scope of BC Enolates.

When the α-position is di-substituted (**1.48**), the reaction doesn't produce the desired BC enolate. We observed almost exclusive BO enolate formation, consistent with our hypothesis that steric factors play a large role in the enolate formation. In addition to SKAs, silyl thioacetals (**1.54**, **1.55**) and silyl ketene acetamides (**1.56**, **1.57**) were

screened without success. Currently, the reaction is only compatible with unsubstituted or mono-α-substituted SKAs.

We next turned our attention to preparing enriched chiral α-BC enolate **1.58** (Scheme 1.10). Unfortunately, the use of SKAs was not a good route for enantioselective synthesis. We also attempted to employ hydrozirconation,[68] dehydrogenative borylation,[18] Grignard addition,[69] turbo Grignard addition,[70] and Reformatsky-type reaction[64] for the preparation of chiral α-1,2-azaborine BC enolates. None of these reactions provided the desired BC enolate. Instead, no reactivity was observed, or the BO species was formed as the sole product.

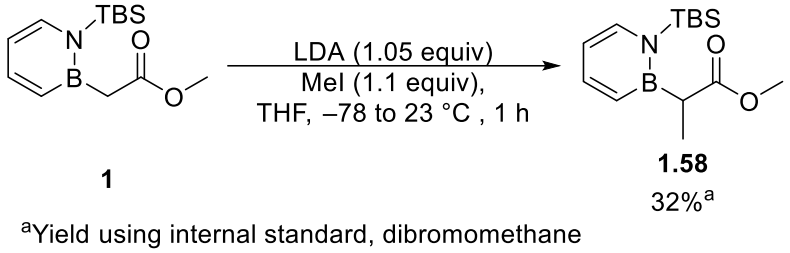

Scheme 1.10: Initial Synthesis via Methylation of Achiral BC Enolate (**1**).

We next attempted to functionalize the simplest BC enolate by methylation at the α-position.[71] The goal would be to form the racemic BC enolate, then separate the enantiomers using chiral HPLC. In initial results, we were able to determine through crude ^{1}H NMR that the product **1.58** had formed in 32% yield using an internal standard dibromomethane (Scheme 1.10). Purification of the racemic α-methylated BC enolate was attempted by silica gel column in an inert atmosphere glovebox, open to air, and

[68] Zhang, D. and Ready, J.M. *J. Am. Chem.* **2007**, *129*, 12088-12089.
[69] Basson, A.J.; Halcovitch, N.R.; and McLaughlin, M.G. *Chem. Eur. J.* **2022**, *28*, e202201107.
[70] Kraspvskiy, A. and Knochel, P. *Angew. Chem. Int. Ed.* **2004**, *43*, 3333-3336.
[71] Chen, T.; Liu, W.; Gu, W.; Niu, S.; Lan, S.; Zhao, Z.; Gong, F.; Liu, J.; Yang, S.; Cotman, A.E.; Song, J.; and Fang, X. *J. Am. Chem. Soc.* **2023**, *145*, 585-599.

distillation. However, all purification methods were deemed unsuccessful due to the decomposition of the product.

1.4.5 Kinetics Analysis

A mixture of BC and BO enolates were obtained during the synthesis using **1.45** with SKAs and derivatives. We hypothesized that the BC enolate could isomerize to the BO enolate through prolonged exposure to heat suggesting the BO enolate is thermodynamically more stable. We conducted a kinetic study where concentration of the BC enolate vs time was plotted at 170 ºC (J-young NMR tube set up containing compound **1** with hexamethylbenzene as the internal standard in ODCB-d4). The kinetic data were collected until there was 17% of compound **1** remaining. A clean conversion to BO enolate was observed. The data was analyzed by plotting, ln(concentration) vs time to determine if the isomerization is first order (Figure 1.11). The linear fit was consistent with a first order isomerization process. On the other hand, when the data was fit for second order kinetics, the data was not linear, again supporting first order kinetics for the isomerization of BC to BO enolates.

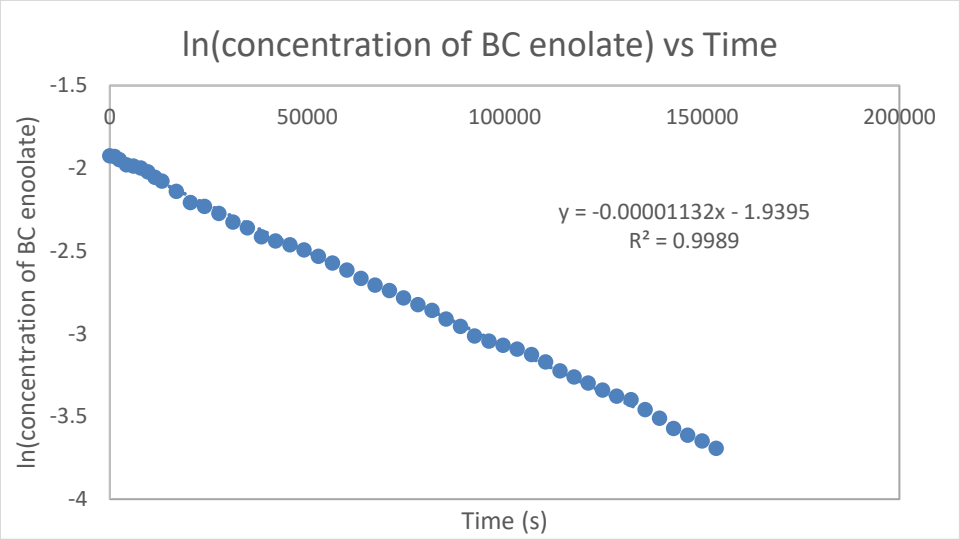

Figure 1.11: Kinetics of Isomerization from BC Enolate to BO Enolate.

Additional rate experiments were performed to further support the first order isomerization mechanism. A "differential rate law experiment" was conducted to further establish the reaction order in BC enolate. This experiment was done with four different concentrations of BC enolate **1** in ODCB-d4 and internal standard hexamethylbenzene in J-young NMR tubes that were heated to 170 ºC. Initial kinetics data were collected by stopping the isomerization at no more than 30% decay of compound **1**. As the isomerization was believed to be first order, the ln(concentration of BC enolate) vs time was plotted as a fitting model to determine the rate constant, k, from the slope of the trendline. Once the rate constant was determined, log(reaction rate) vs log(initial concentration of BC enolate) was plotted where the slope of the trendline corresponds to the order of the reaction (Figure 1.12). The slope of the line is 0.8122, which is more consistent with a first order isomerization process.

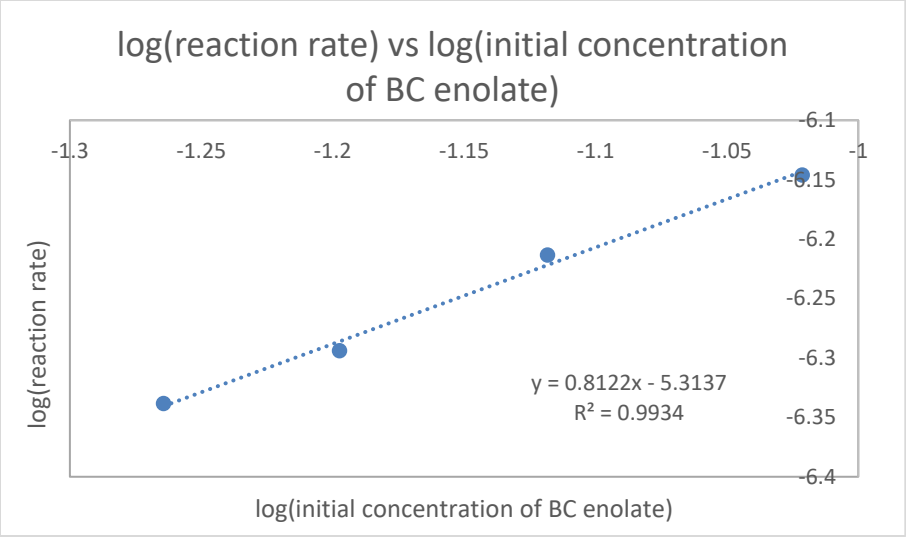

Figure 1.12: Determination of the Reaction Order of the BC to BO Enolate Isomerization Process by Evaluating the Concentration Dependence of the Reaction Rate.

A control experiment was performed to determine if the isomerization occurs at room temperature. Over a period of four days at room temperature the isomerization only proceeded about 3% indicating that isomerization needs heat to occur (Figure 1.13). This observation is consistent with the BC enolate being kinetically stable. The second control experiment was to confirm the reproducibility of the initial rate law data collected for determining the order of isomerization at a given concentration (See Experimental Section, Figure 1.18). We concluded the isomerization kinetics were reproducible with two additional trials at the same temperature and same time providing kinetics data in agreement with each other.

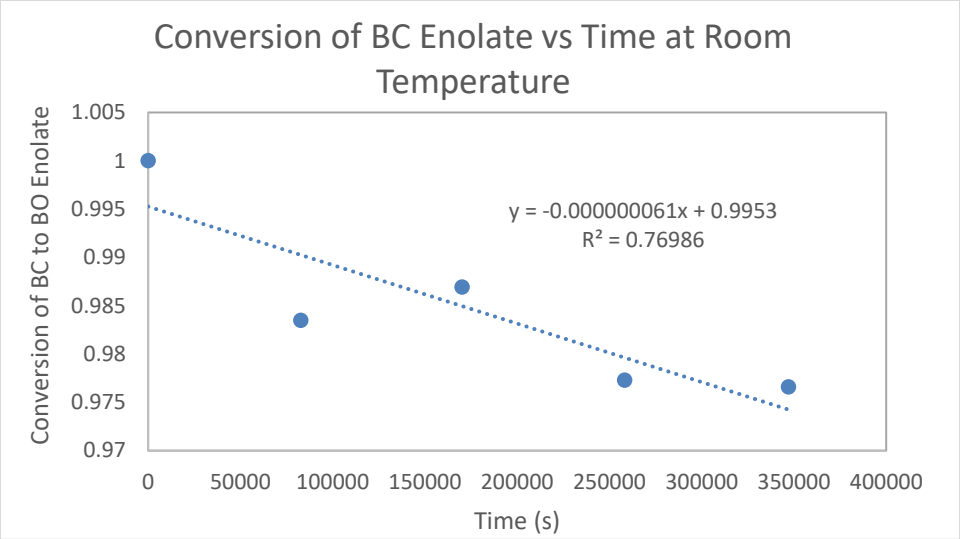

Figure 1.13: Isomerization Control Experiment at Room Temperature.

In addition to the determination of the order of the isomerization, an Eyring analysis was performed.[72] The activation free energy, $\Delta G^{\ddagger}$, activation enthalpy, $\Delta H^{\ddagger}$, and activation entropy, $\Delta S^{\ddagger}$, were determined experimentally. The $\Delta G^{\ddagger}$, $\Delta H^{\ddagger}$, and $\Delta S^{\ddagger}$ were determined as 27.57 kcal/mol, 10.63 kcal/mol, and -56.80 e.u., respectively (Table 1.2). These activation parameters were obtained by using the average rate constants from three separate trials. To determine the parameters, three trials were completed at five different temperatures and the initial kinetics of the decay of the BC enolate until no more than 30% conversion was collected. An average Eyring plot was prepared, where the relationship of plot ln(k/T) vs 1/T is plotted and where k is the average rate constants and T is temperature in Kelvin (Figure 1.14). The $\Delta H^{\ddagger}$ and $\Delta S^{\ddagger}$ can be obtained by the Eyring plot from the slope and y-intercept, respectively. We note that entry 2 in Table 1.2 might be an outlier. Additional data points will need to be collected to further substantiate the numbers.

[72] Eyring, H. *J. Chem. Phys.* **1935**, *3*, 107-115.

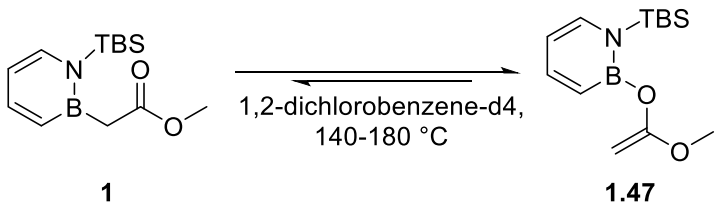

1 **1.47**

Trial	$\Delta H^{\ddagger}$ (kcal/mol)	$\Delta S^{\ddagger}$ (e.u)	$\Delta G^{\ddagger}$ (kcal/mol)
1	12.93	-51.64	28.33
2	9.352	-59.77	27.17
3	12.67	-52.57	28.35
Avg.	**10.63**	**-56.80**	**27.57**

Table 1.2: Activation Parameters for the Isomerization of BC to BO Enolate.

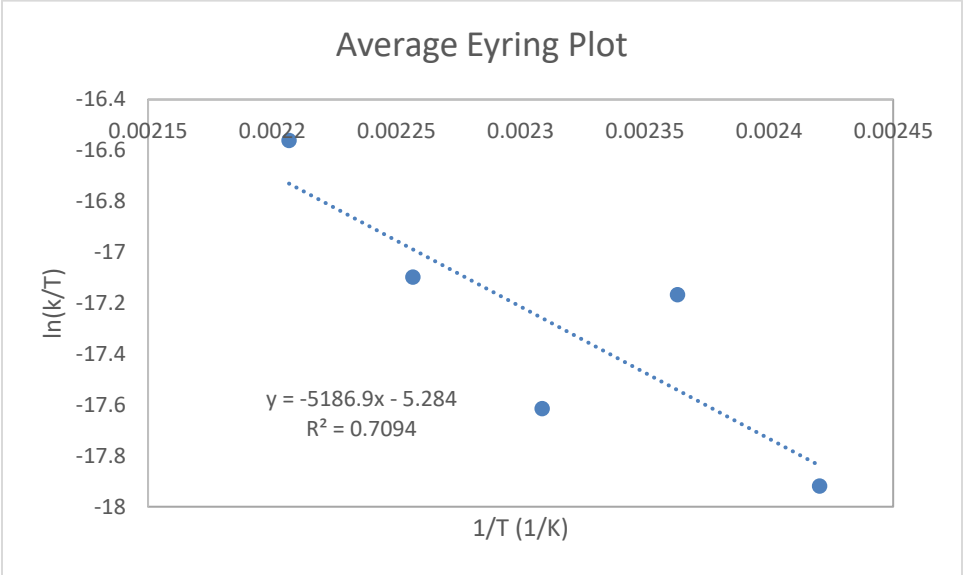

Figure 1.14: Average Eyring Plot for Enolate Isomerization.

Our collaborators at University of Pau also calculated the energy barriers for the isomerization at two different temperatures: 298.15 K (room temperature, green) and 443.15 K (170 ºC, orange) (Figure 1.15). These free energy values (ΔG in kcal/mol) were computed at SMD(o-DiChloroBenzene)-M06-2X/Def2-tzvp level of theory. The activation parameters at both temperatures were also calculated. At room temperature, $\Delta G^{\ddagger}$ is 29.9 kcal/mol, $\Delta H^{\ddagger}$ is 28.5 kcal/mol, and $\Delta S^{\ddagger}$ is -46.81 e.u. In addition, BO enolate

1.47 was found to be lower energy than **1**. At 170 ºC, $\Delta G^{\ddagger}$ is 30.1 kcal/mol, $\Delta H^{\ddagger}$ is 28.3 kcal/mol, and $\Delta S^{\ddagger}$ is -38.85 e.u. While there is sufficient agreement between theory and experiment for $\Delta G^{\ddagger}$; theory and experiment are not in alignment for $\Delta H^{\ddagger}$ and $\Delta S^{\ddagger}$. More experiments and calculations need to be done to refine the values. A first order isomerization should align with a unimolecular mechanism. The transition state for unimolecular mechanism for the BC to BO isomerization is illustrated in Figure 1.15. We proposed that the isomerization occurs in a concerted transition state as opposed to a step-wise transition state mechanism, which agrees with our observed kinetic data.

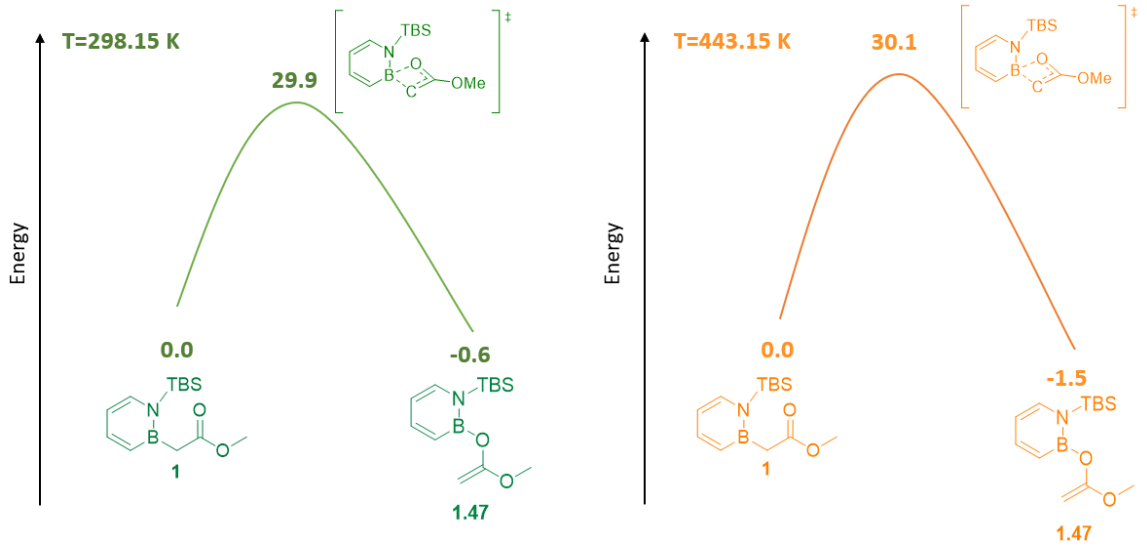

Figure 1.15: Comparison of Energy Barriers at Different Temperatures**.**

1.4.6 Reaction Derivatization

Derivatization of **1** was sought out to be used in organoboron chemistry. The first type of reaction that compound **1** was subjected to was oxidation. Both aqueous and anhydrous conditions were used; however, none of the attempted reaction conditions that

were tried afforded the desired alcohol. We first attempted a protocol from Liu and co-workers[73] using di-tert-butyl peroxide and n-dodecane with the idea that boron will have an aliphatic chain as a side product (Scheme 1.11, equation 1). We also subjected **1** to the oxidation conditions developed by Chiu and co-workers[45] where they used anhydrous conditions to successfully oxidize their BC enolate (**1.41**) (Scheme 1.11, equation 2). Unfortunately, all attempts failed to afford the product, even after nitrogen deprotection and elevated temperature. We also employed conditions that are more common for oxidations of boron. Racherla and co-workers[74] employed oxidation conditions that use hydrogen peroxide and sodium hydroxide at varied the temperature, but we were not able to achieve oxidation of compound **1** under these conditions (Scheme 1.11, equation 3). Another well-known set of conditions is the use of sodium perborate tetrahydrate with water and at varied temperatures (Scheme 1.11, equation 4).[75] Again, these conditions were unsuccessfully applied to **1**. For all the oxidation conditions, we observed decomposition, or no reaction happened with **1** (Scheme 1.11).

[73] Baggett, A.W. and Liu, S.-Y. *J. Am. Chem. Soc.* **2017**, *139*, 15259-15264.
[74] Brown, H.C.; Kulkarni, S.V.; Khanna, V.V.; Patil, V.D.; and Racherla, U.S. *J. Org. Chem.* **1992**, *57*, 6173-6177.
[75] (a) Kabalka, G.W.; Shoup, T.M.; and Goudgaon, N.M. *Tetrahedron. Lett.* **1989**, *30*, 1483-1486. (b) Farthing, C.N. and Marsden, S.P. *Tetrahedron. Lett.* **2000**, *41*, 4235-4238.

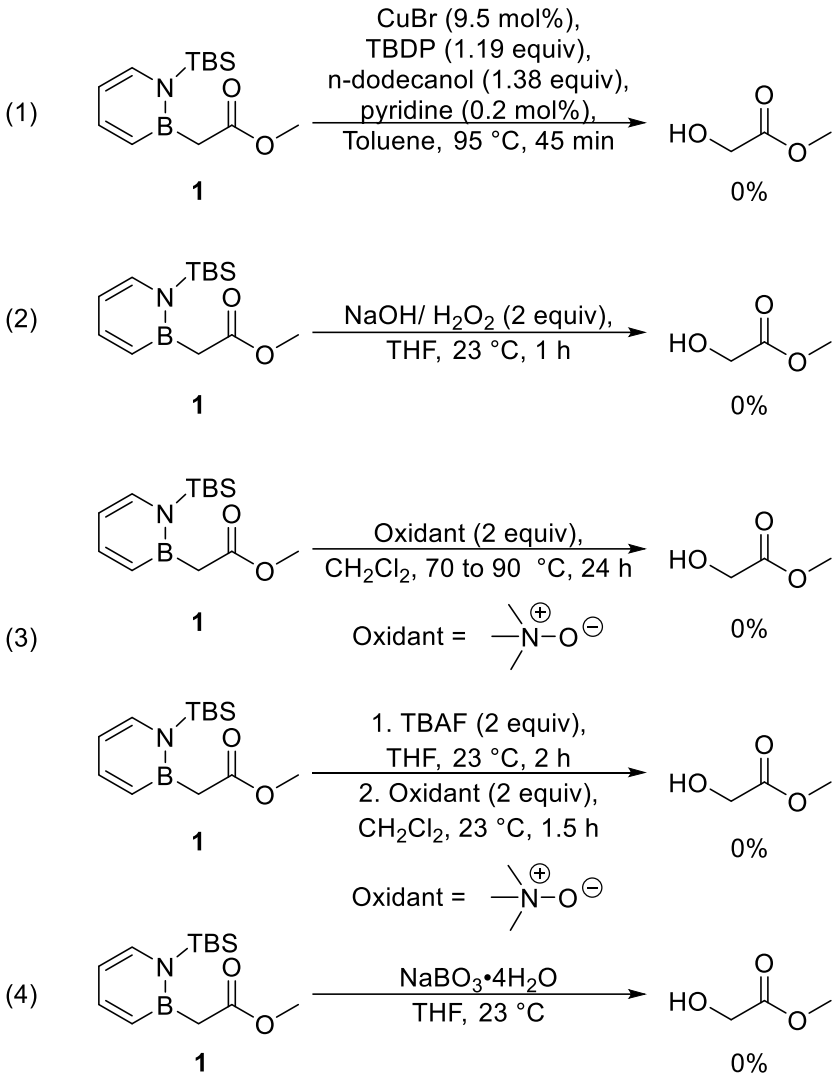

Scheme 1.11: Oxidation Conditions Attempted for BC Enolate **1**

We also attempted to aminate compound **1**. The first set of conditions were from Patridge and co-workers[76] using Chan-Lam amination conditions using aniline, copper (II) acetate, and base. This condition was unsuccessful in forming the aminated product (Scheme 1.12, equation 1). We also attempted amination conditions developed by

[76] Grayson, J.D.; Dennis, F.M.; Robertson, C.C.; and Patridge, B.M. *J. Org. Chem.* **2021**, *86*, 9883-9897.

Singaram and co-workers.[77] Hydroxylamine-O-sulfonic acid was reacted with **1**, but again the amination product could not be obtained (Scheme 1.12, equation 2).

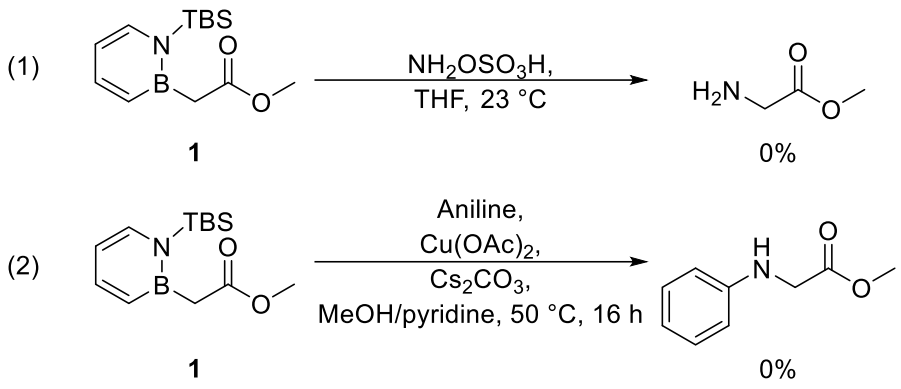

Scheme 1.12: Amination Conditions Attempted for BC Enolate **1.**

We also subjected compound **1** to halogenation and homologation reactions. Aggarwal and co-workers[78] developed an invertive fluorination of aryllithium-activated organoboron compounds using Selectfluor I. These conditions were unsuccessful for halogenating **1** (Scheme 1.13, equation 1). One-carbon homologation conditions were developed by Matteson and co-workers,[79] in which an organoboron compound is treated with an alkyllithium with an α-leaving group. A 1,2-metallate shift occurs to migrate the boron by one carbon. Unfortunately, the Matteson conditions were unsuccessful in the homologation of **1** (Scheme 1.13, equation 2).

[77] Brown, H.C.; Kim, K.-W.; Cole, T.E.; and Singaram, B. *J. Am. Chem. Soc.* **1986,** *108*, 6761-6764.
[78] Sandford, C.; Rasappan, R.; and Aggarwal, V.K. *J. Am. Chem. Soc.* **2015**, *137*, 10100-10103.
[79] Sadhu, K.M. and Matteson, D. S. *Organometallics* **1985**, *4*, 1687-1689.

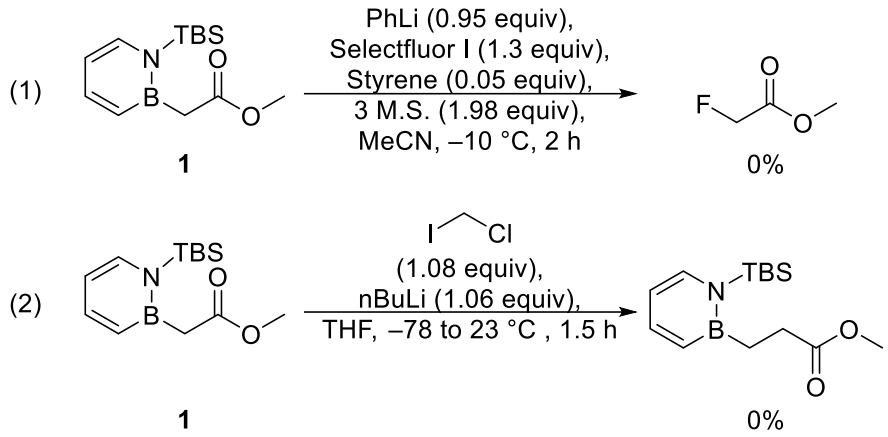

Scheme 1.13: Halogenation and Homologation Conditions Attempted for BC Enolate **1**

Finally, we subjected **1** to Suzuki-Miyaura cross-coupling conditions. The conditions that were attempted were employed by Chiu and co-workers for their BC enolate (**1.41**) (Scheme 1.14).[45] Using palladium as the catalyst, cataXCium A as the ligand, and cesium carbonate as the base, the reaction afforded product **1.46** with 14% yield as determined from the crude ^{1}H NMR with internal standard dibromomethane. However, I did not isolate the product achieved. While bromobenzene was compatible as an electrophile, vinyl bromide was not compatible as an electrophile under these conditions. In Scheme 1.14, we proposed the catalytic cycle for the Suzuki cross-coupling reaction using BC enolate **1**.

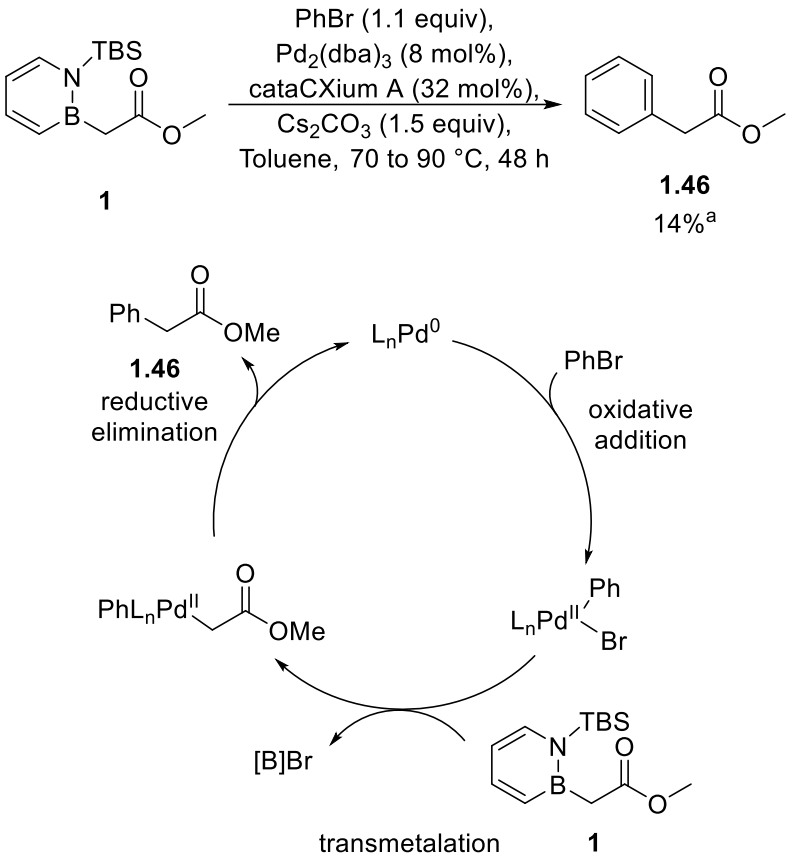

Scheme 1.14: Suzuki Cross-Coupling Reaction using BC Enolate (**1**) and Proposed Catalytic Cycle.

To rule out an alternative mechanism consisting of protodeboronation and enolate arylation, we ran a control experiment that saw no conversion of the coupled product (**1.46**) (Figure 1.17). Thus, product reaction as illustrated in Scheme 1.14 supports the potential of transmetalation of BC enolate **1** (Figure 1.17). The only organoboron functionalization that has provided desired product is Suzuki cross-coupling reaction using bromobenzene.

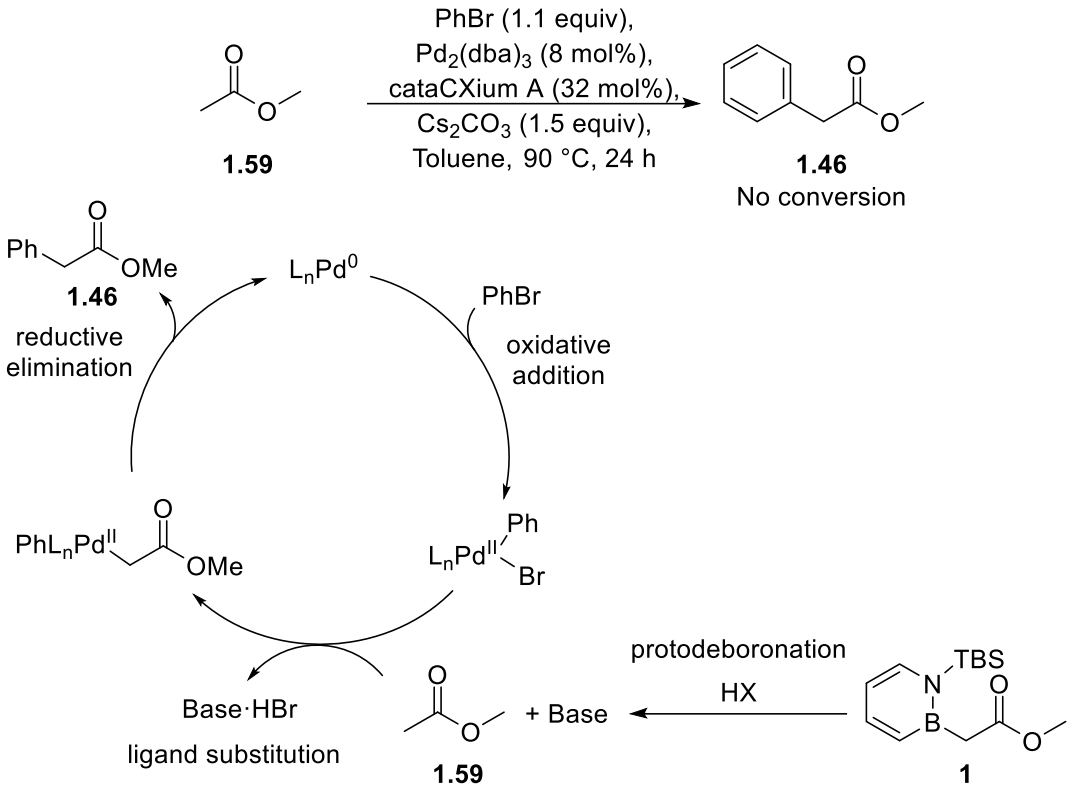

Figure 1.16: Control Experiment using Ester to Determine Potential Mechanism.

1.4.7 Conclusion and Outlook

We synthesized and characterized the first BC enolate (**1**) containing 1,2-azaborine. It was seen through experimental data that the BC enolate isomerizes to the BO enolate through a first order isomerization process. There is a limited scope for the BC enolates containing 1,2-azaborine. When there is mono-α-substitution for the SKAs, there is a mixture of BC and BO enolates that are inseparable. Obtaining a substituted BC enolate containing 1,2-azaborine has shown to be a challenge. Finally, we subjected compound **1** to a variety of organoboron chemistry reactions such as oxidation, amination, halogenation, homologation, and Suzuki cross-coupling. The only

derivatization reaction that showed desired product is the Suzuki cross-coupling reaction. In the future, the scope of the reaction to include stereospecific BC enolates containing 1,2-azaborine and subjecting compound **1** to more organoboron chemistry reactions needs to be explored.

1.5 Experimental Section

1.5.1 General Information

All oxygen- and moisture-sensitive manipulations were performed in oven-dried glassware using either standard Schlenk line techniques or in a glove box under nitrogen. Cannula or gas tight syringes were used to transfer liquid reagents and solvents in all the reactions. Unless otherwise noted, all reagents were obtained from commercial sources (TCI, Millipore-Sigma Aldrich, Strem, Acros, Oakwood, Fisher) and used as received. Solvents such as diethyl ether, dichloromethane, pentane, and tetrahydrofuran were passed through a neutral alumina column and dispensed from Pure Process Technology solvent purification system under argon.

The following compounds were purified prior to use: $CDCl_3$ was purchased from Cambridge Isotope Laboratories and stored containing 4Å molecular sieves prior to use.

^{1}H, ^{13}C, and ^{11}B NMR spectra were measured on a Varian/Agilent VNMRS DD1 system at 11.7 T (500 MHz) with a 5mm PFG OneNMR probe at 25 °C, using the VJ 4.2 software, or a Bruker AVANCE NEO system at 11.7 T (500 MHz) with a 5mm X-nuclei optimized double resonance BBO-H&F Prodigy (N2) CryoProbe or BBFO (He) CryoProbe and sample case, using Topspin 4.1, at the Boston College nuclear magnetic resonance facility. All NMR chemical shifts are reported in ppm; coupling constants are

reported in Hz. ^{1}H and ^{13}C spectra were internally referenced to residual solvent peaks (^{1}H $CDCl_3$: d = 7.26 ppm, toluene-d8: s = 2.08 ppm, ODCB-d4: s = 7.19 ppm; ^{13}C $CDCl_3$: d = 77.16 ppm) and 11B spectra were externally referenced to a standard of BF_3•Et_2O (δ = 0.0 ppm). In ^{13}C NMR analysis, peaks for carbon atoms adjacent to a boron center were generally not observed owing to quadrupolar broadening.

All IR spectra were measured on a Bruker Alpha-P FT-IR equipped with a single crystal diamond ATR module, and values are reported in cm^{-1}.

High-resolution mass spectrometry (HRMS) data were generated in Boston College facilities using direct analysis in real-time (DART) on a JEOL AccuTOF DART spectrometer with the assistance of the director.

Single-crystal X-ray diffraction data were generated in Boston College facilities from measurements with a Bruker Kappa Apex Duo fully automated diffractometer with the assistance of the director.

1.5.2 Procedure for Syntheses

1.5.2.1 Procedure for the Synthesis of 1,2-Azaborine

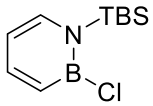

1.20 CAS # 1138164-75-6

1,2-azaborine **1.20** is synthesized according to published procedure.[17,80]

[80] McConnell, C.R.; Haeffner, F.; Baggett, A.W.; and Liu, S.-Y. *J. Am. Chem. Soc.* **2019**, *141*, 9072-9078.

1.5.2.2 Procedure for the Synthesis of BC Enolate (1) containing 1,2-Azaborine

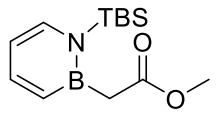

1

Step 1: To an oven-dried 50 mL round-bottom flask with magnetic stir bar, trifluormethylsulfonyloxysilver (1.90 g, 7.38 mmol, 1.89 equiv.) in dichloromethane (20 mL) was added in the glovebox filled with nitrogen. To the reaction flask, 1,2-azaborinetert-butyl-(2-chloroazaborinin-1-yl)-dimethyl-silane (889.3 mg, 3.910 mmol, 1.0 equiv.) was added dropwise at room temperature. The reaction mixture was allowed to stir for one hour. After one hour, the reaction was deemed complete by ^{11}B NMR.

Step 2: In a nitrogen filled glovebox, the crude product was washed with pentane, passed through an acro disc, and then concentrated under vacuum. The concentrated mixture was dissolved in toluene (18 mL). A pressure vessel fitted with a stir bar was charged with tert-butyl-(1-methoxyvinyloxy)-dimethyl-silane (SKA) (735.3 mg, 3.900 mmol, 0.0999 equiv.). The NTBS-BOTf-1,2-azaborine solution was added to the SKA at room temperature. The pressure vessel was fitted with a screw cap and brought outside the glovebox. The pressure vessel was placed in an oil bath at 120 ºC for 20 h. At the conclusion of reaction, the mixture was concentrated under vacuum in the glovebox. The crude mixture was purified via fractional vacuum distillation at an oil bath temperature of 145 ºC, and then the collected fraction was recrystallized using pentane and placed in the freezer to obtain the desired product. Methyl 2-[1-[tert-butyl(dimethyl)silyl]azaborinin-2-yl]acetate (**1**, colorless solid). **^{1}H NMR** (500 MHz, $CDCl_3$) δ 7.54 (dd, *J* = 11.1, 6.3 Hz, 1H), 7.29 (d, *J* = 6.7 Hz, 1H), 6.70 (dd, *J* = 11.1, 1.6 Hz, 1H), 6.32 (dd, *J* = 6.5, 1.5 Hz,

1H), 3.68 (s, 3H), 2.56 (s, 2H), 0.93 (s, 9H), 0.49 (s, 6H). **^{13}C NMR** (125 MHz, $CDCl_3$) δ 175.42, 143.76, 138.39, 128.90, 111.76, 51.36, 30.33, 26.37, 19.11, -1.67. **IR** ν 3070, 2953, 2931, 2888, 2859, 1730, 1608, 1510, 1472, 1457, 1435, 1394, 1363, 1263, 1175, 1135, 1117, 1135, 1117, 1062, 1023, 890, 787, 691, 575 cm^{-1}. **^{11}B NMR** (160 MHz, $CDCl_3$) δ 38.05. **HRMS** (DART) calcd. for $C_{13}H_{25}BNO_2Si$ [$M+H^+$]: 265.1669, found 266.1742.

1.5.2.3 Procedure for the Synthesis of BO Enolate containing 1,2-Azaborine

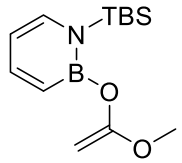

1.47

To an oven-dried round-bottom flask, zinc (287.3 mg, 4.390 mmol, 2.0 equiv.) and CuI (41.8 mg, 0.220 mmol, 0.1 equiv.) in THF (8 mL) was added followed by methyl 2-bromoacetate (672.1 mg, 4.39 mmol, 2.0 equiv.) dropwise in a nitrogen glovebox. Then tert-butyl-(2-chloroazaborinin-1-yl)-dimethyl-silane (**1.20**) (500.0 mg, 2.20 mmol, 1.0 equiv.) was added to the mixture, and allowed to stir for one hour at room temperature. At the conclusion of the hour, the reaction was checked by ^{11}B NMR and determined complete. The material was purified using vacuum distillation with an oil bath at 145 ºC. Tert-butyl-[2-(1-methoxyvinyloxy)azaborinin-1-yl]-dimethyl-silane (**1.47**, colorless oil). **^{1}H NMR** (500 MHz, $CDCl_3$) δ 7.50 (dtd, *J* = 13.4, 7.1, 2.7 Hz, 1H), 7.02 – 6.98 (m, 1H), 6.24 (ddd, *J* = 11.7, 1.3, 0.7 Hz, 1H), 5.90 (ddd, *J* = 6.8, 6.1, 1.4 Hz, 1H), 3.65 (s, 2H), 3.44 (d, *J* = 2.7 Hz, 0H), 3.35 (d, *J* = 2.7 Hz, 0H), 0.89 (s, 5H), 0.36 (s, 3H). **^{13}C NMR**

(125 MHz, $CDCl_3$) δ 162.49, 146.12, 138.05, 118.78, 108.44, 62.88, 55.31, 26.63, 18.69, -3.34. **IR** ν 2953.46, 2929.26, 2857.46, 1745.77, 1660.77, 1608.03, 1509.03, 1464.41, 1293.49, 1270.82, 1155.58, 1121.96, 1072.75, 1009.53, 988.29, 840.55, 809.76, 782.65, 733.07, 694.89 cm^{-1}. **^{11}B NMR** (160 MHz, $CDCl_3$) δ 31.47. **HRMS** (DART) calcd. for $C_{13}H_{25}BNO_2Si$ [$M+H^+$]: 265.1669, found 266.1742.

1.5.2.4 Procedures for the Syntheses of Silylketene Acetals

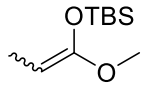

1.50 CAS # 84784-58-7

To an oven-dried round-bottom flask, DIPA (3.42 g, 33.8 mmol, 1.0 equiv.) in THF (25 mL) was added in a glovebox. The flask was brough to a hood where n-BuLi in 2.5M hexanes (2.16 g, 33.8 mmol, 1.0 equiv.) was added at –78 ºC under nitrogen. The resulting mixture was stirred for 30 min before methyl propionate (2.97 g, 33.8 mmol, 1.0 equiv.) was added at –78 ºC dropwise. After 60 min of stirring, the addition of HMPA (3.5 mL) and TBSCl (5.09 g, 33.8 mmol, 1.0 equiv.) in pentane (10 mL) was added to the reaction flask. The reaction was allowed to come to room temperature for 12 hours and then filtered through a pad of celite with pentane in the glovebox. The solution was then concentrated in vacuo and purified via vacuum distillation with an oil bath at 30 ºC.[81] Tert-butyl-[(Z)-1-methoxyprop-1-enoxy]-dimethyl-silane (**1.50**, 10:1 (E:Z), colorless oil).

[81] Denmark, S.E.; Beutner, G.L.; Wynn, T.; and Eastgate, M.D. *J. Am. Chem. Soc.* **2005**, *127*, 3774-3789.

^{1}H NMR (500 MHz, $CDCl_3$) δ 3.67 – 3.63 (m, 0H), 3.54 (s, 1H), 1.49 (d, *J* = 6.6 Hz, 1H), 0.94 (s, 4H), 0.19 – 0.16 (m, 2H).

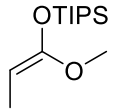

1.51

To an oven-dried round-bottom flask, DIPA (5.74 g, 56.8 mmol, 1.0 equiv.) in THF (115 mL) was added in a glovebox. The flask was brough to a hood where n-BuLi in 2.5M hexanes (3.71 g, 57.9 mmol, 1.02 equiv.) was added at 0 ºC under nitrogen. The resulting mixture was stirred for 30 min before methyl propionate (5.00 g, 56.8 mmol, 1.0 equiv) was added at –78 ºC dropwise. After 90 min of stirring, TIPSOTf (17.74 g, 57.9 mmol, 1.02 equiv) was added to the reaction flask. The reaction was allowed to come to RT for over 2 hours and then filtered through a pad of celite with pentane in the glovebox. The solution was then concentrated in vacuo and purified via vacuum distillation with an oil bath at 30 ºC.[82] Triisopropyl-[(Z)-1-methoxyprop-1-enoxy]silane (**1.51**, 4:1 (E:Z), colorless oil). **^{1}H NMR** (500 MHz, $CDCl_3$) δ 3.72 – 3.65 (m, 0H), 3.63 (s, 1H), 3.59 (s, 1H), 2.33 (q, *J* = 7.2 Hz, 0H), 1.49 (d, *J* = 6.6 Hz, 1H), 1.29 (d, *J* = 7.2 Hz, 1H), 1.25 – 1.14 (m, 2H), 1.14 – 1.03 (m, 14H).

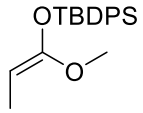

1.52

[82] (a) Zhu, C. and Cook, S.P. *J. Am. Chem. Soc.* **2012**, *134*, 13577-13579. (b) Aben, R.W.M.; Scheeren, H.W. *Tetrahedron Lett.* **1985**, *26*, 1889-1892.

To an oven-dried round-bottom flask with THF (3.6 mL), under nitrogen, KHMDS in 1.0M THF (7.5 mmol) was added at –78 ºC. The reaction mixture was stirred for 30 min, and then methyl propionate (600 mg, 6.81 mmol, 1.0 equiv.) was added. After stirring for another 30 min, TBDPSCl (2.81 g, 10.2 mmol, 1.50 equiv.) was added to the reaction flask. The reaction solution was allowed to RT over two hours. The solution was diluted with pentane. The organic layer was washed with ice-water (3x10 mL) and separated. The organic layer was then dried over sodium sulfate, passed through a funnel with a pad of celite, and concentrated in vacuo. The product was purified via vacuum distillation with an oil bath at 170 ºC.[77] Tert-butyl-[(E)-1-methoxyprop-1-enoxy]-diphenyl-silane (**1.52**, colorless oil). **^{1}H NMR** (500 MHz, $CDCl_3$) δ ^{1}H NMR (500 MHz, $CDCl_3$) δ 7.82 – 7.69 (m, 1H), 7.43 (dtdd, *J* = 10.7, 9.4, 8.1, 4.6 Hz, 1H), 3.50 (qd, *J* = 6.4, 1.9 Hz, 0H), 3.23 (s, *J* = 1.4 Hz, 1H), 1.68 (d, *J* = 6.4, 2.4 Hz, 3H), 1.13 – 1.10 (q, 3H). **^{13}C NMR** (125 MHz, $CDCl_3$) δ 156.72, 135.22, 130.26, 127.87, 54.47, 52.22, 26.51, 20.72, 9.70. **IR** ν 3072.39, 2932.07, 2858.96, 1684.60, 1472.84, 1335.03, 1220.62, 1184.95, 1106.35, 1024.80, 899.86, 821.30, 739.34, 696.94, 610.10, 542.24, 498.61 cm^{-1}. **HRMS** (DART) calcd. for $C_{20}H_{26}O_2Si$ [M+H$^+$]: 326.1702, found 327.1775.

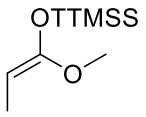

1.53

To an oven-dried round-bottom flask, KHMDS in 1.0M THF (597.7 mg, 3.00 mmol, 1.10 equiv.) was added to THF (2.0 mL) at –78 ºC under nitrogen. The resulting mixture was stirred for 15 min before methyl propionate (240.0 mg, 2.72 mmol, 1.0 equiv) was added. After stirring for 30 min, TTMSSCl (1.00 g, 3.54 mmol, 1.30 equiv.)

in THF (2.0 mL) was added to the reaction flask. The reaction mixture was allowed to warm to RT over 2 hours. Then the solution was diluted with pentane and passed through a pad a celite in the glovebox. The solvent was concentrated in vacuo and then purified via vacuum distillation with an oil bath at 180 ºC.[83] [(Z)-1-methoxyprop-1-enoxy]-tris(trimethylsilyl)silane (**1.53**, colorless oil). **^{1}H NMR** (500 MHz, $CDCl_3$) δ 3.45 (s, 1H), 3.32 (q, *J* = 6.4 Hz, 0H), 1.50 (d, *J* = 6.4 Hz, 1H), 0.18 (s, 9H). **^{13}C NMR** (125 MHz, $CDCl_3$) δ 157.80, 53.97, 49.11, 16.68, -0.19. **IR** ν 2949.52, 2894.34, 1680.57, 1334.72, 1242.78, 1214.85, 1025.20, 827.40, 686.62, 622.60, 508.39 cm^{-1}. **HRMS** (DART) calcd. for $C_{13}H_{35}O_2Si_4$ [$M+H^+$]: 334.1636, found 335.1709.

1.5.2.5 Procedure for the Synthesis of Silyl Thioacetals

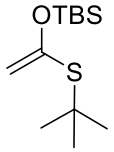

1.54 CAS # 97250-84-5

To an oven-dried round-bottom flask, diisopropylamine (459.1 mg, 4.54 mmol, 1.20 equiv.) in THF (6.0 mL) in a glovebox. The solution was brought to the hood, under nitrogen, and cooled to 0 ºC. Once this temperature is reached, n-BuLi in 2.5M Hexanes (290.6 mg, 4.54 mmol, 1.20 equiv.) was added slowly. After 20 min at 0 ºC, the solution was cooled to –78 ºC, and then a solution of S-tert-butyl ethanethioate (500.0 mg, 3.78 mmol, 1.0 equiv.) in HMPA (1.62 mL) was slowly added over 5 min. After stirring for 30 min, a solution of TBSCl (683.8 mg, 4.54 mmol, 1.20 equiv.) and HMPA (1.62 mL) in

[83] Eggert, A.; Etling, C.; Millbrodt, L.; Schulz, G.; and Kalesse, M. *Org. Lett.* **2021**, *23*, 8722-8726.

hexane (0.76 mL) was added slowly. Then the reaction solution was warmed to RT, diluted with ice-cold pentane, and washed with water (2x25 mL). The organic phase was separated, dried over anhydrous magnesium sulfate, and passed through a filter. The filtrate was concentrated in vacuo. The desired product was purified via vacuum distillation with an oil bath at 95 ºC. Tert-butyl-(1-tert-butylsulfanylvinyloxy)-dimethyl-silane (**1.54**, colorless oil).[84] **^{1}H NMR** (500 MHz, $CDCl_3$) δ 4.71 (d, *J* = 1.4 Hz, 1H), 4.67 (d, *J* = 1.3 Hz, 1H), 1.40 – 1.36 (m, 9H), 0.94 (d, *J* = 1.4 Hz, 9H), 0.20 (d, *J* = 1.4 Hz, 6H).

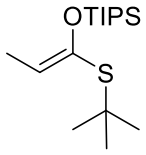

1.55

To an oven-dried round-bottom flask, diisopropylamine (38.1 mg, 0.376 mmol, 1.10 equiv.) in THF (2.0 mL) in a glovebox. Then the flask it brought to a hood, under nitrogen, and cooled to 0 ºC. Once at 0 ºC, n-BuLi in 2.5M hexanes (24.1 mg, 0.376 mmol, 1.10 equiv.) was added slowly. The reaction flask was warmed to RT and stirred for one hour. After one hour, the solution was cooled to –78 ºC and *sec*-tert-butyl propanethioate (50.0 mg, 0.341 mmol, 1.0 equiv.) in THF (0.5 mL) was added dropwise over a period of 5 min. Upon the completion of addition to the reaction, the reaction stirred for 40 min. Then to the stirring reaction, TIPSOTF (115.2 mg, 0.376 mmol, 1.10 equiv.) was added in one portion. The reaction was stirred for one hour and was allowed

[84] Gennari, C.; Beretta, M.G.; Bernardi, A.; Moro, G.; Scolastico, C.; and Todeschini, R. *Tetrahedron* **1986**, *42*, 893-909.

to warm to RT. The solution was rinsed with pentane and then concentrated in vacuo.[85] [(E)-1-tert-butylsulfanylprop-1-enoxy]-triisopropyl-silane (**1.55**, white amorphous solid). **^{1}H NMR** (500 MHz, $CDCl_3$) δ 5.33 (q, *J* = 6.8 Hz, 1H), 1.74 (d, *J* = 6.8 Hz, 3H), 1.38 (s, 8H), 1.10 (d, *J* = 7.1 Hz, 16H), 1.05 (d, *J* = 4.9 Hz, 12H). **^{13}C NMR** (125 MHz, $CDCl_3$) δ 146.32, 114.94, 47.11, 31.76, 18.04, 15.15, 12.61. **IR** ν 2943, 2866, 1705, 1624, 1458, 1363, 1256, 1168, 1039, 882, 803, 642 cm^{-1}. **HRMS** (DART) calcd. for $C_{16}H_{35}OSiS$ $[M+H^+]$: 302.2100, found 303.2172.

1.5.2.6 General Procedure for the Synthesis of Silyl Ketene Acetamides

To an oven-dried round-bottom flask, 1-morpholinopropan-1-one (5.59 mmol) in THF (28.0 mL) was added in a glovebox. The flask was brought to a hood under nitrogen where it was cooled to –78 ºC. Once the desired temperature is achieved, KHMDS in 1M THF (6.15 mmol) was added dropwise to the reaction flask. The solution was stirred for 30 min and then a solution of TBSCl or TIPSCl (6.15 mmol) in THF (7.0 mL) slowly. When the solution is completely added, the reaction flask was warmed to 0 ºC for 30 min and then warmed to RT. Once the reaction flask is warmed to RT, the solvent is concentrated in vacuo. Then in the glovebox, pentane (15 mL) was added to the flask and passed through a filter with dried celite. Then in the hood, the solution was concentrated again in vacuo. For specific purification details, mentioned alongside the structure below.[86]

---

[85] (a) Davis, A.P.; Plunkett, S.J.; and Muir, J.E. *Chem. Commun.* **1998**, 1797-1798. (b) "Toward the First Asymmetric Total Synthesis of (–)-Euonyminol" Matthew J. Webber's Thesis from Imperial College London pp. 1-197.
[86] Denmark, S.E. and Heemstra, J.R. *J. Org. Chem.* **2007**, *72*, 5668-5688.

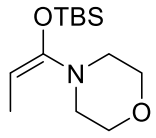

1.56 The desired product was purified using vacuum distillation in an oil bath at 80 ºC. (**1.56**, colorless oil). **^{1}H NMR** (500 MHz, $CDCl_3$) δ 3.75 (q, *J* = 6.6 Hz, 1H), 3.70 – 3.64 (m, 1H), 2.78 – 2.72 (m, 1H), 1.53 (d, *J* = 6.6 Hz, 3H), 0.96 (d, *J* = 0.9 Hz, 2H), 0.14 (s, 1H). **^{13}C NMR** (125 MHz, $CDCl_3$) δ 154.17, 82.62, 66.81, 49.41, 25.89, 18.23, 10.53, -4.45. **IR** ν 2958, 2929, 2856, 1667, 1329, 1298, 1214, 1204, 1118, 1056, 866, 833, 778, 691, 609, 505 cm^{-1}. **HRMS** (DART) calcd. for $C_{13}H_{28}NO_2Si$ [$M+H^+$]: 257.1811, found 258.1884.

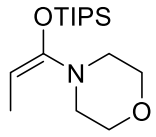

1.57 The desired product was purified using vacuum distillation in an oil bath at 110 ºC. (**1.57**, colorless oil). **^{1}H NMR** (500 MHz, $CDCl_3$) δ 3.75 (q, *J* = 6.6 Hz, 0H), 3.70 – 3.66 (m, 1H), 2.79 – 2.73 (m, 1H), 1.57 (d, *J* = 6.7 Hz, 1H), 1.27 – 1.13 (m, 1H), 1.13 – 1.09 (m, 6H). **^{13}C NMR** (125 MHz, $CDCl_3$) δ 155.01, 83.21, 66.76, 50.13, 18.02, 13.27, 10.71. **IR** ν 2944, 2865, 1666, 1463, 1329, 1212, 1202, 1118, 1059, 919, 882, 862, 824, 673, 552 cm^{-1}. **HRMS** (DART) calcd. for $C_{16}H_{34}NO_2Si$ [$M+H^+$]: 299.2281, found 300.2353.

1.5.3 Kinetic Experiments

1.5.3.1 General Procedure for Integrated Rate Law Experiment

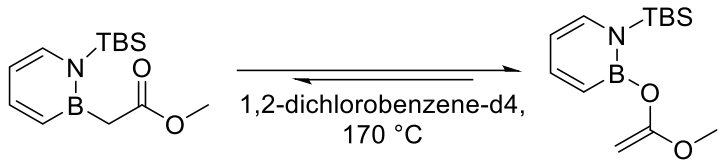

In a nitrogen glovebox, a stock solution was made with methyl 2-[1-[tert-butyl(dimethyl)silyl]azaborinin-2-yl]acetate (21.2 mg, 0.0799 mmol, 1.0 equiv.), hexamethylbenzene (13.0 mg, 0.0799 mmol, 1.0 equiv.), and ODCB-d4 (0.4 mL) in a vial to set up a J-young NMR tube experiment. Initial ^{1}H and ^{11}B NMRs for each tube were taken to determine the initial ratio of internal standard and starting material. Each tube was placed in a temperature-controlled oil bath maintained at 170 °C in a fume hood. ^{1}H NMR spectra were taken periodically to determine the decay of the Boron-Carbon enolate. Analysis of the decay was done observing the disappearance of the α-ketone protons where the observation peak integration is from 2.52 to 2.49 ppm using hexamethylbenzene as the internal standard where the internal standard integration is set to 18 and from 2.1 to 2.03 ppm.

1.5.3.2 General Procedure for Differential Rate Law Experiment

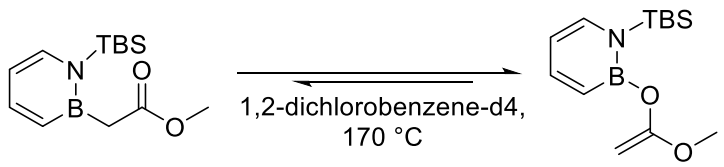

In a nitrogen glovebox, a stock solution was made with methyl 2-[1-[tert-butyl(dimethyl)silyl]azaborinin-2-yl]acetate (50.0 mg, 0.189 mmol, 1.0 equiv.), hexamethylbenzene (30.6 mg, 0.189 mmol, 1.0 equiv.), and ODCB-d4 (2.0 mL) in a vial to set up four J-young NMR tube experiments. Each J-young NMR tube will have a different concentration and aliquots added to them: #1: 0.4 mL of the stock solution, #2: 0.4 mL of stock solution + 0.1 mL ODCB-d4, #3: 0.4 mL of the stock solution + 0.2 mL ODCB-d4, and #4: 0.4 mL of stock solution + 0.3 mL ODCB-d4. Initial ^{1}H and ^{11}B NMRs for each tube were taken to determine the initial ratio of internal standard and starting material. Each tube was placed in a temperature-controlled oil bath maintained at 170 °C in a fume hood. ^{1}H NMR spectra were taken periodically to determine the decay of the Boron-Carbon enolate. Analysis of the decay was done observing the disappearance of the α-ketone protons where the observation peak integration is from 2.52 to 2.49 ppm using hexamethylbenzene as the internal standard where the internal standard integration is set to 18 and from 2.1 to 2.03 ppm.

1.5.3.2.1 Mathematical Procedure for Determining Reaction Order

To determine the reaction order from the experimental data, we needed to first plot ln(concentration of BC enolate) vs. time (in seconds) for the isomerization from the BC to BO enolate. At a given starting concentration, the isomerization was monitored over a period of time and the concentration of the BC enolate decreased. The concentration of the BC enolate was calculated using concentration of BC enolate = initial concentration of BC enolate/ conversion, where conversion = integration of product signal/ initial integration of product signal (with relation to the internal standard).

From the ln(concentration of BC enolate) vs time plot, the rate constant, k [s^{-1}], can be extracted from the slope. We did this for all other concentrations. Once the rate constants for all concentrations are determined, we plotted log(rate of reaction) vs log(initial concentration of BC enolate) (where the rate = k*(initial concentration of BC enolate)) to extract the reaction order from the slope. From the plot, the slope of the line determines the order of the reaction.

1.5.3.3 General Procedure for Eyring Analysis

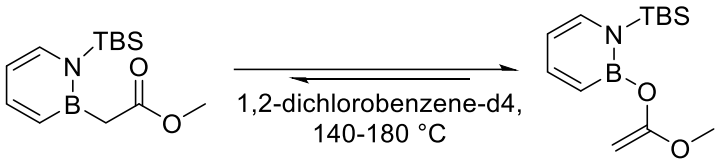

In a nitrogen glovebox, a stock solution was made of methyl 2-[1-[tert-butyl(dimethyl)silyl]azaborinin-2-yl]acetate (11.1 mg, 0.0419 mmol, 1.0 equiv.), hexamethylbenzene (6.8 mg 0.21 mmol, 1.0 equiv.) and ODCB-d4 (2.0 mL) in a vial to perform five j-young NMR tube experiments. To each j-young tube, 0.4 mL of the stock solution in ODCB-d4 was added. Initial ^{1}H and ^{11}B NMRs for each tube were taken to determine the initial ratio of internal standard and starting material. Each tube was placed in temperature-controlled oil baths ranging from 140 to 180 °C in a fume hood. ^{1}H NMR spectra were taken periodically to determine the decay of the Boron-Carbon enolate. Analysis of the decay was done observing the disappearance of the α-ketone protons where the observation peak integration is from 2.52 to 2.49 ppm using

hexamethylbenzene as the internal standard where the internal standard integration is set to 18 and from 2.1 to 2.03 ppm. Each temperature was repeated for three trials.[87]

1.5.3.3.1 Mathematical Procedure for Determining Activation Parameters

To determine the activation parameters from the experimental data, for all five temperatures used the rate constants needed to be determined for further usage. For each individual temperature, we needed to first plot ln(concentration of BC enolate) vs. time (in seconds) for the isomerization from the BC to BO enolate. At a given concentration, the isomerization was monitored over a period of time and the concentration of the BC enolate decreased. The concentration of the BC enolate was calculated using concentration of BC enolate = initial concentration of BC enolate/ conversion, where conversion = integration of product signal/ initial integration of product signal (with relation to the internal standard). The rate constant, k [s^{-1}], can be extracted from the slope.

Once the rate constants for all the temperatures are determined, we plotted ln(k/T) vs T (in Kelvin) using all five temperatures for one trial. From this graph the slope gives us $\Delta H^{\ddagger}$, and $\Delta S^{\ddagger}$ is determined from the y-intercept of the linear line. Using these two values, we were able to then determine $\Delta G^{\ddagger}$ for the individual trial. This was repeated for the other two trials. For the average activation parameters, the rate constants used came from the average rate constants for the individual temperatures to be used in the same plot.

[87] Robichuad, H.M.; Ishibashi, J.S.A.; Ozaki, T.; Lamine, W.; Miqueu, K.; and Liu, S.-Y. *Org. Biomol. Chem.* **2023**, *21*, 3778-3783.

1.5.3.4 Control Experiment for Isomerization Order Data Collection Reproducibility

At a given concentration, 0.1093 M, of BC enolate (**1**) was prepared as the procedure above (1.5.3.2) presents for determining the order of the isomerization. The control experiment was done in an oil bath of 160 ºC using two j-young NMR tubes with the same concentration. Each tube was monitored using ^{1}H NMR via hexamethylbenzene as the internal standard. Proton NMRs were taken periodically to determine the decay of the Boron-Carbon enolate. Analysis of the decay was done observing the disappearance of the α-hydrogen protons where the observation peak integration is from 2.52 to 2.49 ppm using hexamethylbenzene as the internal standard where the internal standard integration is set to 18 and from 2.1 to 2.03 ppm.

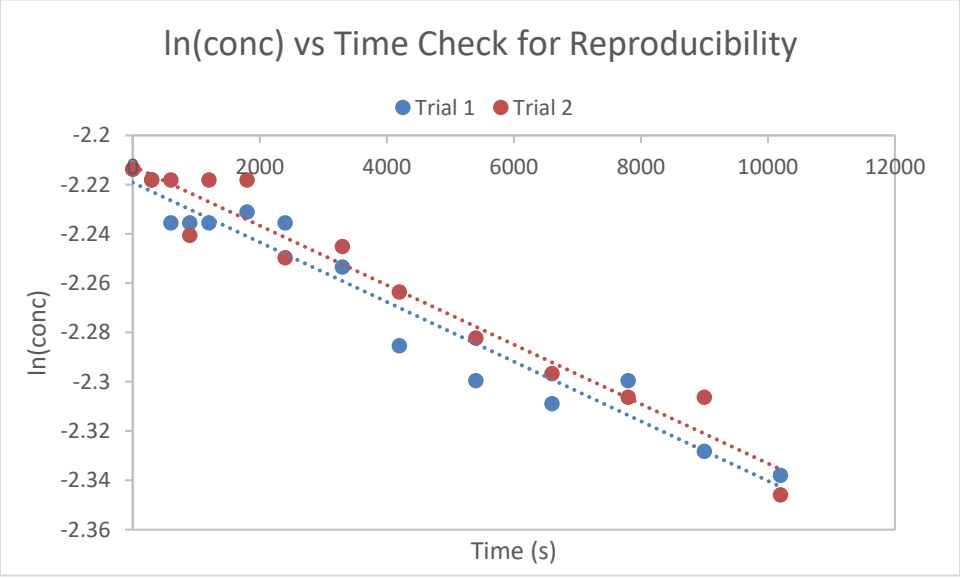

Figure 1.17: Reproducibility Check for Isomerization of Compound **1.**

1.5.4 X-ray Crystallographic Data

Data for Compound **1**

Table 1. Crystal data and structure refinement for C13H24BNO2Si.

Identification code	C13H24BNO2Si	
Empirical formula	C13 H24 B N O2 Si	
Formula weight	265.23	
Temperature	173(2) K	
Wavelength	1.54178 Å	
Crystal system	Monoclinic	
Space group	$P2_1/n$	
Unit cell dimensions	a = 12.9358(8) Å	a= 90°.
	b = 8.0895(5) Å	b= 108.487(2)°.
	c = 15.6926(10) Å	g = 90°.
Volume	1557.40(17) $Å^3$	
Z	4	
Density (calculated)	1.131 Mg/m^3	
Absorption coefficient	1.278 mm^{-1}	
F(000)	576	
Crystal size	0.380 x 0.320 x 0.220 mm^3	
Theta range for data collection	3.875 to 66.720°.	
Index ranges	-15<=h<=15, -9<=k<=9, -18<=l<=18	
Reflections collected	26251	

Independent reflections	2733 [R(int) = 0.0284]
Completeness to theta = 66.720°	99.2 %
Absorption correction	Semi-empirical from equivalents
Max. and min. transmission	0.7528 and 0.6622
Refinement method	Full-matrix least-squares on F^2
Data / restraints / parameters	2733 / 0 / 165
Goodness-of-fit on F^2	1.036
Final R indices [I>2sigma(I)]	R1 = 0.0308, wR2 = 0.0834
R indices (all data)	R1 = 0.0312, wR2 = 0.0838
Extinction coefficient	n/a
Largest diff. peak and hole	0.307 and -0.199 e.$Å^{-3}$

Table 2. Atomic coordinates ($x10^4$) and equivalent isotropic displacement parameters ($Å^2 x\ 10^3$) for C13H24BNO2Si. U(eq) is defined as one third of the trace of the orthogonalized U^{ij} tensor.

	x	y	z	U(eq)
Si(1)	4808(1)	8101(1)	6576(1)	24(1)
O(1)	2502(1)	2848(1)	5460(1)	42(1)
O(2)	1575(1)	3909(1)	4128(1)	56(1)
N(1)	3405(1)	7674(1)	6471(1)	24(1)
B(1)	2648(1)	6599(2)	5838(1)	26(1)
C(1)	1794(2)	1429(2)	5249(1)	62(1)
C(2)	2287(1)	4031(2)	4834(1)	32(1)
C(3)	3024(1)	5478(2)	5146(1)	34(1)

C(4)	1488(1)	6566(2)	5866(1)	33(1)
C(5)	1217(1)	7460(2)	6496(1)	34(1)
C(6)	2013(1)	8415(2)	7129(1)	33(1)
C(7)	3043(1)	8509(2)	7097(1)	29(1)
C(8)	5077(1)	7807(2)	5484(1)	39(1)
C(9)	5057(1)	10329(2)	6875(1)	34(1)
C(10)	5710(1)	6725(2)	7480(1)	31(1)
C(11)	5433(1)	6925(2)	8357(1)	41(1)
C(12)	6902(1)	7248(2)	7654(1)	48(1)
C(13)	5580(1)	4898(2)	7197(1)	40(1)

Table 3. Bond lengths [Å] and angles [°] for C13H24BNO2Si.

Si(1)-N(1)	1.8026(10)
Si(1)-C(9)	1.8643(13)
Si(1)-C(8)	1.8682(13)
Si(1)-C(10)	1.8884(13)
O(1)-C(2)	1.3360(16)
O(1)-C(1)	1.4399(19)
O(2)-C(2)	1.1998(16)
N(1)-C(7)	1.3901(15)
N(1)-B(1)	1.4442(17)
B(1)-C(4)	1.5154(18)
B(1)-C(3)	1.6038(18)

C(1)-H(1A)	0.9800
C(1)-H(1B)	0.9800
C(1)-H(1C)	0.9800
C(2)-C(3)	1.4909(18)
C(3)-H(3A)	0.9900
C(3)-H(3B)	0.9900
C(4)-C(5)	1.357(2)
C(4)-H(4)	0.9500
C(5)-C(6)	1.413(2)
C(5)-H(5)	0.9500
C(6)-C(7)	1.3514(18)
C(6)-H(6)	0.9500
C(7)-H(7)	0.9500
C(8)-H(8A)	0.9800
C(8)-H(8B)	0.9800
C(8)-H(8C)	0.9800
C(9)-H(9A)	0.9800
C(9)-H(9B)	0.9800
C(9)-H(9C)	0.9800
C(10)-C(11)	1.536(2)
C(10)-C(13)	1.5373(19)
C(10)-C(12)	1.5379(18)
C(11)-H(11A)	0.9800

C(11)-H(11B)	0.9800
C(11)-H(11C)	0.9800
C(12)-H(12A)	0.9800
C(12)-H(12B)	0.9800
C(12)-H(12C)	0.9800
C(13)-H(13A)	0.9800
C(13)-H(13B)	0.9800
C(13)-H(13C)	0.9800

N(1)-Si(1)-C(9)	107.27(5)
N(1)-Si(1)-C(8)	111.53(6)
C(9)-Si(1)-C(8)	106.66(6)
N(1)-Si(1)-C(10)	108.64(5)
C(9)-Si(1)-C(10)	111.35(6)
C(8)-Si(1)-C(10)	111.32(7)
C(2)-O(1)-C(1)	115.69(11)
C(7)-N(1)-B(1)	118.12(10)
C(7)-N(1)-Si(1)	113.43(8)
B(1)-N(1)-Si(1)	128.45(8)
N(1)-B(1)-C(4)	116.91(11)
N(1)-B(1)-C(3)	121.38(11)
C(4)-B(1)-C(3)	121.71(11)
O(1)-C(1)-H(1A)	109.5

O(1)-C(1)-H(1B)	109.5
H(1A)-C(1)-H(1B)	109.5
O(1)-C(1)-H(1C)	109.5
H(1A)-C(1)-H(1C)	109.5
H(1B)-C(1)-H(1C)	109.5
O(2)-C(2)-O(1)	122.66(13)
O(2)-C(2)-C(3)	126.27(13)
O(1)-C(2)-C(3)	111.05(11)
C(2)-C(3)-B(1)	111.50(11)
C(2)-C(3)-H(3A)	109.3
B(1)-C(3)-H(3A)	109.3
C(2)-C(3)-H(3B)	109.3
B(1)-C(3)-H(3B)	109.3
H(3A)-C(3)-H(3B)	108.0
C(5)-C(4)-B(1)	119.91(12)
C(5)-C(4)-H(4)	120.0
B(1)-C(4)-H(4)	120.0
C(4)-C(5)-C(6)	120.32(11)
C(4)-C(5)-H(5)	119.8
C(6)-C(5)-H(5)	119.8
C(7)-C(6)-C(5)	120.76(12)
C(7)-C(6)-H(6)	119.6
C(5)-C(6)-H(6)	119.6

C(6)-C(7)-N(1)	123.82(12)
C(6)-C(7)-H(7)	118.1
N(1)-C(7)-H(7)	118.1
Si(1)-C(8)-H(8A)	109.5
Si(1)-C(8)-H(8B)	109.5
H(8A)-C(8)-H(8B)	109.5
Si(1)-C(8)-H(8C)	109.5
H(8A)-C(8)-H(8C)	109.5
H(8B)-C(8)-H(8C)	109.5
Si(1)-C(9)-H(9A)	109.5
Si(1)-C(9)-H(9B)	109.5
H(9A)-C(9)-H(9B)	109.5
Si(1)-C(9)-H(9C)	109.5
H(9A)-C(9)-H(9C)	109.5
H(9B)-C(9)-H(9C)	109.5
C(11)-C(10)-C(13)	108.97(11)
C(11)-C(10)-C(12)	108.56(12)
C(13)-C(10)-C(12)	109.08(11)
C(11)-C(10)-Si(1)	110.30(9)
C(13)-C(10)-Si(1)	111.39(9)
C(12)-C(10)-Si(1)	108.48(10)
C(10)-C(11)-H(11A)	109.5
C(10)-C(11)-H(11B)	109.5

H(11A)-C(11)-H(11B)	109.5
C(10)-C(11)-H(11C)	109.5
H(11A)-C(11)-H(11C)	109.5
H(11B)-C(11)-H(11C)	109.5
C(10)-C(12)-H(12A)	109.5
C(10)-C(12)-H(12B)	109.5
H(12A)-C(12)-H(12B)	109.5
C(10)-C(12)-H(12C)	109.5
H(12A)-C(12)-H(12C)	109.5
H(12B)-C(12)-H(12C)	109.5
C(10)-C(13)-H(13A)	109.5
C(10)-C(13)-H(13B)	109.5
H(13A)-C(13)-H(13B)	109.5
C(10)-C(13)-H(13C)	109.5
H(13A)-C(13)-H(13C)	109.5
H(13B)-C(13)-H(13C)	109.5

Symmetry transformations used to generate equivalent atoms:

Table 4. Anisotropic displacement parameters ($Å^2 x\ 10^3$) for C13H24BNO2Si. The anisotropic displacement factor exponent takes the form:$-2p^2\ [\ h^2a^{*2}U^{11}+...+2hka^*b^*U^{12}]$

	U^{11}	U^{22}	U^{33}	U^{23}	U^{13}	U^{12}
Si(1)	24(1)	23(1)	27(1)	-2(1)	11(1)	-2(1)
O(1)	48(1)	34(1)	36(1)	3(1)	-1(1)	-3(1)

O(2)	67(1)	49(1)	33(1)	3(1)	-11(1)	-17(1)
N(1)	23(1)	24(1)	24(1)	-1(1)	9(1)	1(1)
B(1)	28(1)	25(1)	25(1)	2(1)	7(1)	0(1)
C(1)	75(1)	36(1)	63(1)	8(1)	7(1)	-15(1)
C(2)	38(1)	31(1)	27(1)	-5(1)	7(1)	0(1)
C(3)	36(1)	34(1)	32(1)	-8(1)	12(1)	-5(1)
C(4)	27(1)	34(1)	34(1)	0(1)	6(1)	-4(1)
C(5)	25(1)	40(1)	39(1)	8(1)	13(1)	3(1)
C(6)	32(1)	40(1)	32(1)	-1(1)	15(1)	7(1)
C(7)	29(1)	32(1)	28(1)	-5(1)	9(1)	2(1)
C(8)	45(1)	40(1)	41(1)	-5(1)	26(1)	-9(1)
C(9)	36(1)	27(1)	38(1)	-3(1)	12(1)	-6(1)
C(10)	22(1)	31(1)	40(1)	3(1)	9(1)	2(1)
C(11)	43(1)	45(1)	34(1)	9(1)	8(1)	8(1)
C(12)	23(1)	53(1)	64(1)	3(1)	7(1)	-1(1)
C(13)	36(1)	30(1)	56(1)	4(1)	16(1)	6(1)

Table 5. Hydrogen coordinates ($x10^4$) and isotropic displacement parameters ($Å^2 x\ 10^3$) for C13H24BNO2Si.

	x	y	z	U(eq)
H(1A)	2017	637	5747	92
H(1B)	1041	1778	5157	92
H(1C)	1843	905	4700	92

H(3A)	3025	6156	4621	40
H(3B)	3777	5082	5442	40
H(4)	951	5920	5444	39
H(5)	489	7443	6511	41
H(6)	1822	8999	7583	40
H(7)	3549	9185	7527	35
H(8A)	5128	6623	5371	59
H(8B)	5764	8350	5511	59
H(8C)	4480	8294	4998	59
H(9A)	4429	10983	6523	50
H(9B)	5712	10698	6743	50
H(9C)	5161	10476	7517	50
H(11A)	5514	8088	8542	62
H(11B)	4680	6572	8260	62
H(11C)	5929	6244	8828	62
H(12A)	7091	7126	7099	72
H(12B)	6994	8404	7849	72
H(12C)	7381	6545	8123	72
H(13A)	5756	4760	6638	61
H(13B)	6076	4220	7670	61
H(13C)	4827	4548	7103	61

Table 6. Torsion angles [°] for C13H24BNO2Si.

C(9)-Si(1)-N(1)-C(7)	-37.42(10)
C(8)-Si(1)-N(1)-C(7)	-153.86(9)
C(10)-Si(1)-N(1)-C(7)	83.07(9)
C(9)-Si(1)-N(1)-B(1)	142.83(11)
C(8)-Si(1)-N(1)-B(1)	26.38(12)
C(10)-Si(1)-N(1)-B(1)	-96.69(11)
C(7)-N(1)-B(1)-C(4)	4.23(16)
Si(1)-N(1)-B(1)-C(4)	-176.02(9)
C(7)-N(1)-B(1)-C(3)	-175.01(11)
Si(1)-N(1)-B(1)-C(3)	4.74(17)
C(1)-O(1)-C(2)-O(2)	-2.3(2)
C(1)-O(1)-C(2)-C(3)	176.56(13)
O(2)-C(2)-C(3)-B(1)	101.27(16)
O(1)-C(2)-C(3)-B(1)	-77.55(14)
N(1)-B(1)-C(3)-C(2)	157.01(11)
C(4)-B(1)-C(3)-C(2)	-22.19(17)
N(1)-B(1)-C(4)-C(5)	-3.06(18)
C(3)-B(1)-C(4)-C(5)	176.18(12)
B(1)-C(4)-C(5)-C(6)	-0.4(2)
C(4)-C(5)-C(6)-C(7)	2.7(2)
C(5)-C(6)-C(7)-N(1)	-1.4(2)
B(1)-N(1)-C(7)-C(6)	-2.17(18)
Si(1)-N(1)-C(7)-C(6)	178.04(11)

N(1)-Si(1)-C(10)-C(11)	-53.94(10)
C(9)-Si(1)-C(10)-C(11)	63.98(11)
C(8)-Si(1)-C(10)-C(11)	-177.14(9)
N(1)-Si(1)-C(10)-C(13)	67.20(10)
C(9)-Si(1)-C(10)-C(13)	-174.87(9)
C(8)-Si(1)-C(10)-C(13)	-55.99(11)
N(1)-Si(1)-C(10)-C(12)	-172.72(9)
C(9)-Si(1)-C(10)-C(12)	-54.80(12)
C(8)-Si(1)-C(10)-C(12)	64.09(11)

Symmetry transformations used to generate equivalent atoms

1.5.5 Computational Analysis

All calculations were performed on the real systems with the Gaussian 16 package[88] and the functional M06-2X.[89] All atoms have been described with def2-TZVP basis set.[90] All stationary points involved were fully optimized by taking into consideration the solvent effect (o-dichlorobenzene) by means of the universal Solvation

[88] **Gaussian 16**, Revision **B.01**, Frisch, M. J.; Trucks, G. W.; Schlegel, H. B.; Scuseria, G. E.; Robb, M. A.; Cheeseman, J. R.; Scalmani, G.; Barone, V.; Petersson, G. A.; Nakatsuji, H.; Li, X.; Caricato, M.; Marenich, A. V.; Bloino, J.; Janesko, B. G.; Gomperts, R.; Mennucci, B.; Hratchian, H. P.; Ortiz, J. V.; Izmaylov, A. F.; Sonnenberg, J. L.; Williams-Young, D.; Ding, F.; Lipparini, F.; Egidi, F.; Goings, J.; Peng, B.; Petrone, A.; Henderson, T.; Ranasinghe, D.; Zakrzewski, V. G.; Gao, J.; Rega, N.; Zheng, G.; Liang, W.; Hada, M.; Ehara, M.; Toyota, K.; Fukuda, R.; Hasegawa, J.; Ishida, M.; Nakajima, T.; Honda, Y.; Kitao, O.; Nakai, H.; Vreven, T.; Throssell, K.; Montgomery, J. A., Jr.; Peralta, J. E.; Ogliaro, F.; Bearpark, M. J.; Heyd, J. J.; Brothers, E. N.; Kudin, K. N.; Staroverov, V. N.; Keith, T. A.; Kobayashi, R.; Normand, J.; Raghavachari, K.; Rendell, A. P.; Burant, J. C.; Iyengar, S. S.; Tomasi, J.; Cossi, M.; Millam, J. M.; Klene, M.; Adamo, C.; Cammi, R.; Ochterski, J. W.; Martin, R. L.; Morokuma, K.; Farkas, O.; Foresman, J. B.; Fox, D. J. Gaussian, Inc., Wallingford CT, **2016.**

[89] Zhao, Y.; Truhlar, D. G., *Theor Chem Acc.,* **2008**, 120, 215–241.

[90] Weigend, F.; Ahlrichs, R., *Phys. Chem. Chem. Phys*., **2005**, 7, 3297-3305.

Model based on solute electron Density (SMD). [91] Frequency calculations were undertaken to confirm the nature of the stationary points, yielding one imaginary frequency for transition states (TS), corresponding to the expected process, and all of them positive for *minima*. The connectivity of the transition states and their adjacent *minima* was confirmed by intrinsic reaction coordinate (IRC)[92] calculations. Standard thermodynamic corrections (T = 298 K, 1 atm) have been considered to express reaction paths in terms of standard Gibbs free energy. For real experimental conditions T=443 K, since the temperature setting does not affect the structural optimization, the Gibbs free energies are obtained from the calculated single point energy at T=443K with the Zero-point energy correction. All the energies that appear in this article are in kcal/mol. Geometrical structures were plotted with the CYLview 2.0 programs.[93]

Relative stability of B-C and B-O enolates was determine through different computational programs. The energy (ΔG in kcal/mol) for the ground state BC and BO enolates were computed at SMD(o-DiChloroBenzene) (Table 1.3).

[91] Marenich, A. V.; Cramer, C. J.; Truhlar, D. G., J. Phys. Chem. B 2009, 113, 6378-6396.
[92] (a) Fukui, K., *Acc. Chem. Res.*, **1981**, *14*, 363. (b) Hratchian, H. P.; Schlegel, H. B., in *Theory and Applications of Computational Chemistry: The First 40 Years*, Ed. Dykstra, C. E.; Frenking, G.; Kim, K. S.; Scuseria, G., Elsevier, Amsterdam, **2005**, 195.
[93] CYLview20; Legault, C. Y., Université de Sherbrooke, 2020 (http://www.cylview.org)

Functional	Azaborine_Enolate	
	BN_BO_Enolate 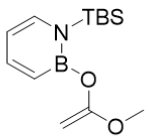	BN_BC_Enolate 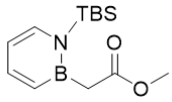
B3LYP-D3/6-31G**	0.0	-2.49
B3LYP/6-31G**	0.0	-3.20
M06-2X/6-31G**	0.0	-0.68
M06-2X/6-311G**	0.0	-1.30
wb97xd/6-311G**	0.0	-4.74
M06-2X/def2-TZVP	0.0	0.60 ✓
M06-2X/def2-TZVP// M06-2X/def2-QZVP	0.0	0.58

Table 1.3: Benchmark Screening of Computational Analysis Programs

The z-matrix coordinates of the optimized BC and BO enolate structures were computed (temperature does not affect optimization) at ground state. The z-matrix coordinates were also optimized for the transition state structure of the isomerization of BC to BO enolate.

Ground State Matrices for the BC Enolate

	x	y	z
C	0.183144	2.527902	-0.545350
O	-0.123493	2.809894	-1.678132
O	1.455177	2.552058	-0.123290
C	2.432237	2.916088	-1.098676
H	2.403790	2.228258	-1.943666
H	2.257720	3.931256	-1.454165
H	3.393339	2.854376	-0.595547

C	-0.761238	2.150226	0.554731
H	-1.762626	2.108955	0.135131
H	-0.740656	2.994671	1.251728
C	-0.285897	-1.516577	1.907388
C	0.306054	-1.323349	3.114520
C	0.620270	-0.010339	3.553583
H	-0.515998	-2.526770	1.590843
H	0.528877	-2.184277	3.729405
H	1.097135	0.107397	4.522287
H	0.568414	2.056099	3.146364
B	-0.352441	0.865349	1.426470
C	0.319361	1.066241	2.774600
N	-0.623932	-0.503715	1.038050
Si	-1.251115	-1.106473	-0.547542
C	0.239198	-1.609513	-1.597957
C	1.075311	-2.686819	-0.900822
H	0.484933	-3.573601	-0.656156
H	1.888892	-3.004536	-1.562146
H	1.529527	-2.313986	0.020278
C	1.129417	-0.394527	-1.871999
H	1.985559	-0.690668	-2.488610
H	0.593002	0.393176	-2.406136
H	1.525177	0.028344	-0.943403

C	-0.284823	-2.165558	-2.928267
H	-0.918363	-3.044522	-2.780418
H	-0.860908	-1.420041	-3.482047
H	0.556768	-2.468489	-3.560450
C	-2.345036	-2.581572	-0.192267
H	-1.796663	-3.492619	0.051521
H	-3.027300	-2.363842	0.633632
H	-2.954527	-2.789092	-1.075181
C	-2.296526	0.155697	-1.429868
H	-1.745709	1.012129	-1.818004
H	-2.761789	-0.357816	-2.276206
H	-3.103575	0.516665	-0.788367

Sum of electronic and zero-point Energies = -1029.113254

Sum of electronic and thermal Free Energies = -1029.161901

Transition State Matrices for the Isomerization of BC to BO Enolate

	x	**y**	**z**
C	4.197559	-0.415356	1.020612
O	4.800963	-1.511894	0.697111
O	4.727130	0.742257	0.760808
C	6.040943	0.759267	0.164456
H	6.735013	0.190784	0.780509
H	5.998396	0.342189	-0.839456
H	6.327731	1.805291	0.128724

C	3.103540	-0.664079	1.862329
H	2.295987	-1.224103	1.406841
H	2.795957	0.108251	2.556190
C	3.612369	-4.456045	2.714028
C	4.321678	-4.337340	3.857641
C	5.150115	-3.175742	4.086242
H	3.044778	-5.363625	2.537815
H	4.290258	-5.141875	4.579100
H	5.769327	-3.160076	4.978713
H	5.795834	-1.292810	3.414308
B	4.218217	-2.192411	1.969505
C	5.157165	-2.150876	3.212858
N	3.564175	-3.502488	1.711971
Si	2.866365	-4.032792	0.167092
C	4.167136	-4.969330	-0.845968
C	4.882406	-5.994561	0.039292
H	4.183820	-6.702841	0.494325
H	5.592991	-6.574366	-0.560630
H	5.442919	-5.510299	0.842809
C	5.204521	-4.006654	-1.429012
H	5.937604	-4.563985	-2.023340
H	4.744049	-3.261936	-2.083952
H	5.745526	-3.473291	-0.644840

C	3.464904	-5.704958	-1.993735
H	2.756618	-6.450706	-1.624657
H	2.921833	-5.018657	-2.649318
H	4.205554	-6.228336	-2.608521
C	1.431993	-5.180156	0.536023
H	1.739588	-6.181968	0.841820
H	0.797676	-4.764070	1.322986
H	0.818461	-5.283838	-0.362684
C	2.185041	-2.599971	-0.824214
H	2.896631	-1.794046	-1.001691
H	1.879984	-2.990894	-1.799790
H	1.290451	-2.181976	-0.357082

Sum of electronic and zero-point Energies = -1029.065866

Sum of electronic and thermal Free Energies = -1029.114232

Ground State Matrices for the BO Enolate

	x	**y**	**z**
C	0.138311	2.818852	0.137759
O	0.249993	1.479823	0.048053
O	0.928496	3.479337	-0.728785
C	2.231130	2.931971	-0.931599
H	2.736002	2.772819	0.024284
H	2.183655	1.993271	-1.481921
H	2.778491	3.670883	-1.511689

C	-0.720805	3.457237	0.929576
H	-1.413913	2.899106	1.541995
H	-0.734831	4.536299	0.945881
C	-0.235058	-1.625078	1.930161
C	0.315169	-1.365255	3.144207
C	0.846216	-0.075021	3.435524
H	-0.646372	-2.605377	1.722706
H	0.337441	-2.149859	3.887340
H	1.272721	0.086603	4.421130
H	1.241030	1.892858	2.778550
B	0.240639	0.613674	1.150135
C	0.825240	0.926796	2.513220
N	-0.311264	-0.696070	0.921384
Si	-1.103693	-1.162014	-0.630601
C	0.227715	-1.778136	-1.818768
C	0.918150	-3.014253	-1.234247
H	0.216486	-3.836286	-1.073914
H	1.691216	-3.370035	-1.924175
H	1.406134	-2.792037	-0.281041
C	1.278462	-0.694448	-2.072919
H	2.020409	-1.060164	-2.791594
H	0.834137	0.215565	-2.482854
H	1.807841	-0.424562	-1.155502

C	-0.446661	-2.149728	-3.144851
H	-1.196020	-2.935117	-3.014785
H	-0.935567	-1.287101	-3.605688
H	0.301859	-2.522340	-3.852513
C	-2.319345	-2.525073	-0.236202
H	-1.853682	-3.468158	0.052875
H	-2.993764	-2.216886	0.567118
H	-2.931096	-2.715672	-1.121623
C	-2.055236	0.286778	-1.319373
H	-1.423811	0.983159	-1.870974
H	-2.833914	-0.082640	-1.991628
H	-2.547111	0.842048	-0.516583

Sum of electronic and zero-point Energies = -1029.112147

Sum of electronic and thermal Free Energies = -1029.162852

1.5.5.1 Bond Length Comparison

The comparison of selected bond lengths of the M06-2X/Def2-tzvp optimized structure and crystal structure (in parentheses) of BC enolate (**1**) were calculated (Figure 1.18).

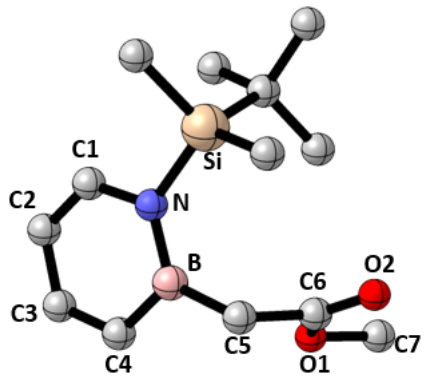

B-N: 1.449 (1.444) Å , B-C5: 1.606 (1.604) Å ;
N-Si: 1.809 (1.803) Å , C1-N: 1.377 (1.390) Å ;
C1-C2: 1.358 (1.351) Å , C2-C3: 1.420 (1.413) Å ;
C3-C4: 1.362 (1.357) Å , C4-B: 1.520 (1.515) Å ;
C5-C6: 1.498 (1.491) Å , C6-O1: 1.340 (1.336) Å ;
C6-O2: 1.207 (1.200) Å , O1-C7: 1.428 (1.440) Å .

Figure 1.18: Comparison of Experimental and Theoretical Bond Lengths for Compound **1**

1.5.6 NMR Spectra

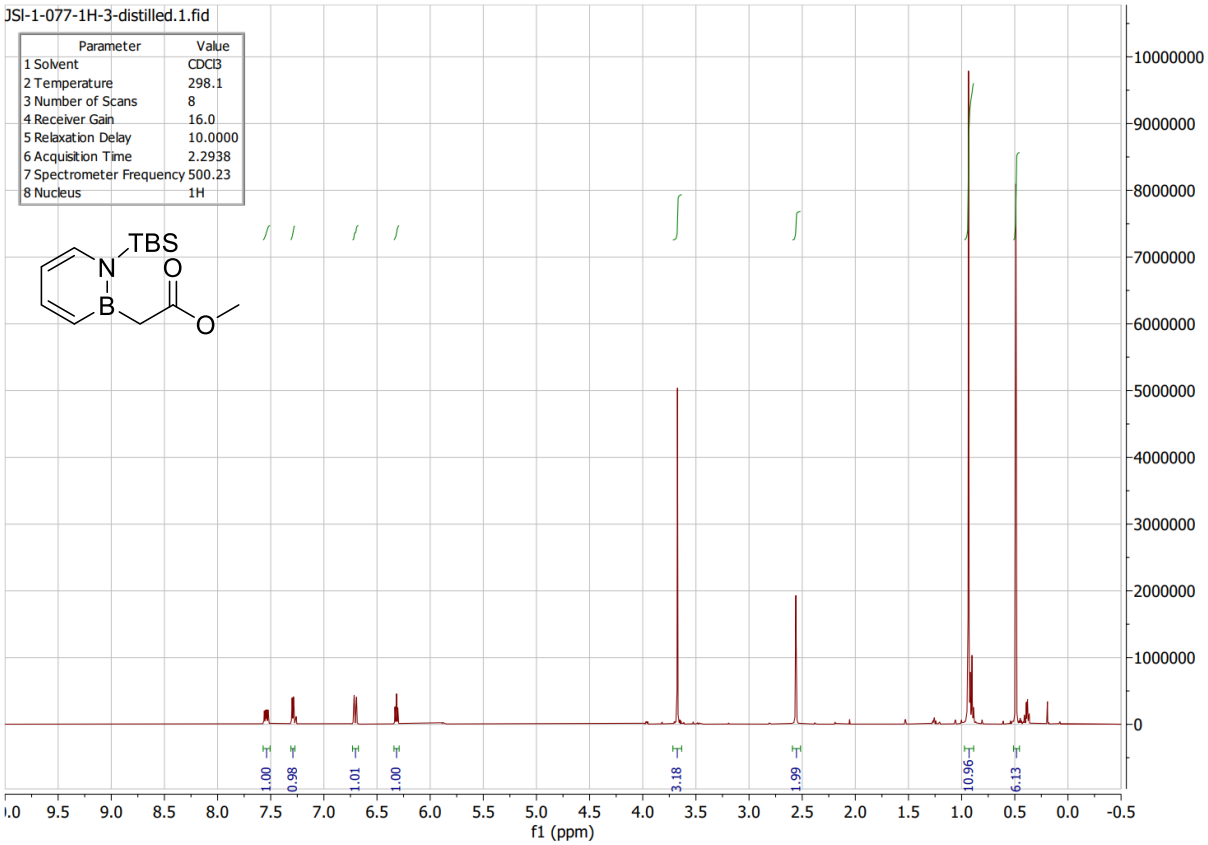

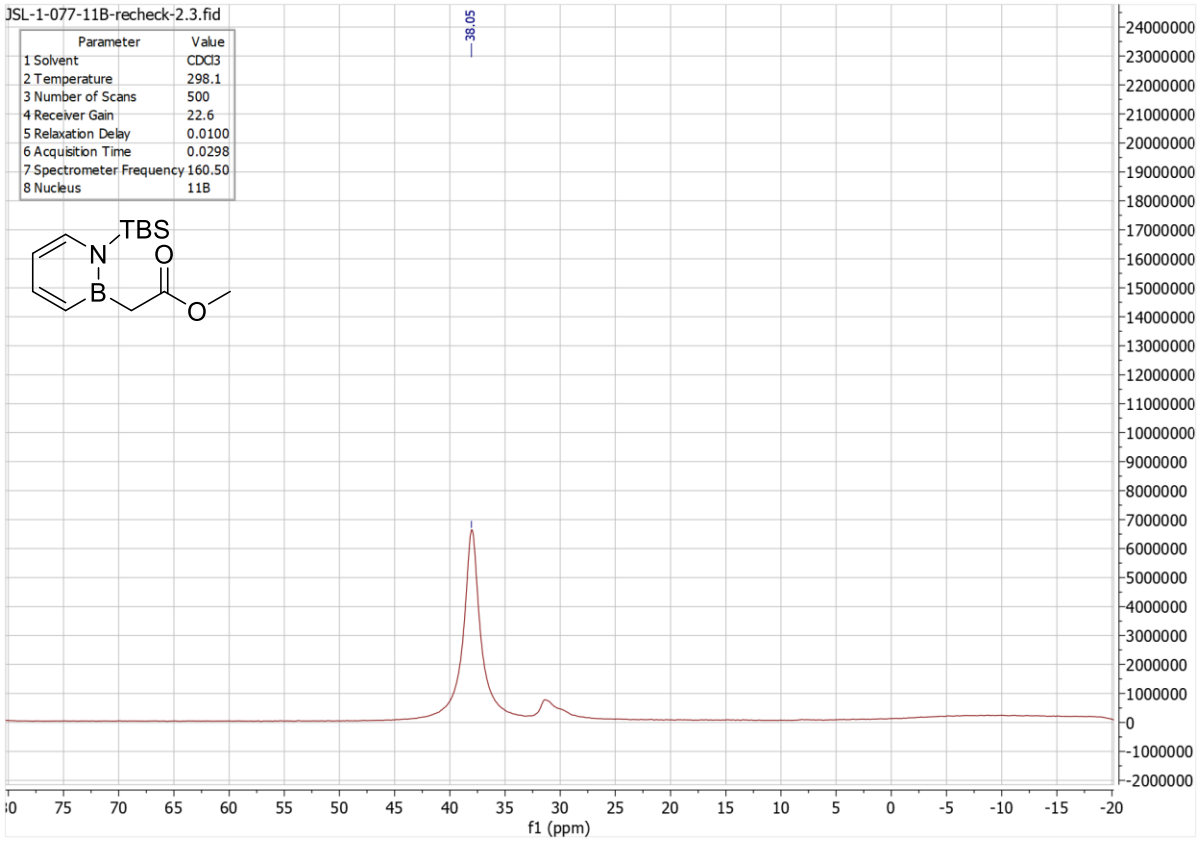
JSL-1-077-11B-recheck-2.3.fid
Parameter Value
1 Solvent CDCl3
2 Temperature 298.1
3 Number of Scans 500
4 Receiver Gain 22.6
5 Relaxation Delay 0.0100
6 Acquisition Time 0.0298
7 Spectrometer Frequency 160.50
8 Nucleus 11B
38.05
TBS
N
O
B
O
f1 (ppm)

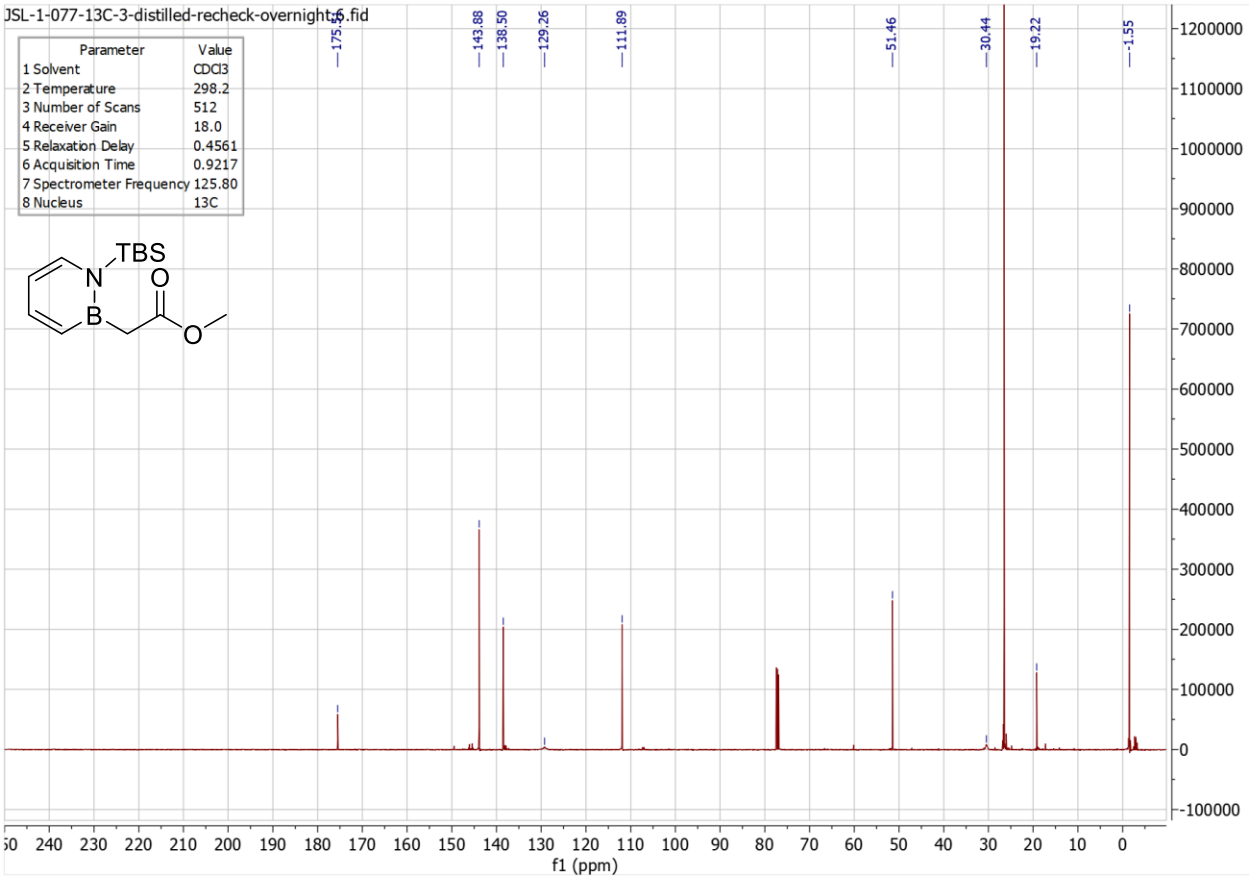
JSL-1-077-13C-3-distilled-recheck-overnight.6.fid
Parameter Value
1 Solvent CDCl3
2 Temperature 298.2
3 Number of Scans 512
4 Receiver Gain 18.0
5 Relaxation Delay 0.4561
6 Acquisition Time 0.9217
7 Spectrometer Frequency 125.80
8 Nucleus 13C
175.55
143.88
138.50
129.26
111.89
51.46
30.44
19.22
-1.55
TBS
N
O
B
O
f1 (ppm)

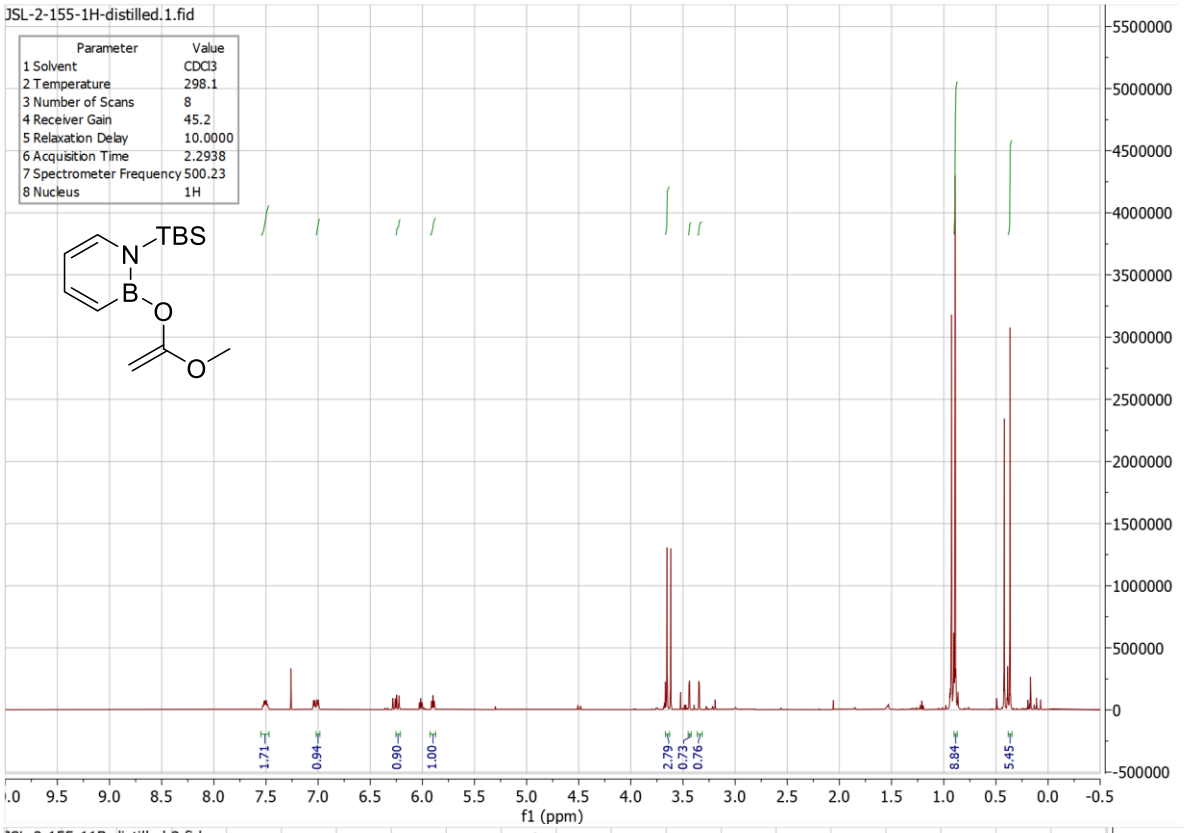
JSL-2-155-1H-distilled.1.fid
Parameter Value
1 Solvent CDCl3
2 Temperature 298.1
3 Number of Scans 8
4 Receiver Gain 45.2
5 Relaxation Delay 10.0000
6 Acquisition Time 2.2938
7 Spectrometer Frequency 500.23
8 Nucleus 1H
TBS
N
B
O
O
1.71
0.94
0.90
1.00
2.79
0.73
0.76
8.84
5.45
f1 (ppm)

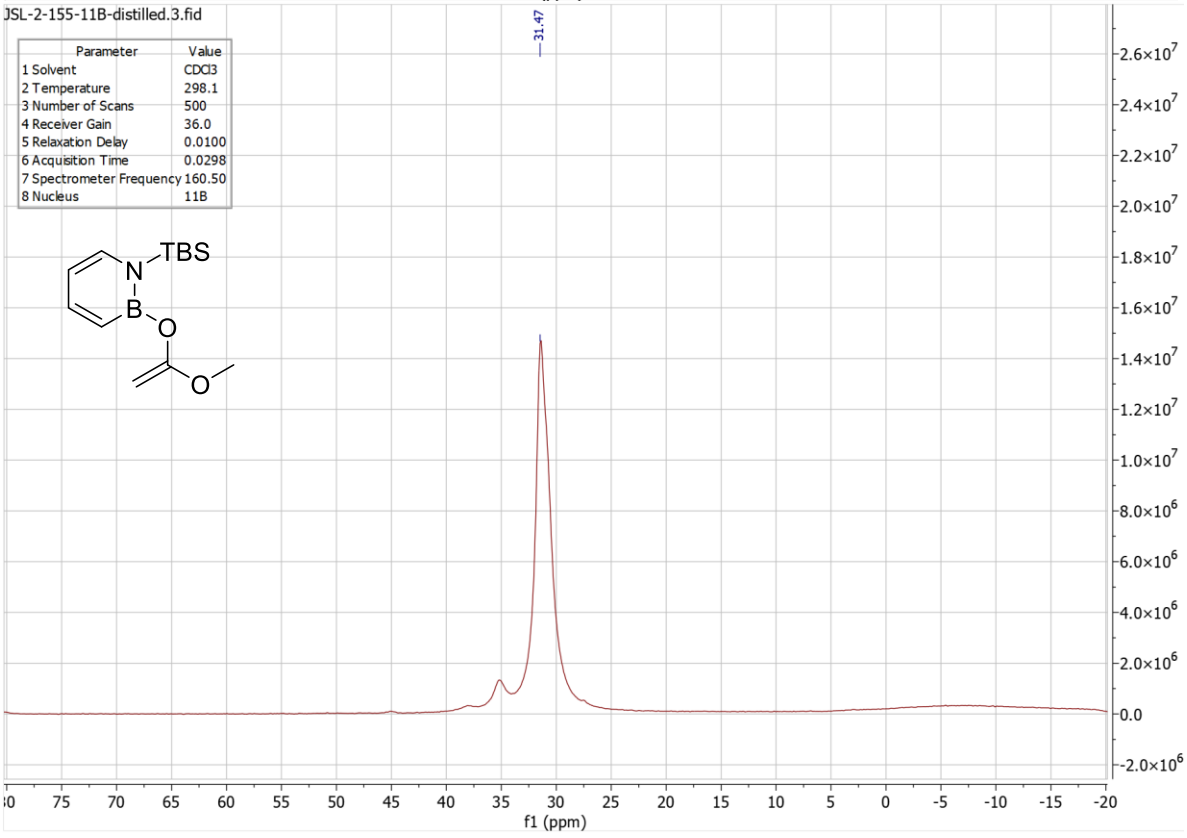
JSL-2-155-11B-distilled.3.fid
Parameter Value
1 Solvent CDCl3
2 Temperature 298.1
3 Number of Scans 500
4 Receiver Gain 36.0
5 Relaxation Delay 0.0100
6 Acquisition Time 0.0298
7 Spectrometer Frequency 160.50
8 Nucleus 11B
TBS
N
B
O
O
31.47
f1 (ppm)

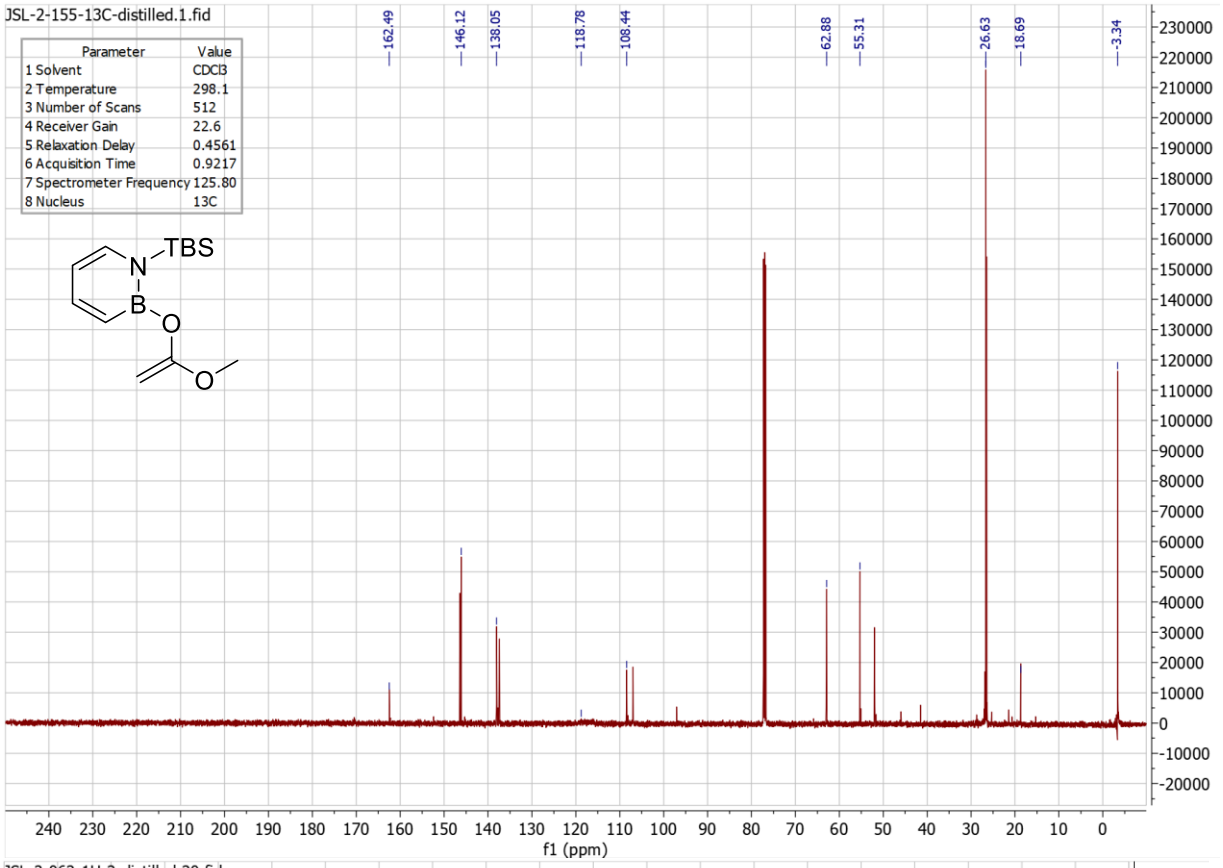
JSL-2-155-13C-distilled.1.fid
Parameter Value
1 Solvent CDCl3
2 Temperature 298.1
3 Number of Scans 512
4 Receiver Gain 22.6
5 Relaxation Delay 0.4561
6 Acquisition Time 0.9217
7 Spectrometer Frequency 125.80
8 Nucleus 13C
TBS
N
B
O
O
162.49
146.12
138.05
118.78
108.44
62.88
55.31
26.63
18.69
-3.34
f1 (ppm)

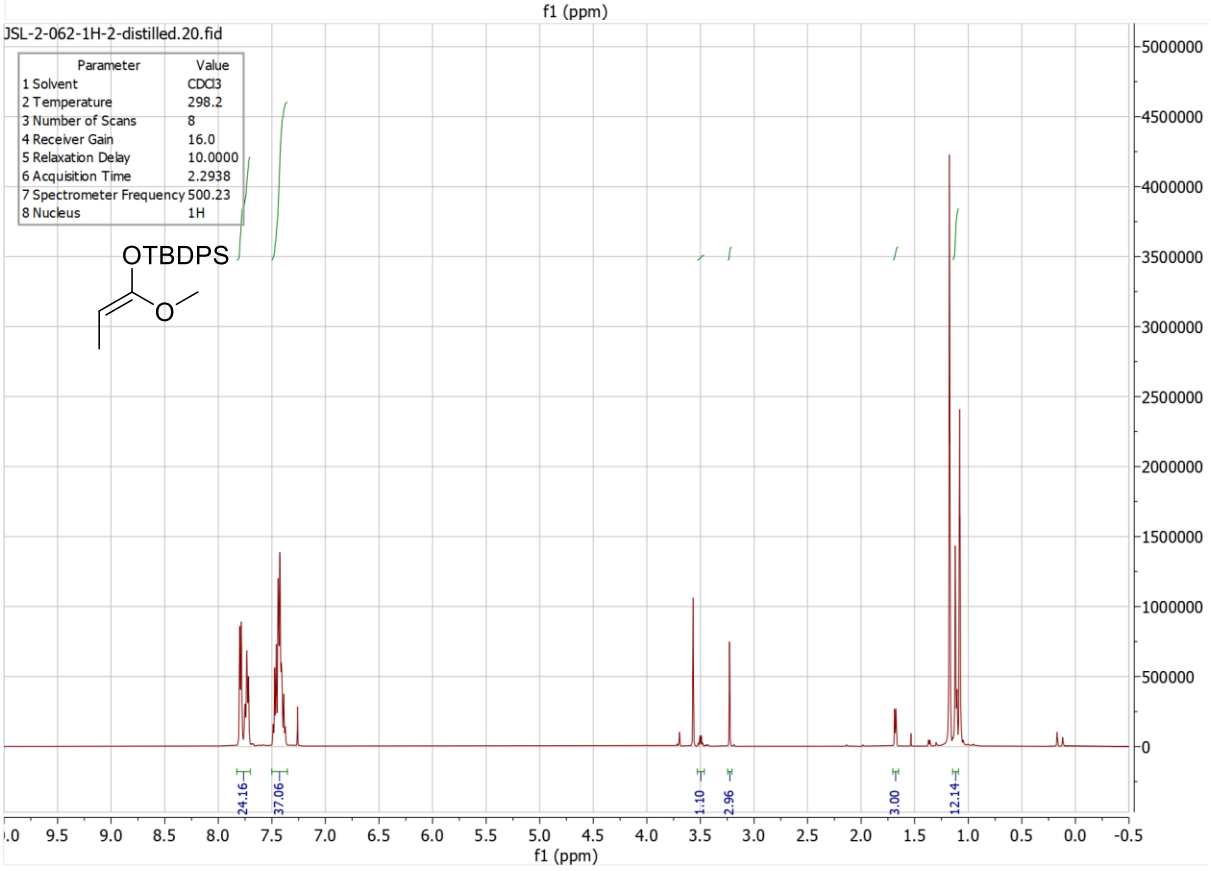
JSL-2-062-1H-2-distilled.20.fid
Parameter Value
1 Solvent CDCl3
2 Temperature 298.2
3 Number of Scans 8
4 Receiver Gain 16.0
5 Relaxation Delay 10.0000
6 Acquisition Time 2.2938
7 Spectrometer Frequency 500.23
8 Nucleus 1H
OTBDPS
O
24.16
37.06
1.10
2.96
3.00
12.14
f1 (ppm)

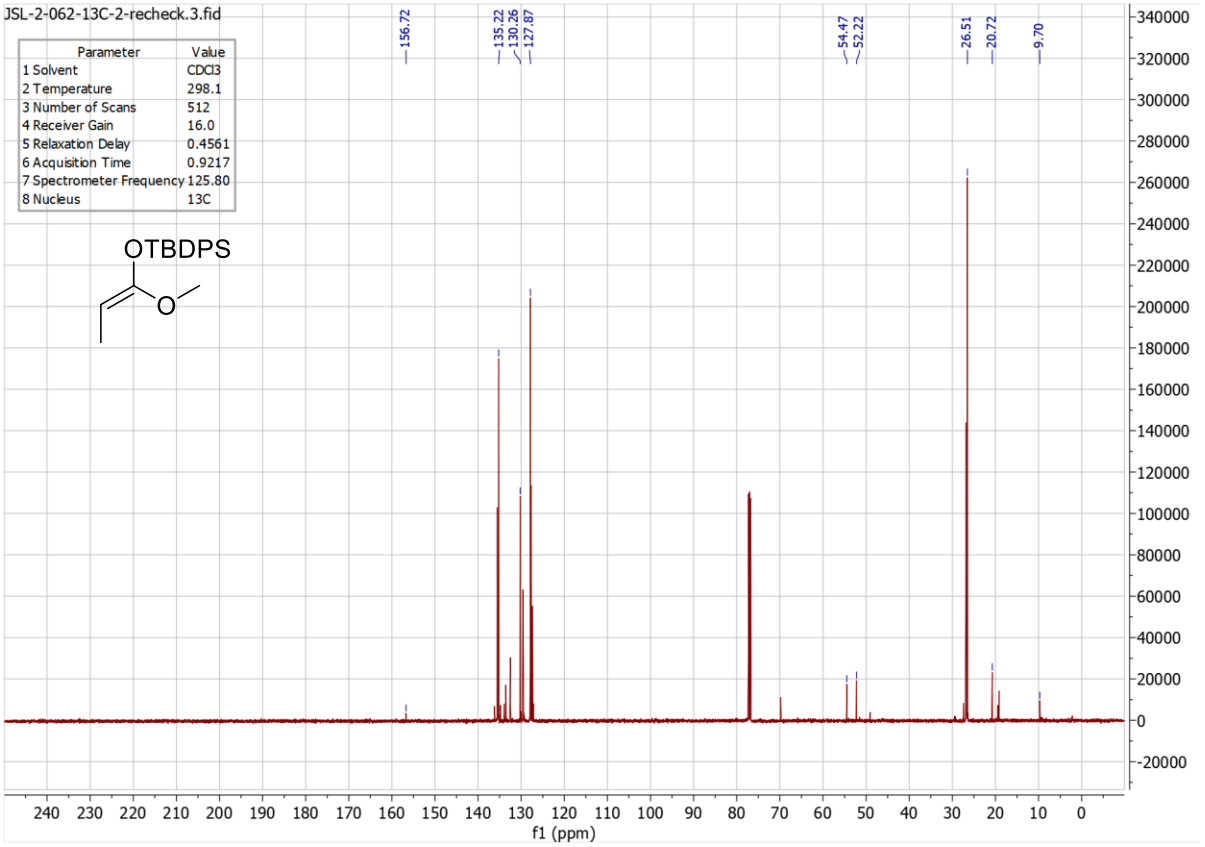
JSL-2-062-13C-2-recheck.3.fid
Parameter Value
1 Solvent CDCl3
2 Temperature 298.1
3 Number of Scans 512
4 Receiver Gain 16.0
5 Relaxation Delay 0.4561
6 Acquisition Time 0.9217
7 Spectrometer Frequency 125.80
8 Nucleus 13C
OTBDPS
O
156.72
135.22
130.26
127.87
54.47
52.22
26.51
20.72
9.70
f1 (ppm)

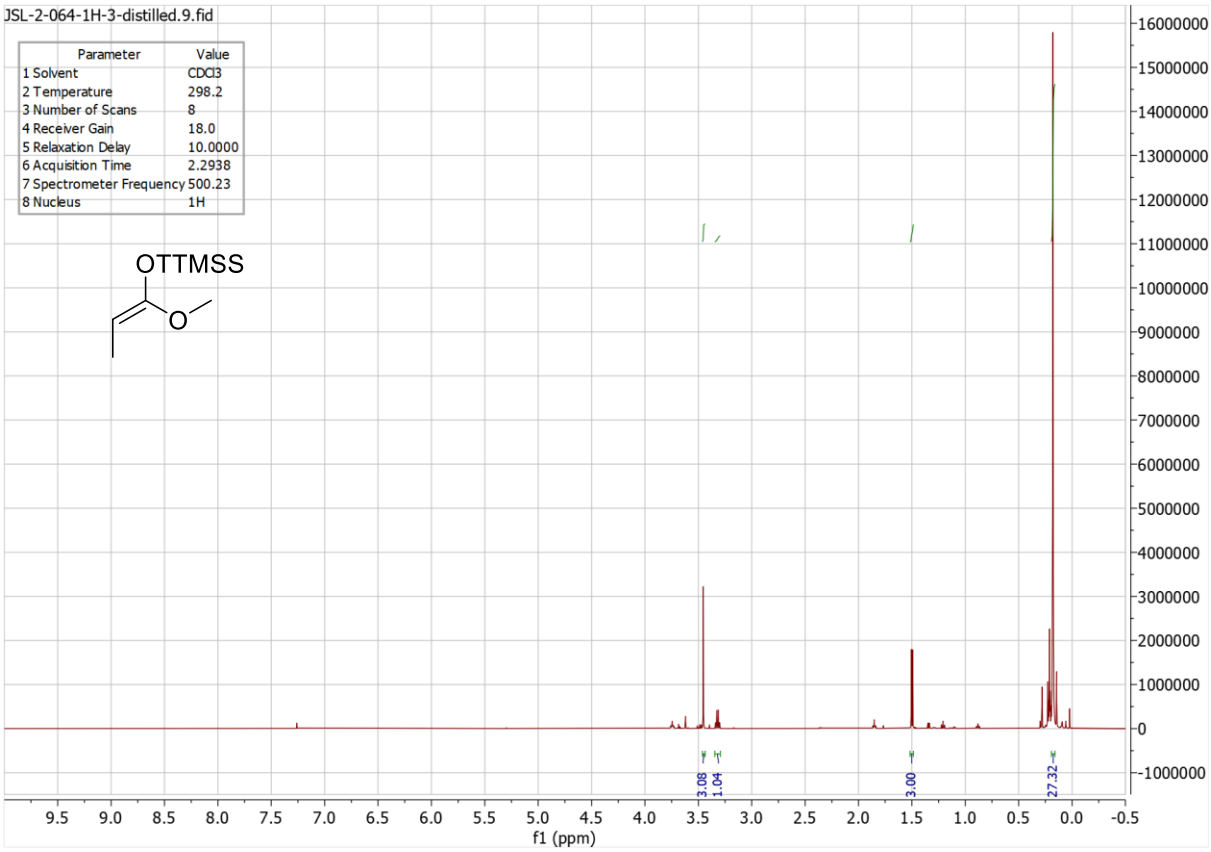
JSL-2-064-1H-3-distilled.9.fid
Parameter Value
1 Solvent CDCl3
2 Temperature 298.2
3 Number of Scans 8
4 Receiver Gain 18.0
5 Relaxation Delay 10.0000
6 Acquisition Time 2.2938
7 Spectrometer Frequency 500.23
8 Nucleus 1H
OTTMSS
O
3.08
1.04
3.00
27.32
f1 (ppm)

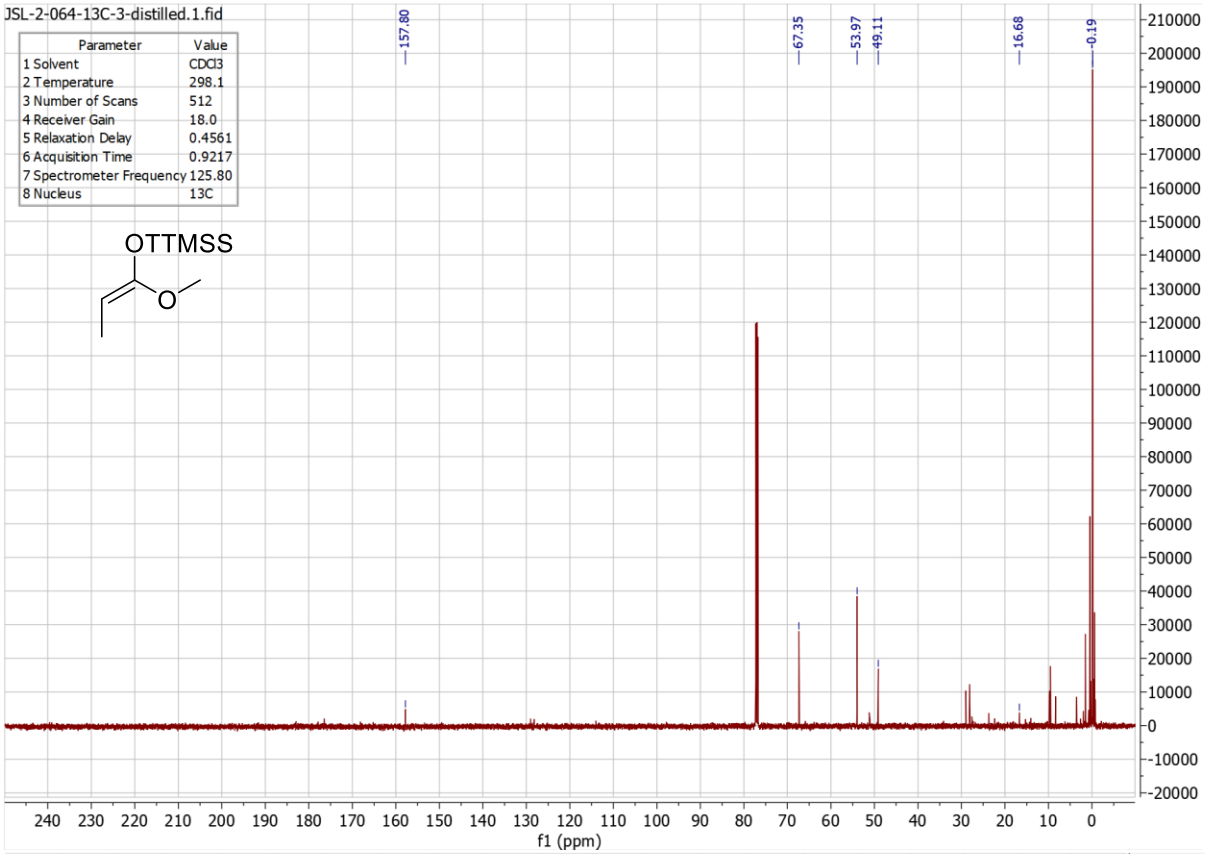
JSL-2-064-13C-3-distilled.1.fid
Parameter Value
1 Solvent CDCl3
2 Temperature 298.1
3 Number of Scans 512
4 Receiver Gain 18.0
5 Relaxation Delay 0.4561
6 Acquisition Time 0.9217
7 Spectrometer Frequency 125.80
8 Nucleus 13C
OTTMSS
O
157.80
67.35
53.97
49.11
16.68
0.19
f1 (ppm)

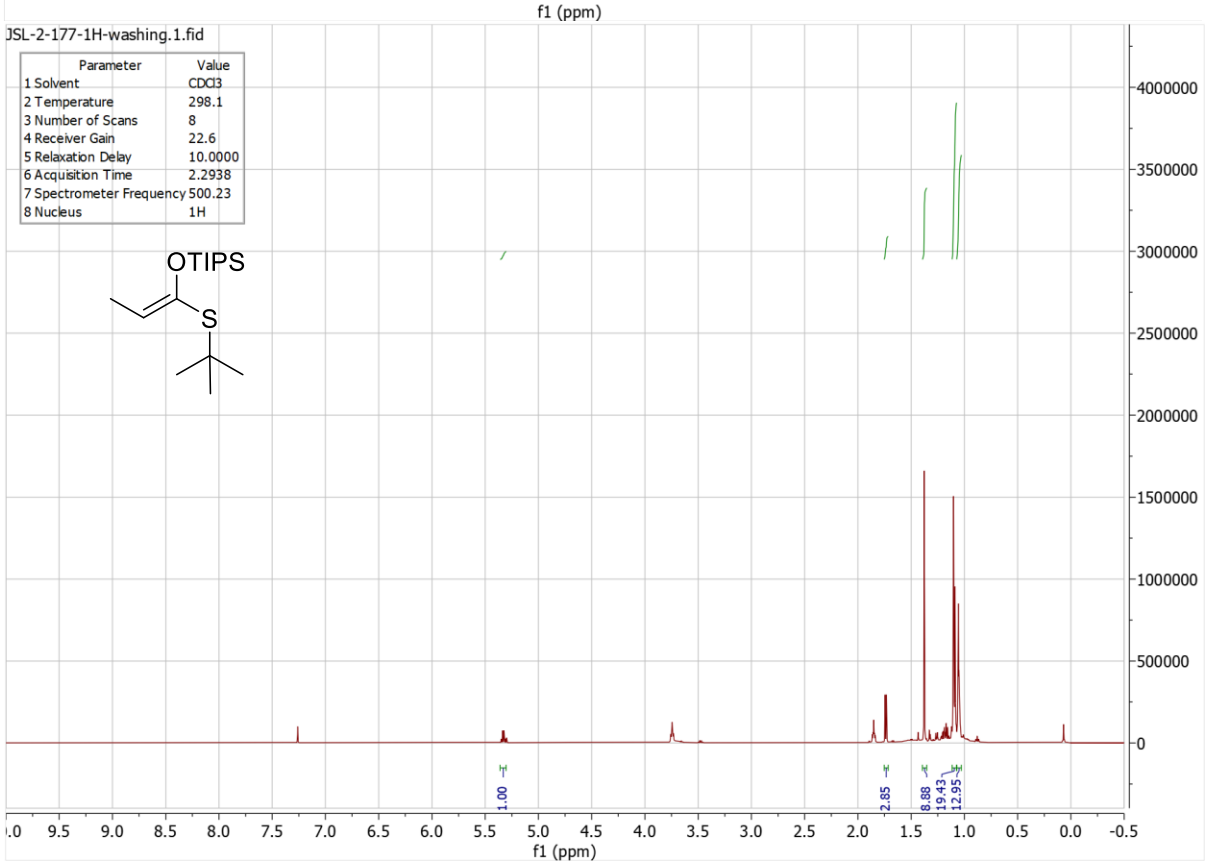
JSL-2-177-1H-washing.1.fid
Parameter Value
1 Solvent CDCl3
2 Temperature 298.1
3 Number of Scans 8
4 Receiver Gain 22.6
5 Relaxation Delay 10.0000
6 Acquisition Time 2.2938
7 Spectrometer Frequency 500.23
8 Nucleus 1H
OTIPS
S
1.00
2.85
8.88
19.43
12.95
f1 (ppm)

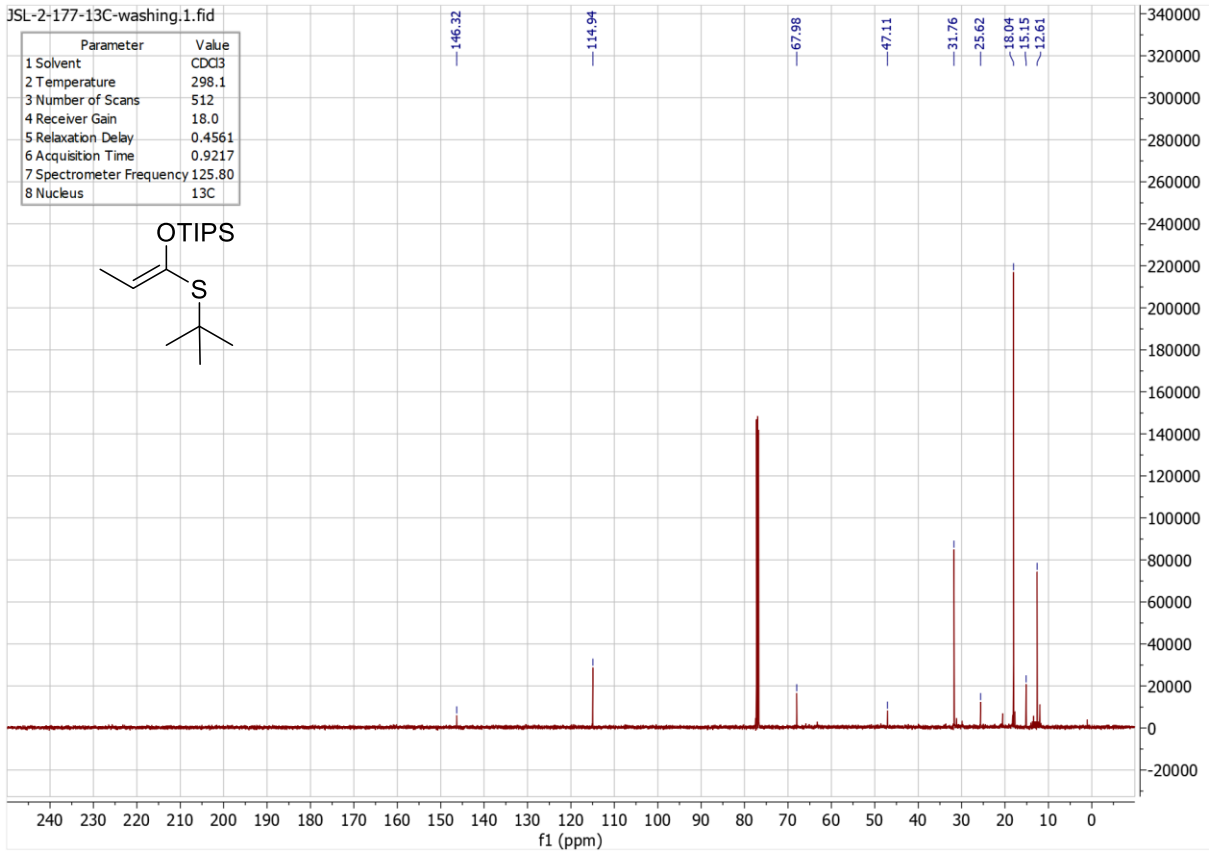
JSL-2-177-13C-washing.1.fid
Parameter Value
1 Solvent CDCl3
2 Temperature 298.1
3 Number of Scans 512
4 Receiver Gain 18.0
5 Relaxation Delay 0.4561
6 Acquisition Time 0.9217
7 Spectrometer Frequency 125.80
8 Nucleus 13C
OTIPS
S
146.32
114.94
67.98
47.11
31.76
25.62
18.04
15.15
12.61
f1 (ppm)

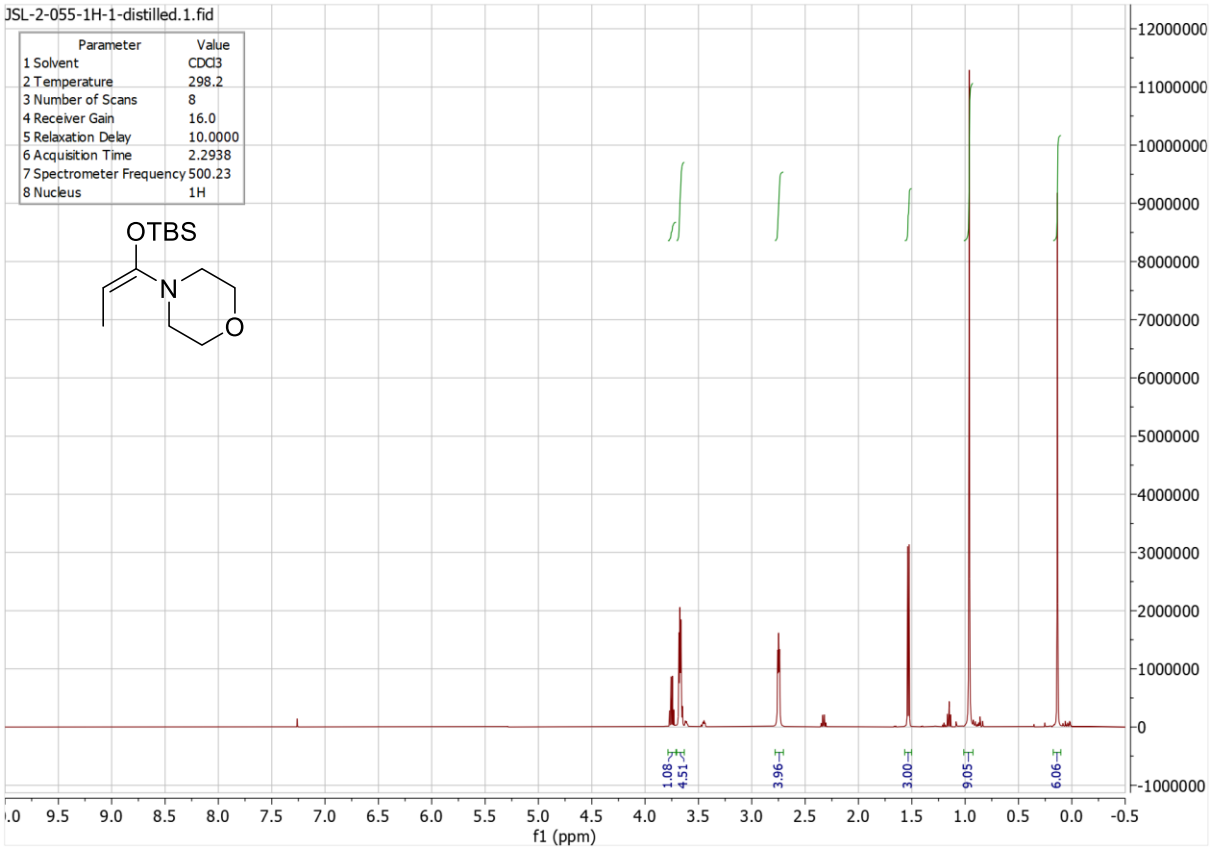
JSL-2-055-1H-1-distilled.1.fid
Parameter Value
1 Solvent CDCl3
2 Temperature 298.2
3 Number of Scans 8
4 Receiver Gain 16.0
5 Relaxation Delay 10.0000
6 Acquisition Time 2.2938
7 Spectrometer Frequency 500.23
8 Nucleus 1H
OTBS
N
O
1.08
4.51
3.96
3.00
9.05
6.06
f1 (ppm)

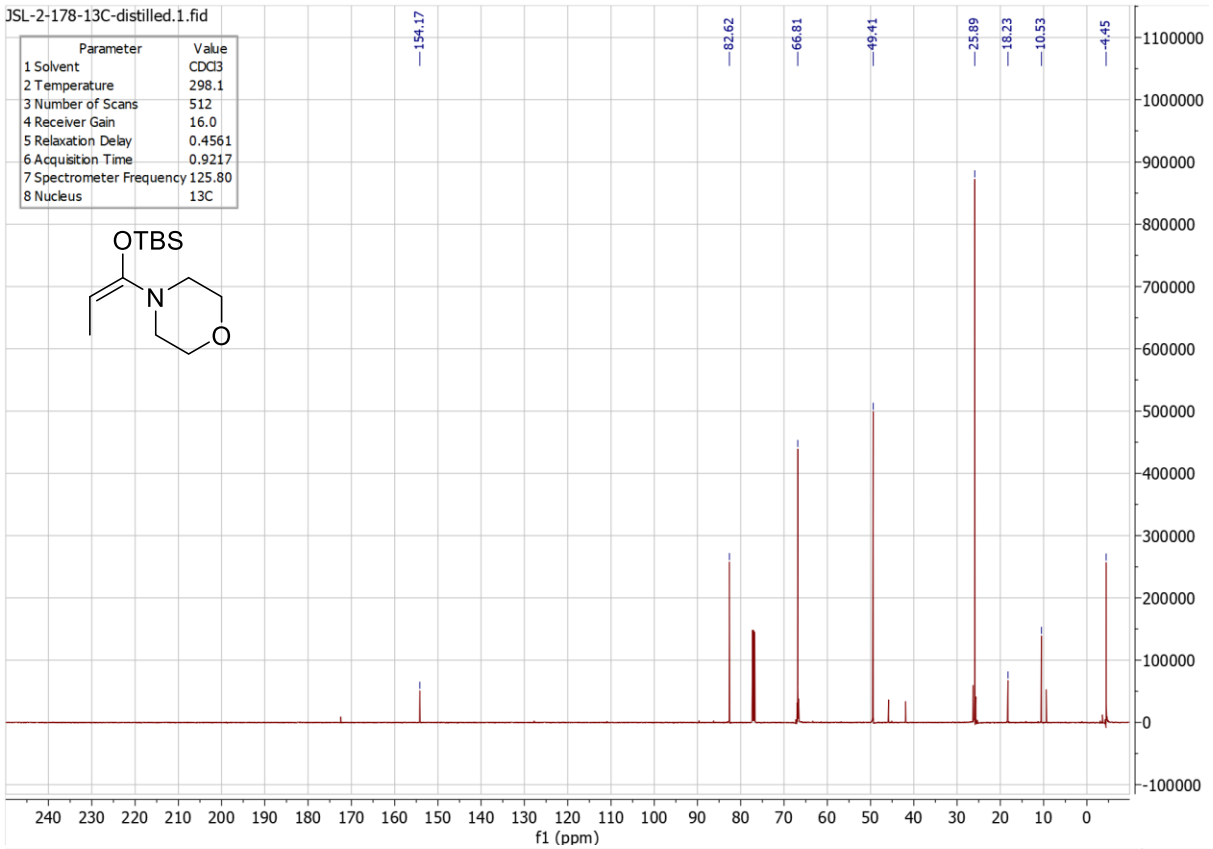
JSL-2-178-13C-distilled.1.fid
Parameter Value
1 Solvent CDCl3
2 Temperature 298.1
3 Number of Scans 512
4 Receiver Gain 16.0
5 Relaxation Delay 0.4561
6 Acquisition Time 0.9217
7 Spectrometer Frequency 125.80
8 Nucleus 13C
OTBS
N
O
154.17
82.62
66.81
49.41
25.89
18.23
10.53
-4.45
f1 (ppm)

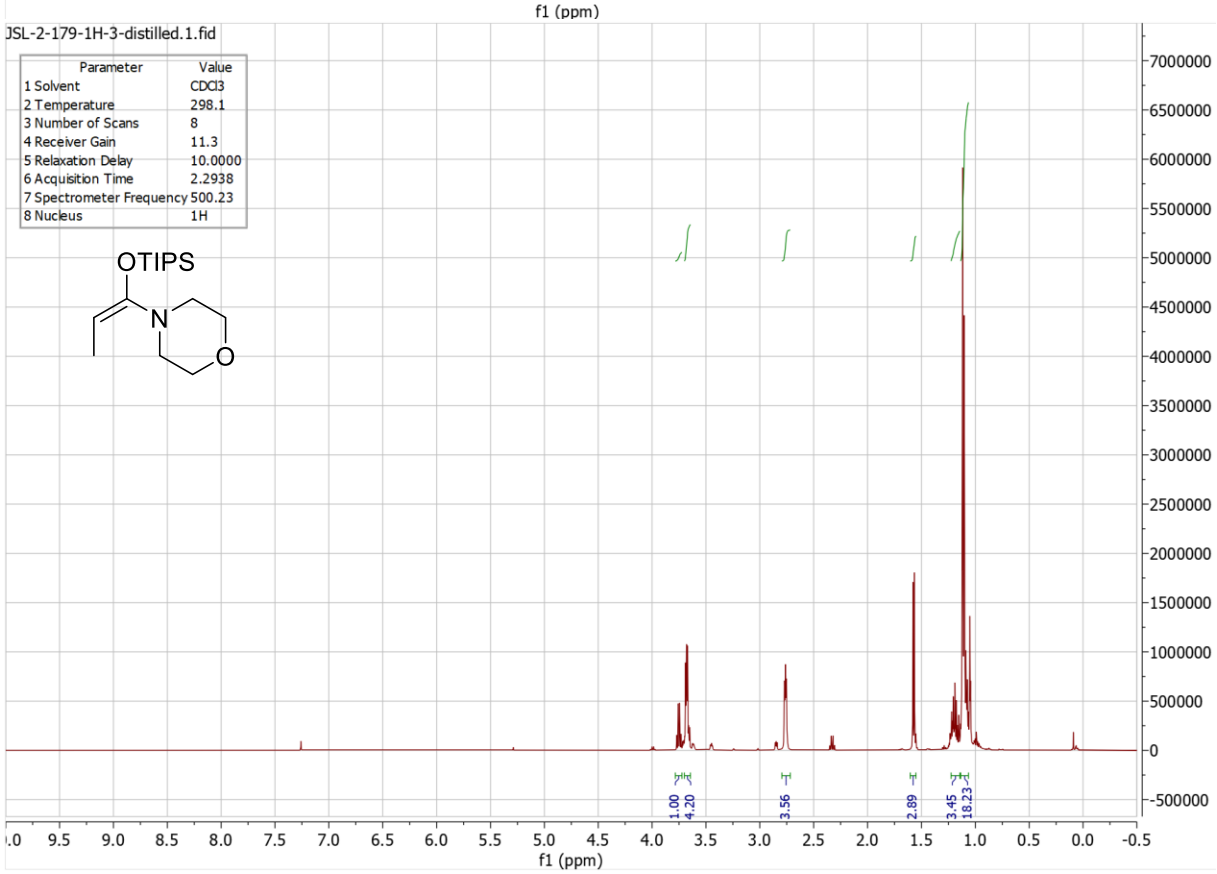
JSL-2-179-1H-3-distilled.1.fid
Parameter Value
1 Solvent CDCl3
2 Temperature 298.1
3 Number of Scans 8
4 Receiver Gain 11.3
5 Relaxation Delay 10.0000
6 Acquisition Time 2.2938
7 Spectrometer Frequency 500.23
8 Nucleus 1H
OTIPS
N
O
1.00
4.20
3.56
2.89
3.45
18.23
f1 (ppm)

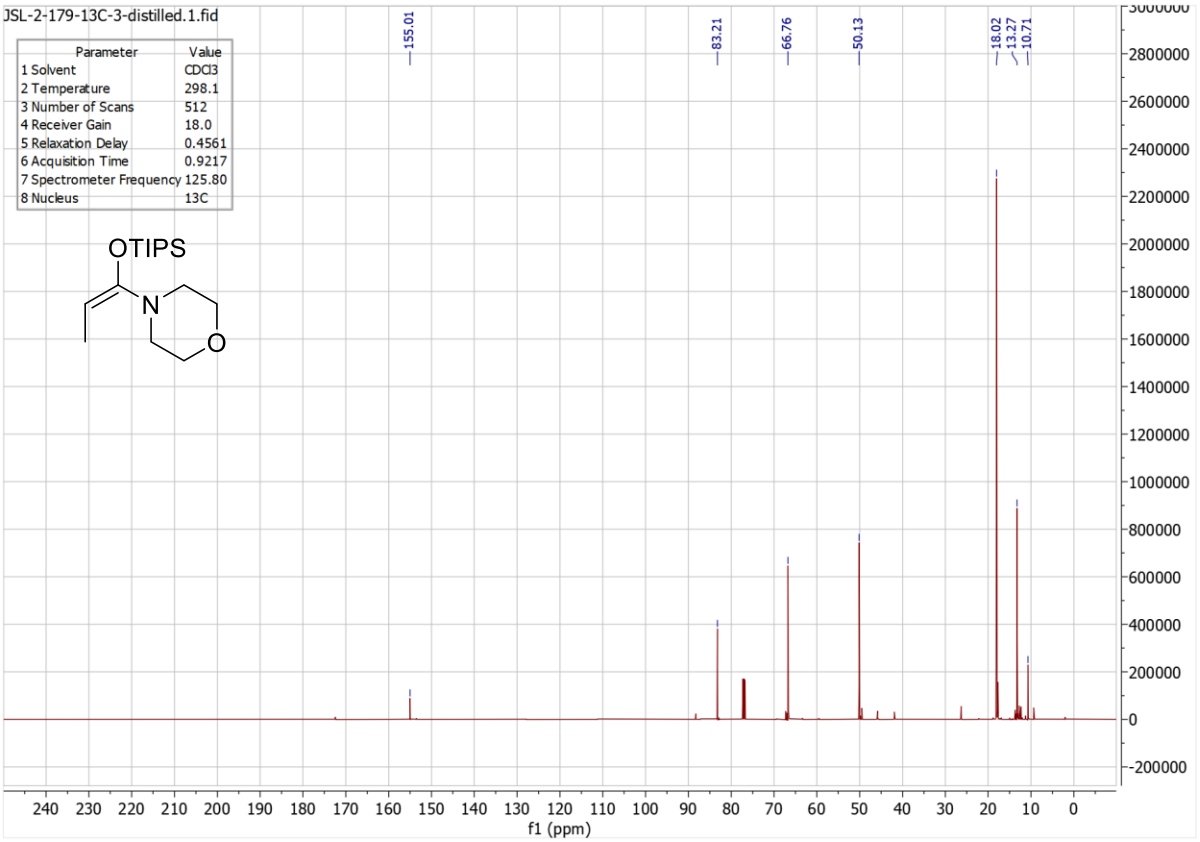
JSL-2-179-13C-3-distilled.1.fid
Parameter Value
1 Solvent CDCl3
2 Temperature 298.1
3 Number of Scans 512
4 Receiver Gain 18.0
5 Relaxation Delay 0.4561
6 Acquisition Time 0.9217
7 Spectrometer Frequency 125.80
8 Nucleus 13C
OTIPS
N
O
155.01
83.21
66.76
50.13
18.02
13.27
10.71
f1 (ppm)

1.5.6.1 Analysis of Achiral Boron-Carbon Enolate (1)

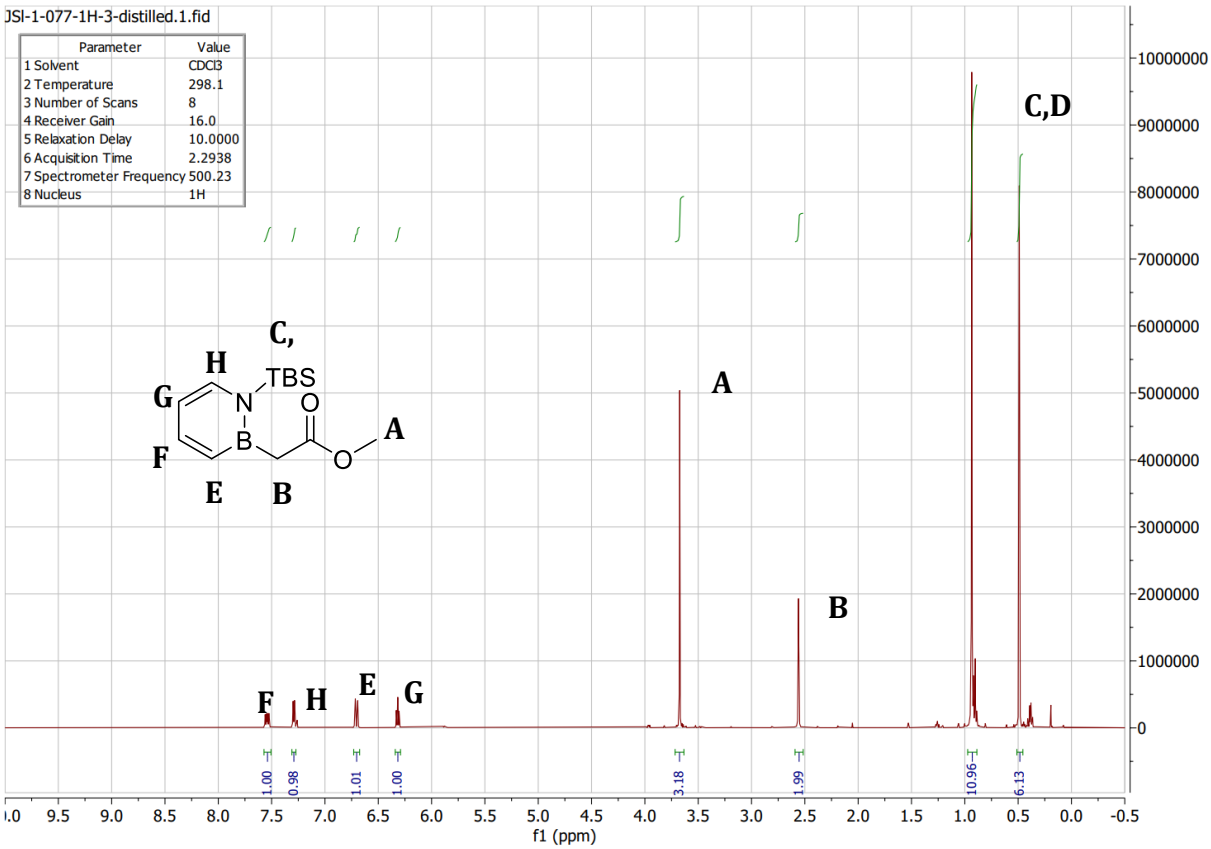
JSI-1-077-1H-3-distilled.1.fid
Parameter Value
1 Solvent CDCl3
2 Temperature 298.1
3 Number of Scans 8
4 Receiver Gain 16.0
5 Relaxation Delay 10.0000
6 Acquisition Time 2.2938
7 Spectrometer Frequency 500.23
8 Nucleus 1H
C,
H
TBS
G
N
O
B
A
F
O
E
B
A
B
C,D
F
H
E
G
1.00
0.98
1.01
1.00
3.18
1.99
10.96
6.13
f1 (ppm)

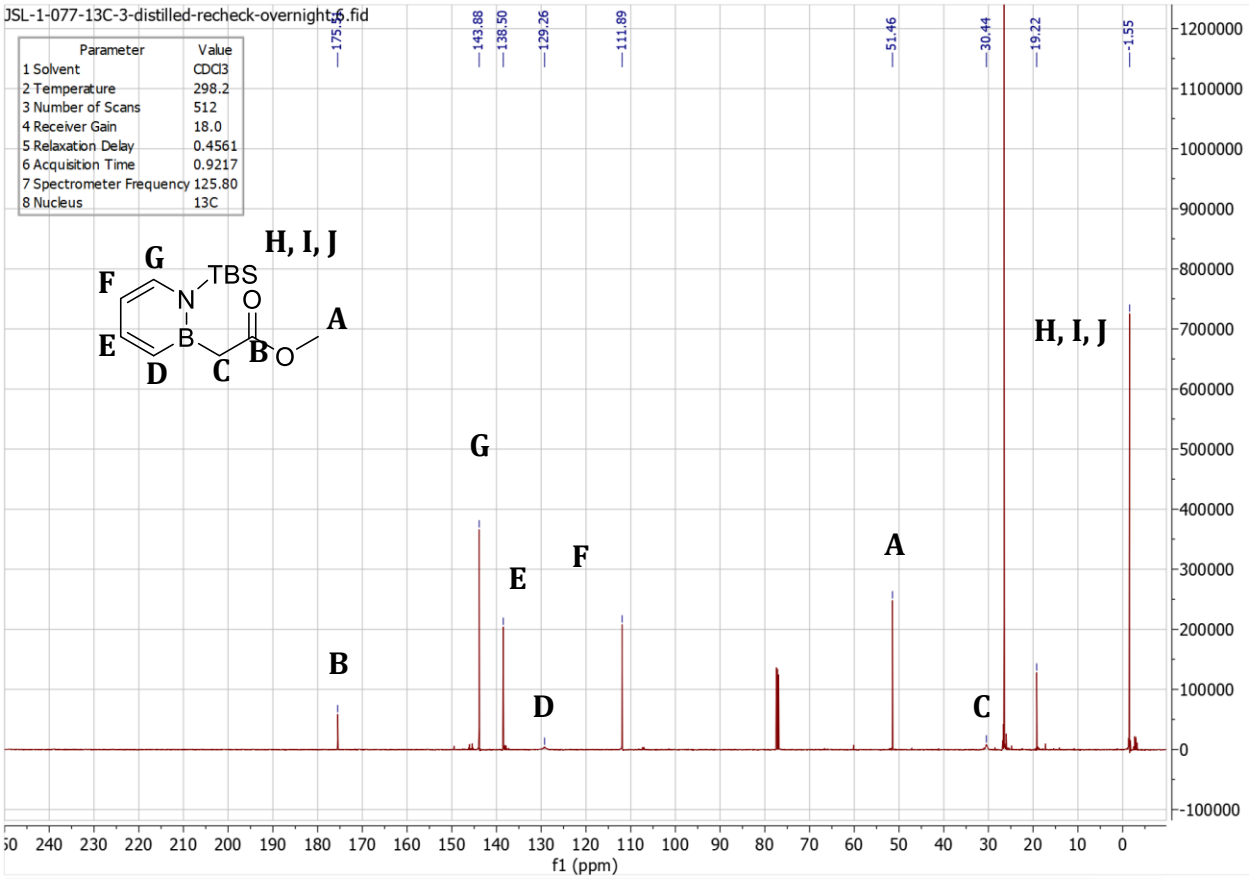
JSL-1-077-13C-3-distilled-recheck-overnight-6.fid
Parameter Value
1 Solvent CDCl3
2 Temperature 298.2
3 Number of Scans 512
4 Receiver Gain 18.0
5 Relaxation Delay 0.4561
6 Acquisition Time 0.9217
7 Spectrometer Frequency 125.80
8 Nucleus 13C
175.55
143.88
138.50
129.26
111.89
51.46
30.44
19.22
-1.55
H, I, J
G
F
TBS
N
O
A
E
B
O
D
C
H, I, J
G
E
F
A
B
D
C
f1 (ppm)

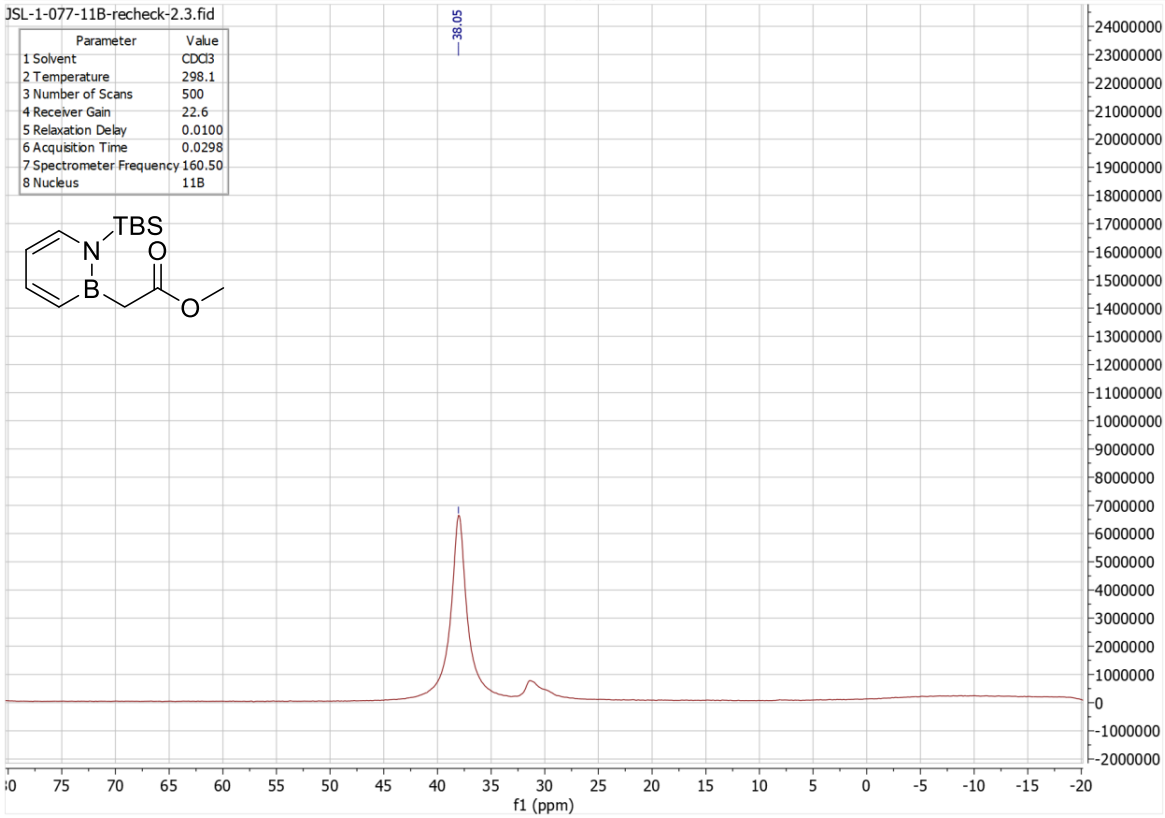
JSL-1-077-11B-recheck-2.3.fid
Parameter Value
1 Solvent CDCl3
2 Temperature 298.1
3 Number of Scans 500
4 Receiver Gain 22.6
5 Relaxation Delay 0.0100
6 Acquisition Time 0.0298
7 Spectrometer Frequency 160.50
8 Nucleus 11B
38.05
TBS
N
O
B
O
f1 (ppm)

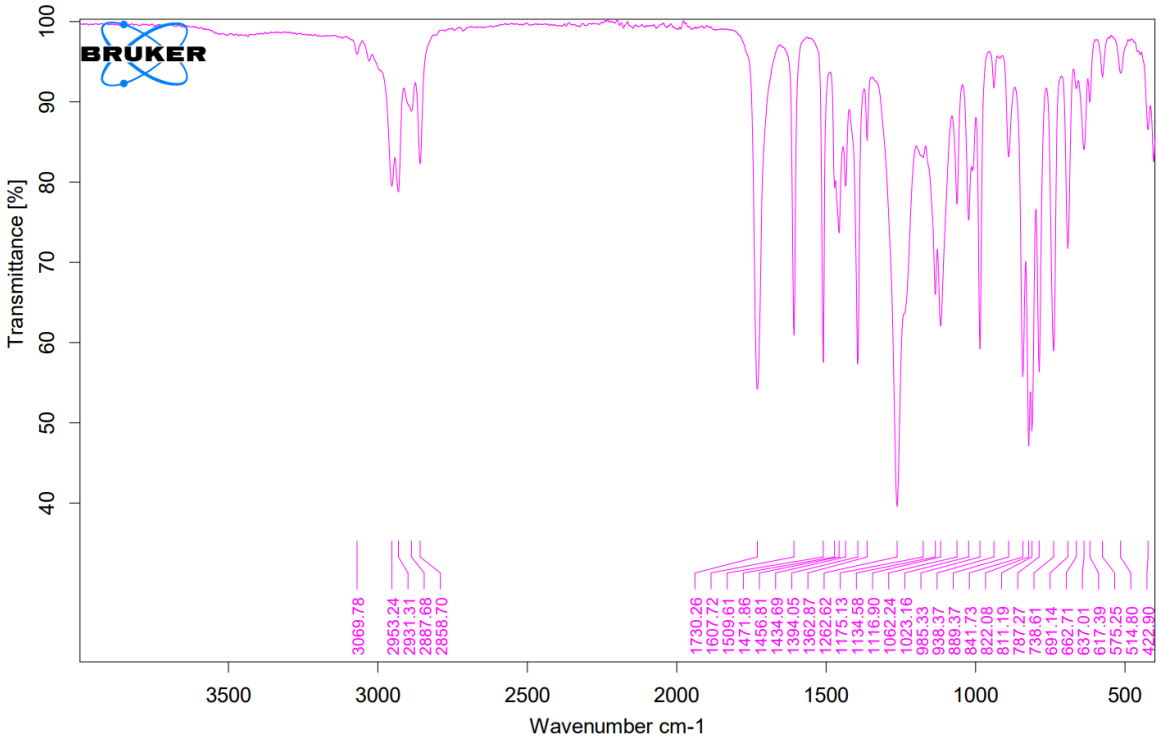
BRUKER
Transmittance [%]
100
90
80
70
60
50
40
3069.78
2953.24
2931.31
2887.68
2858.70
1730.26
1607.72
1509.61
1471.86
1456.81
1434.69
1394.05
1362.87
1262.62
1175.13
1134.58
1116.90
1062.24
1023.16
985.33
938.37
889.37
841.73
822.08
811.19
787.27
738.61
691.14
662.71
637.01
617.39
575.25
514.80
422.90
3500
3000
2500
2000
1500
1000
500
Wavenumber cm-1

1.5.6.2 Analysis of Achiral Boron-Oxygen Enolate (1.47)

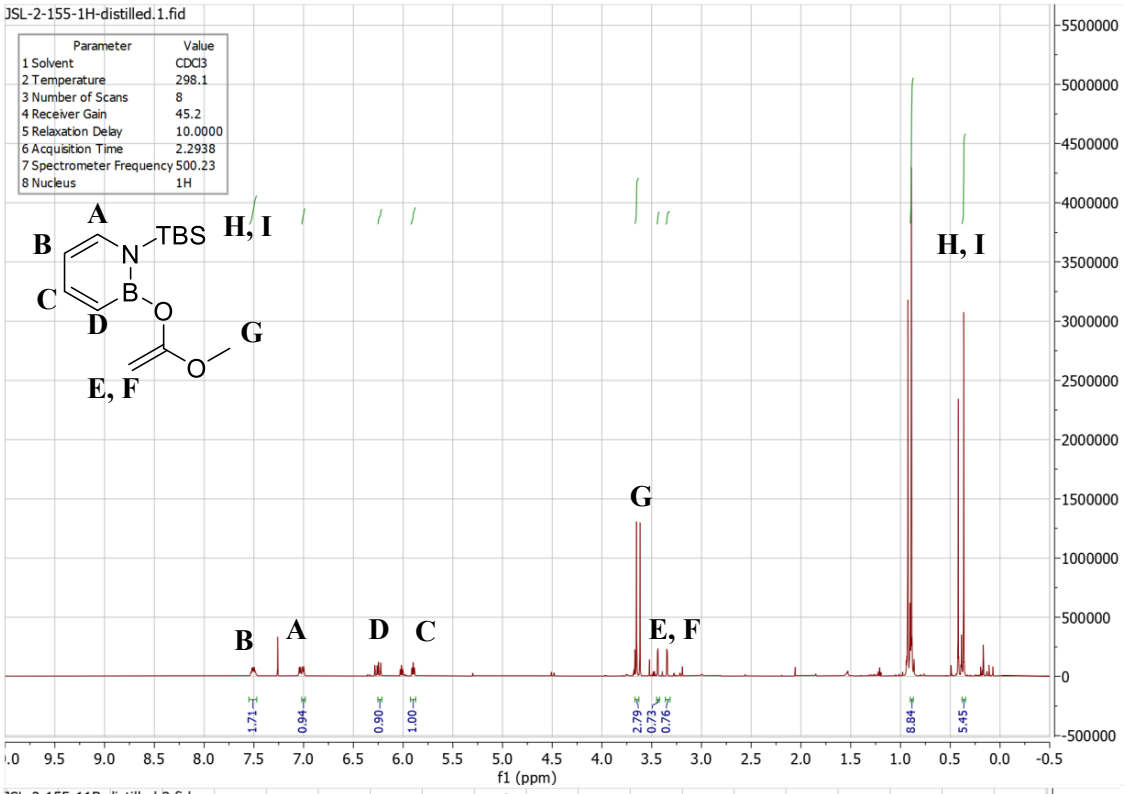

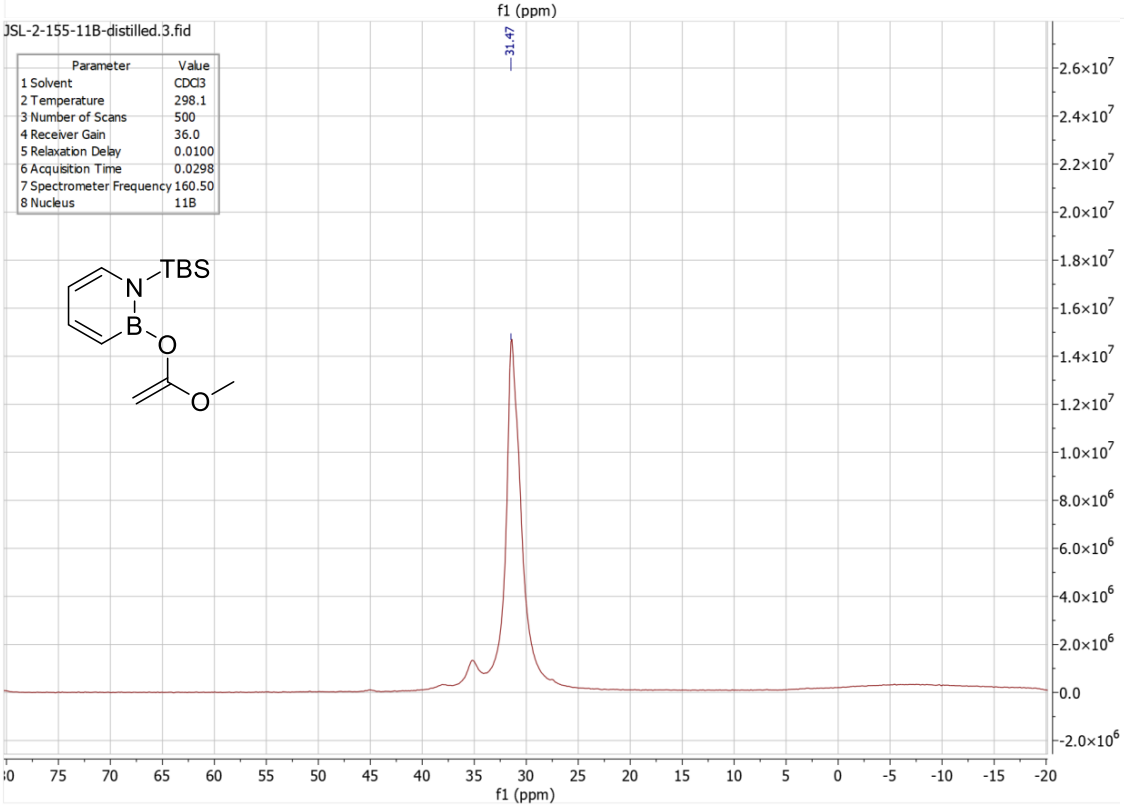

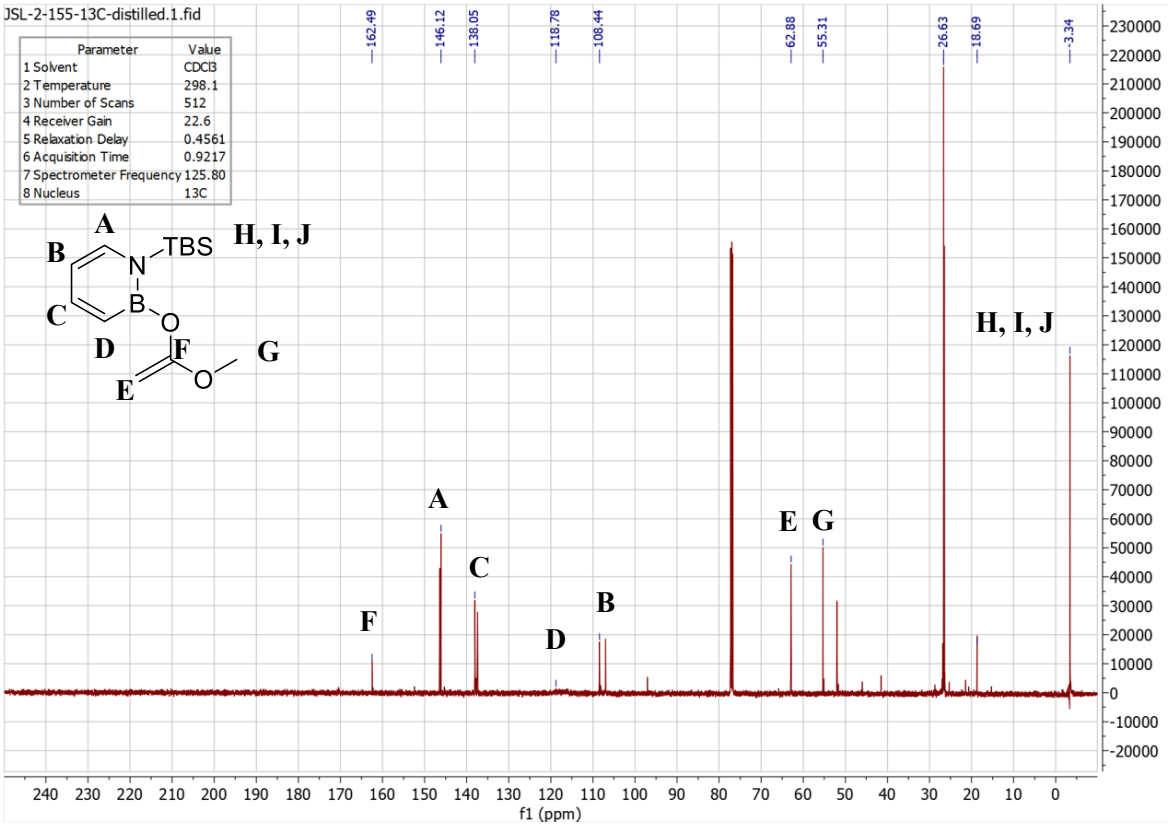
JSL-2-155-13C-distilled.1.fid
Parameter Value
1 Solvent CDCl3
2 Temperature 298.1
3 Number of Scans 512
4 Receiver Gain 22.6
5 Relaxation Delay 0.4561
6 Acquisition Time 0.9217
7 Spectrometer Frequency 125.80
8 Nucleus 13C
A
B
C
D
E
F
G
TBS
N
B
O
O
H, I, J
162.49
146.12
138.05
118.78
108.44
62.88
55.31
26.63
18.69
-3.34
H, I, J
A
C
F
D
B
E G
f1 (ppm)

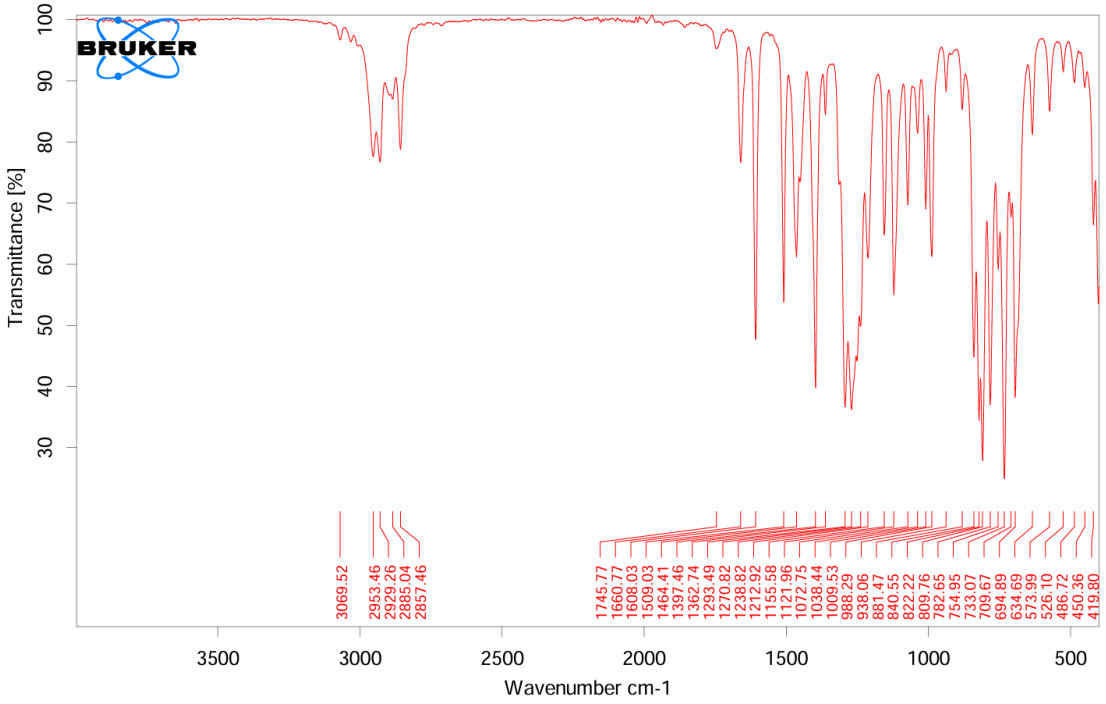
BRUKER
Transmittance [%]
Wavenumber cm-1
3069.52
2953.46
2929.26
2885.04
2857.46
1745.77
1660.77
1608.03
1509.03
1464.41
1397.46
1362.74
1293.49
1270.82
1238.82
1212.92
1155.58
1121.96
1072.75
1038.44
1009.53
988.29
938.06
881.47
840.55
822.22
809.76
782.65
754.95
733.07
709.67
694.89
634.69
573.99
526.10
486.72
450.36
419.80

1.5.6.3 Determining the Yield for the Suzuki Cross-Coupling Reaction using BC Enolate 1

The yield for the Suzuki cross-coupling reaction using BC enolate (**1**) shown in Scheme 1.1 was determined using dibromomethane as the internal standard. The signal for dibromomethane in ^{1}H NMR is at 4.93 ppm in $CDCl_3$ solvent which integrates to 2 protons. The desired product signal that we are monitoring is at 3.69 ppm corresponding to the methoxy protons which should integrate to 3 protons. To determine the crude NMR yield using dibromomethane the equation is as follows: percent (%) yield = (product signal integration/ internal standard integration)*(number of protons in internal standard/ number of protons in product signal)x100.